LONG-TERM VARIABILITY OF HUMAN HEALTH-RELATED SOLAR ULTRAVIOLET-B RADIATION DOSES FROM THE 1980S TO THE END OF THE 21ST CENTURY

Human health

Ozone

UV-B

Air quality

Climate

AUTHORS

Christos Zerefos, Ilias Fountoulakis, Kostas Eleftheratos, Andreas Kazantzidis

CORRESPONDENCE

zerefos@geol.uoa.gr

CLINICAL HIGHLIGHTS

Solar ultraviolet-B (UV-B) radiation has played a crucial role for the evolution of life on Earth. Optimal UV-B exposure behaviors, which ensure balance between the risks and benefits of exposure to UV-B, depend on both environmental and physiological factors, and cannot be easily determined. The present review provides the current state of knowledge on the effects of UV-B radiation to humans. The physical mechanisms that control the levels of solar UV-B radiation at the Earth's surface are also discussed. A comprehensive review of the studies reporting on current trends in the levels of UV-B at the surface and model projections of its future levels is examined and reveals the important role of man-made climatic changes in the evolution of the solar UV-B at the ground. The review provides evidence that, despite the success of the Montreal Protocol, the future evolution of the levels of solar UV-B radiation at the Earth's surface has important uncertainties caused by the expected changes in our climate. Therefore, it is recommended that the usual precautionary measures to protect from excess exposure of humans to solar UV-B radiation should continue to apply in the decades to come.

REVIEW ARTICLE

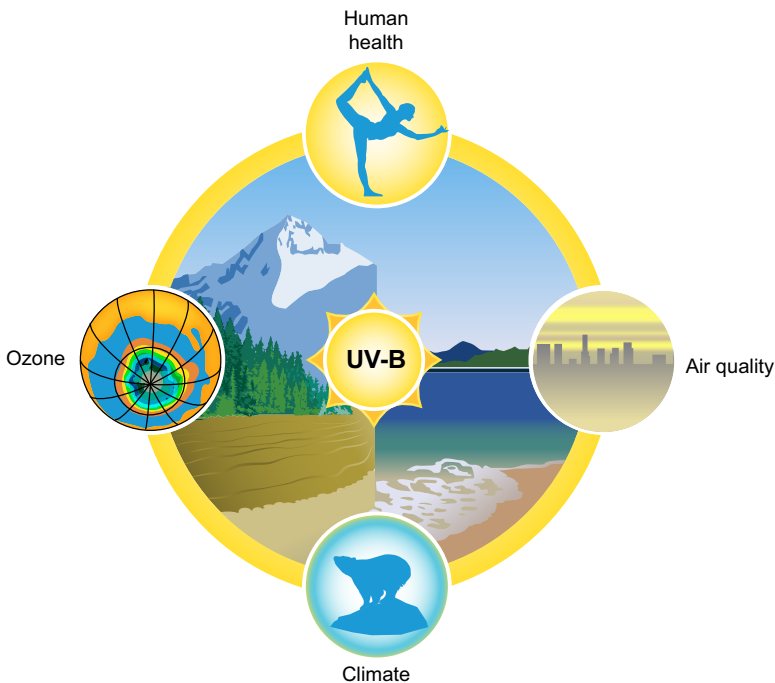# LONG-TERM VARIABILITY OF HUMAN HEALTH-RELATED SOLAR ULTRAVIOLET-B RADIATION DOSES FROM THE 1980S TO THE END OF THE 21ST CENTURY

Christos Zerefos,[1,2,3,4] Ilias Fountoulakis,[1,5,6] Kostas Eleftheratos,[2,6] and Andreas Kazantzidis[7]

[1]Research Centre for Atmospheric Physics and Climatology, Academy of Athens, Athens, Greece; [2]Biomedical Research Foundation, Academy of Athens, Athens, Greece; [3]Navarino Environmental Observatory, Messinia, Greece; [4]Mariolopoulos-Kanaginis Foundation, Athens, Greece; [5]Institute for Astronomy, Astrophysics, Space Applications and Remote Sensing, National Observatory of Athens (IAASARS/NOA), Athens, Greece; [6]Department of Geology and Geoenvironment, National and Kapodistrian University of Athens, Athens, Greece; and [7]Laboratory of Atmospheric Physics, Physics Department, University of Patras, Patras, Greece

Abstract

Solar ultraviolet-B (UV-B) radiation has played a crucial role in the evolution of life on Earth. UV exposure presents both risks and benefits to humans. Optimal UV-B exposure behaviors, that ensure balance between the risks and benefits of exposure to UV-B depend both on environmental and physiological factors and cannot be easily determined. The present review provides the current state of knowledge relative to the effects of UV-B radiation to humans. The physical mechanisms that control the levels of solar UV-B radiation at the Earth's surface are also discussed. A comprehensive review of the studies reporting on current trends in the levels of solar UV-B radiation at the surface and model projections of its future levels is examined and reveals the important role of man-made climatic changes in its evolution. The review provides evidence that despite the success of the Montreal Protocol, the future evolution of the levels of solar UV-B radiation at the Earth's surface has important uncertainties caused by the expected changes in our climate. Therefore, it is recommended that the usual precautionary measures to protect from excess exposure of humans to solar UV-B radiation should continue to apply in the decades to come.

climate change; effective UV doses; Montreal Protocol; solar ultraviolet radiation; solar UV-B variability

1. INTRODUCTION

Life on Earth is protected from a number of dangerous forms of energy coming from the sun and from space. The upper and lower layers of the atmosphere not only serve as a shield but also act as a barrier that keeps the mean global air temperature above 14°C. This is effected by the so-called greenhouse gases (GHGs; CO_2, methane, N_2O, water vapor), without the presence of which our planet would have ground temperatures on the order of -18°C. Our protection from high-energy particles and radiation coming from the sun is provided mainly by their absorption in the upper layers of the atmosphere, mainly by oxygen atoms, ozone molecules, and other constituents. Overall, the atmosphere is composed of 78% nitrogen and 21% oxygen, and the remaining 1% includes greenhouse gases and other minor constituents.

Ozone is formed in the upper layers of the atmosphere by the interaction of solar ultraviolet radiation with molecular oxygen, and it protects us from dangerous parts of ultraviolet-B (UV-B). It should be remembered that the UV part of the solar spectrum carries to the Earth only 9% of the total solar energy. These photons enter into a large number of photochemical reactions. The interaction of solar light and solar particles with the upper layers of the polar atmosphere is responsible for

CLINICAL HIGHLIGHTS

Solar ultraviolet-B (UV-B) radiation has played a crucial role for the evolution of life on Earth. Optimal UV-B exposure behaviors, which ensure balance between the risks and benefits of exposure to UV-B, depend on both environmental and physiological factors, and cannot be easily determined. The present review provides the current state of knowledge on the effects of UV-B radiation to humans. The physical mechanisms that control the levels of solar UV-B radiation at the Earth's surface are also discussed. A comprehensive review of the studies reporting on current trends in the levels of UV-B at the surface and model projections of its future levels is examined and reveals the important role of man-made climatic changes in the evolution of the solar UV-B at the ground. The review provides evidence that, despite the success of the Montreal Protocol, the future evolution of the levels of solar UV-B radiation at the Earth's surface has important uncertainties caused by the expected changes in our climate. Therefore, it is recommended that the usual precautionary measures to protect from excess exposure of humans to solar UV-B radiation should continue to apply in the decades to come.

spectacular visual phenomena, such as those seen in the celestial curtains of aurora borealis and aurora australis.

For historical purposes, it is noted here that air (our atmospheric envelope) is not an essential element, as it was considered by ancient philosophers (1). Rather, it is a mixture of gases that were discovered during the enlightenment period (2). In 1840, Schönbein discovered that during electric sparks or after thunderstorm activity there was a particular odor (smell) in the surrounding air, and he attributed it to the presence of an "unknown" gas. He named it "ozone" from the Greek verb $\acute{o}\zeta\omega$, "I smell" (3). Since then, the absorption of solar UV radiation by ozone has been studied by Fabry and Buisson (4), and its seasonal and interannual variability garnered attention in the first decades of the twentieth century (see sect. 3).

Various studies have reported that atmospheric ozone protects humans and animals from the dangerous UV part of the solar spectrum (5, 6). Angell and Korshover, in a series of articles dating back to the 1960s (7–9), discovered that ozone concentrations fluctuated over short and long periods of time. Other cyclical or quasi-cyclical phenomena that affect the total column of ozone were discovered in the 1980s (10). Such were the El Niño southern oscillation and the amplitude of the solar cycle by Angell and Korshover; the first estimate of the amplitude of the 11-yr solar cycle in stratospheric temperatures (which depend on the ozone abundance) was first modeled by Zerefos and Crutzen (11). At that time, modeling of ozone was done with atmospheric chemistry models based only on oxygen. The models were improved by Paul Crutzen to include nitrogen species in the early 1970s, which marked the era of modern atmospheric chemistry. All of these studies have

shown that ozone concentrations vary not only by simple chemical reactions with oxygen molecules (12) but also by interaction between dynamics of the atmospheric engine and by more complex chemical and photochemical reactions (2, 13).

In the 1970s, the calibration of homogeneous satellite measurements created a revolution in the measurement of long-term ozone changes (ozone trends) (14). The final clue came with the discovery of the "ozone hole" (15, 16) and the establishment of the Montreal Protocol on Substances that Deplete the Ozone Layer (commonly referred to as the Montreal Protocol), the landmark multilateral environmental agreement that regulates the production and consumption of nearly 100 manmade chemicals referred to as ozone-depleting substances (ODSs; see for example Ref. 17).

2. SIGNIFICANCE OF UV-B RADIATION FOR HUMANS AND THE ECOSYSTEMS

UV radiation extends at wavelengths between 100 and 400 nm and is divided into the UV-C (100–280 nm), the UV-B (280–315 nm), and the UV-A (315–400 nm) subregions of the solar spectrum. Although UV radiation is only a small fraction (∼9%) of the electromagnetic radiation emitted by the sun, it is of exceptional biological significance. Solar UV-C radiation is absorbed mainly by oxygen and its constituents in the upper atmosphere. Stratospheric ozone also absorbs UV-C radiation as well as most of the UV-B radiation, and only a very small fraction of the solar UV-B radiation reaches the surface of the Earth (18, 19). The inverse relationship between ozone and UV-B was first quantified by Bass and Paur (20), and it was experimentally proven under clear skies in the 1990s by spectroradiometry (21, 22).

UV-B radiation that reaches the surface of the Earth is a very small fraction of the total solar radiation (<1%), although its biological significance is remarkable (23). Exposure to UV-B radiation is vital for many living organisms, including humans (24–29), and has played a key role in the evolutionary process. For example, the production of vitamin D in the human skin, driven by UV-B radiation, is the main evolutionary force that caused white skin development when humans migrated from central Africa to northern latitudes (30, 31).

Because humans are part of the natural environment, changes driven by UV-B in the function of ecosystems have both direct and indirect impacts on humans. During exposure to sunlight, the UV-B photons enter the skin and photolyze 7-dehydrocholesterol to previtamin D_3, which in turn is isomerized by the body's temperature to vitamin D_3 (32). Several studies have indicated

that vitamin D enhances immune function (33) and protects humans from infections (34–37), autoimmune diseases (38, 39), mental disorders (40, 41), and cancer (42–44). Additional beneficial effects of UV radiation are summarized in the study of Juzeniene and Moan (27).

Overexposure to UV-B radiation can be detrimental and is related to numerous health issues (45–47). For example, it can cause DNA damage (48) and is among the main environmental risk factors for melanoma and nonmelanoma skin cancers (49) (**FIGURE 1**). It is also related to suppression of immune response (52) and induction of erythema in the human skin (53). UV-B is also related to eye diseases (54–56) such as cataracts. Interaction between UV-B radiation and specific environmental contaminants can also result in harmful effects for humans and ecosystems (57, 58). It must be noted that excessive exposure to UV radiation has been found to lead to the degradation of vitamin D instead of contributing to its formation (59), which shows the significance of maintaining optimal exposures to UV sunlight.

Appropriate weighting factors, commonly referred as action spectra, are used (50, 60–62) for the quantification of the ability of solar UV radiation to induce biological effects on humans, plants, and animals. Action spectra represent the relative efficiency of the irradiance (i.e., the intensity of the total radiation that reaches a plane parallel surface) at each wavelength to cause biological effects. Biological doses are calculated after multiplying the irradiance at each wavelength by the appropriate weighting factor and then integrating over the full range of UV wavelengths. Three biologically active spectra that are widely used and are of great interest for humans are the spectra for

- erythemal irradiance, that is, the spectrum that describes the effectiveness of different wavelengths relative to their ability to induce erythema in the human skin. The erythemal irradiance action spectrum is well studied and has been defined by the International Commission on Illumination (CIE) (thus, it is commonly referred to as the CIE action spectrum) (53).
- the formation of the provitamin D_3 in the human skin. The particular action spectrum is under debate (63, 64), and different studies propose different action spectra (see **FIGURE 1**) (65–67).
- DNA damage. The action spectrum for DNA damage is well defined (48), although various equations have been proposed for its quantitation (e.g., Refs. 68, 69).

Although in all the above cases UV-A wavelengths also contribute to the integrated doses, the greatest contribution comes from UV-B.

In addition to its direct effects on the health of living organisms, solar UV-B radiation affects life on earth indirectly through several physical and chemical processes. For example, UV-B radiation is very important for tropospheric air quality (70, 71) and affects the biogeochemical cycles that subsequently determine the Earth's environmental conditions (for more information see for example Ref. 72).
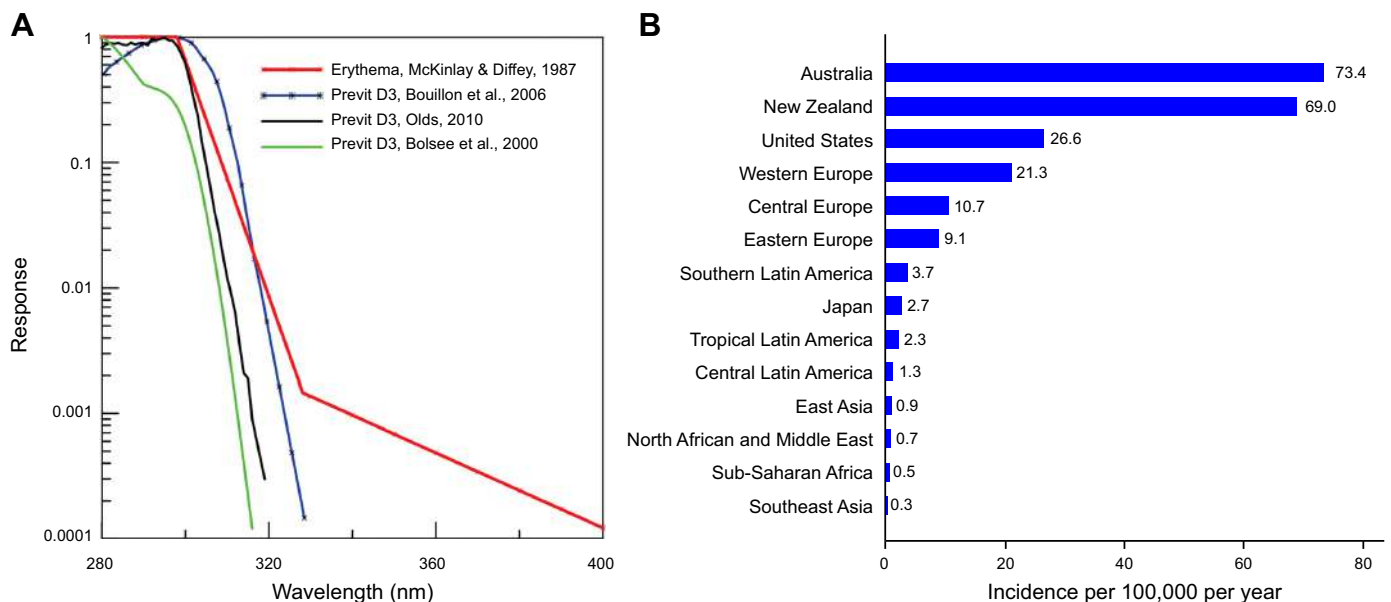

FIGURE 1. *A*: biological action spectra for erythema and production of previtamin (Previt) D_3. Adapted from Ref. 50 with permission from *Photochemical and Photobiological Sciences*. *B*: estimates of the incidence (new diagnoses) of cutaneous malignant melanoma for selected locations (note that these estimates are not adjusted for the differing age distributions of the populations). Reproduced from Ref. 51 with permission from *Photochemical and Photobiological Sciences*.

3. DISCOVERY AND FIRST EFFORTS TO MEASURE UV

UV radiation is considered to have been first discovered by the German scientist Johann Wilhelm Ritter (73) in 1801. Ritter noticed that silver chloride-soaked paper was transformed faster from white to black when it was exposed to invisible rays just beyond the violet end of the spectrum. He named the radiation that caused this effect "(de-)oxidizing rays" (74, 75). Throughout the nineteenth century, significant progress regarding the understanding of the properties of UV radiation was achieved, while the term "chemical rays" was commonly used to describe it (75).

The relationship between sunlight and ozone, as well as the role of stratospheric ozone, was initially discussed at the end of the nineteenth century and established at the beginning of the twentieth century (75, 76). Cornu and Spottiswoode (77) noted that solar UV radiation that reaches the Earth's surface decreases rapidly with decreasing wavelength for wavelengths shorter than 300 nm; the cutoff in solar UV radiation that reaches the Earth's surface at ~293 nm is due to attenuation by ozone, most of which occurs in the stratosphere (78, 79). Miethe and Lehmann (78) determined that the lower limit in the wavelength of photons that reach the Earth's surface is between 291.21 and 291.55 nm. A first detailed study of the spectral composition of sunlight in the UV region and the absorption characteristics of ozone was performed by Fabry and Buisson (4, 79). The interactions of solar UV radiation with atmospheric constituents and the spatiotemporal variability of UV radiation were also further discussed in other studies that were published in the same period (80–82).

The discussion relative to the potential biological effects of the "chemical rays" started at the beginning of the nineteenth century (83), and many studies relative to the effects of UV radiation on humans (e.g., Refs. 84–87) and on other living organisms (e.g., Refs. 88, 89) were already published in the first four decades of the twentieth century. It is worth noting that a first effort to quantify the correlation between UV-B radiation and erythema in the human skin was performed in 1928 (90). These first studies confirmed the very significant role of solar UV radiation in life on Earth.

Efforts to systematically measure the levels of solar UV radiation operationally for biological purposes began during the interwar period (e.g., Refs. 91–95). These first broadband UV measurements were performed with simple sensors and were highly uncertain. Since then, gradual progress in the field of radiometric measurements has been achieved and has led to improved understanding of the characteristics of solar UV radiation that reaches the Earth's surface. Measurements of spectral solar UV radiation at particular wavelengths have been performed since the beginning of the nineteenth century (4, 79) and were used to retrieve the total column of ozone (a measurement of the total amount of atmospheric ozone in a given column). The total column of ozone was estimated from the difference between the irradiances at wavelengths where absorption by ozone differed significantly. Thus, absolute calibration of the sensors was not necessary, and these measurements cannot provide information for the absolute variations of the irradiance.

High-quality spectro-radiometric measurements, not only in the UV region, were not generally available before the 1970s mainly because of poor calibration techniques, poor traceability, a lack of temperature compensation in the instruments deployed, and generally unsatisfactory maintenance (96). The quality of the measurements of solar irradiance was improved substantially in the 1970s and the 1980s when the first ground-based networks for the monitoring of solar irradiance were developed, which were traceable to national and international reference standards (96).

4. CONCERN FOR UV-B INCREASES BECAUSE OF THE SEVERE DESTRUCTION OF THE OZONE LAYER IN THE 1980S AND 1990S

Extensive destruction of the stratospheric ozone over Antarctica was first reported in the mid-1980s (16, 97, 98) and was attributed to anthropogenic emissions of ODSs since the 1970s. The most effective ODSs are humanmade chemicals [halocarbons and chlorofluorocarbons (CFCs)] that were mainly used in refrigerants, solvents, and propellants and as foam-blowing agents. ODS have long lifetimes in the troposphere and can enter the stratosphere, where they release atoms from the halogens through photodissociation, which subsequently catalyze the breakdown of ozone into oxygen. Atmospheric conditions during the Antarctic spring favor the chemical destruction of ozone due to the presence of ODSs, and these circumstances result in the extensive destruction of the ozone layer. In the following years, decreasing stratospheric ozone was also reported over the Arctic (99–101) and over middle latitudes (102–104). Stratospheric ozone depletion resulted in increased surface solar UV-B irradiance over many regions of the world, including areas in the densely populated middle latitudes of the Northern Hemisphere (21, 22, 105–107). Further decreases in stratospheric ozone in the future would result in extremely high UV-B levels, with

detrimental impacts for human health and the functionality of ecosystems. It is estimated that two million cases of skin cancer in humans per year will be prevented by 2030 because of the adoption of measures suggested by the Montreal Protocol (108).

Increased awareness among the scientific community and public authorities led to the signing of the Montreal Protocol, which is the only United Nations (UN) treaty to have been signed by all UN Member States. The Montreal Protocol, which was adopted in September 1987, prohibited the emissions of the most severe ODSs and prevented a further decrease in the levels of stratospheric ozone as well as a subsequent increase in the levels of UV-B (109–111). McKenzie et al. (111) simulated the levels of UV-B radiation assuming that the Montreal Protocol measures were not adopted and showed that the UV index at middle latitudes would have been already ∼20% higher with respect to current levels (**FIGURE 2**) and would have increased by approximately a factor of 4 (i.e., 400%) between 1990 and 2100.

Stratospheric ozone depletion has decelerated since the mid-1990s, and the first signs of recovery are now evident (113, 114) because adoption of the Montreal Protocol drastically limited the emissions of ODS (115). Nevertheless, more measurements and more time are needed to confirm that total ozone is indeed recovering (116, 377). Global climate model simulations predict that stratospheric ozone will fully recover after 2050 and may even exceed pre-1970s levels until the end of the century, depending on the socioeconomic scenarios considered for the simulations (117). However, as discussed in the following sections, projections of surface solar UV-B levels are still very uncertain.

5. UV-B MONITORING IN THE POST-MONTREAL PROTOCOL ERA

Increased concern for the potential evolution of the levels of UV-B irradiance in the 1980s resulted in a significant international effort for limitation of the uncertainties in UV-B measurements (**FIGURE 3**). Until the end of the 1970s, measurements of total ozone and spectral solar UV irradiance were performed manually (118). The first instruments performing automated measurements of the latter quantities were the Brewer spectrophotometers that were developed in the late 1970s (119) and became commercially available at the beginning of the 1980s (120, 121). The Brewer spectrophotometer was originally developed to perform automated measurements of the total column of ozone as an improvement of the Dobson instrument (22, 118, 119, 122). In the late 1980s it was modified to measure spectral solar UV
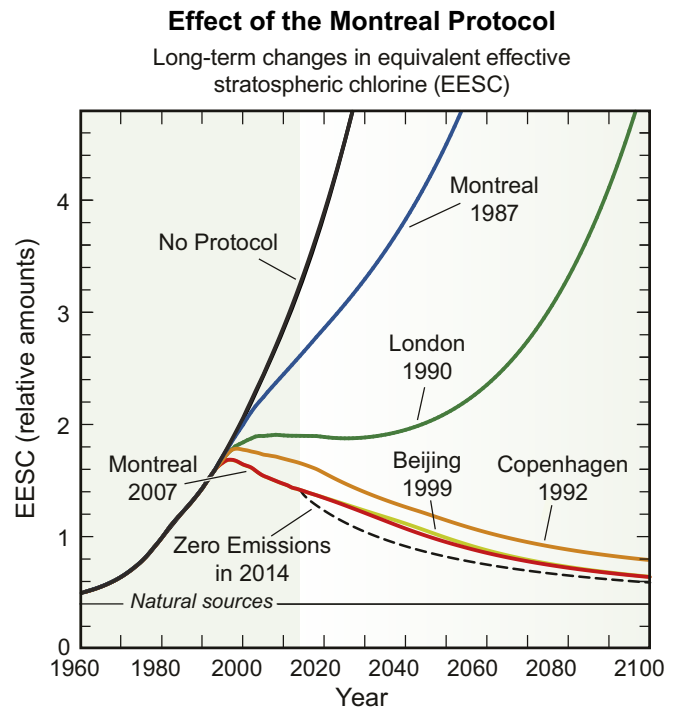

Effect of the Montreal Protocol

Long-term changes in equivalent effective stratospheric chlorine (EESC)

FIGURE 2. Projections of future abundances of ozone-depleting substances (ODSs) expressed as values of equivalent effective stratospheric chlorine (EESC) for the middle latitude stratosphere for *1*) no Montreal Protocol provisions, *2*) the provisions of the original 1987 Montreal Protocol and some of its subsequent amendments and adjustments, and *3*) zero emissions of ODSs starting in 2014. The city names and years indicate where and when changes to the original 1987 Protocol provisions were agreed. EESC is a relative measure of the potential for stratospheric ozone depletion that combines the contributions of chlorine and bromine from ODS surface observations. Without the Protocol, EESC values are projected to have increased significantly in the 21st century. Only with the Copenhagen (1992) and subsequent amendments and adjustments do EESC values show a long-term decrease. Reproduced from Ref. 112 with permission from World Meteorological Organization/United Nations Environment Programme.

irradiance (123). Since then, >200 such instruments have been deployed worldwide, constituting a large network (124–126).

Nowadays, improved spectral sensors (**FIGURE 4**) (compared with those deployed in the 1980s) have been developed, providing highly accurate measurements in a wider range of wavelengths extending up to the visible region (e.g., Refs. 127, 128), and many UV monitoring networks have been developed (e.g., Refs. 129–133). In addition to the improvement in the technology of the sensors, numerous national and international intercomparison campaigns for spectral and broadband UV monitoring instruments have been performed (e.g., Refs. 135–139) that allowed identification and constraint of the uncertainties in UV measurements and established maintenance and calibration pro-cedures (132, 140–143). Standardization of the
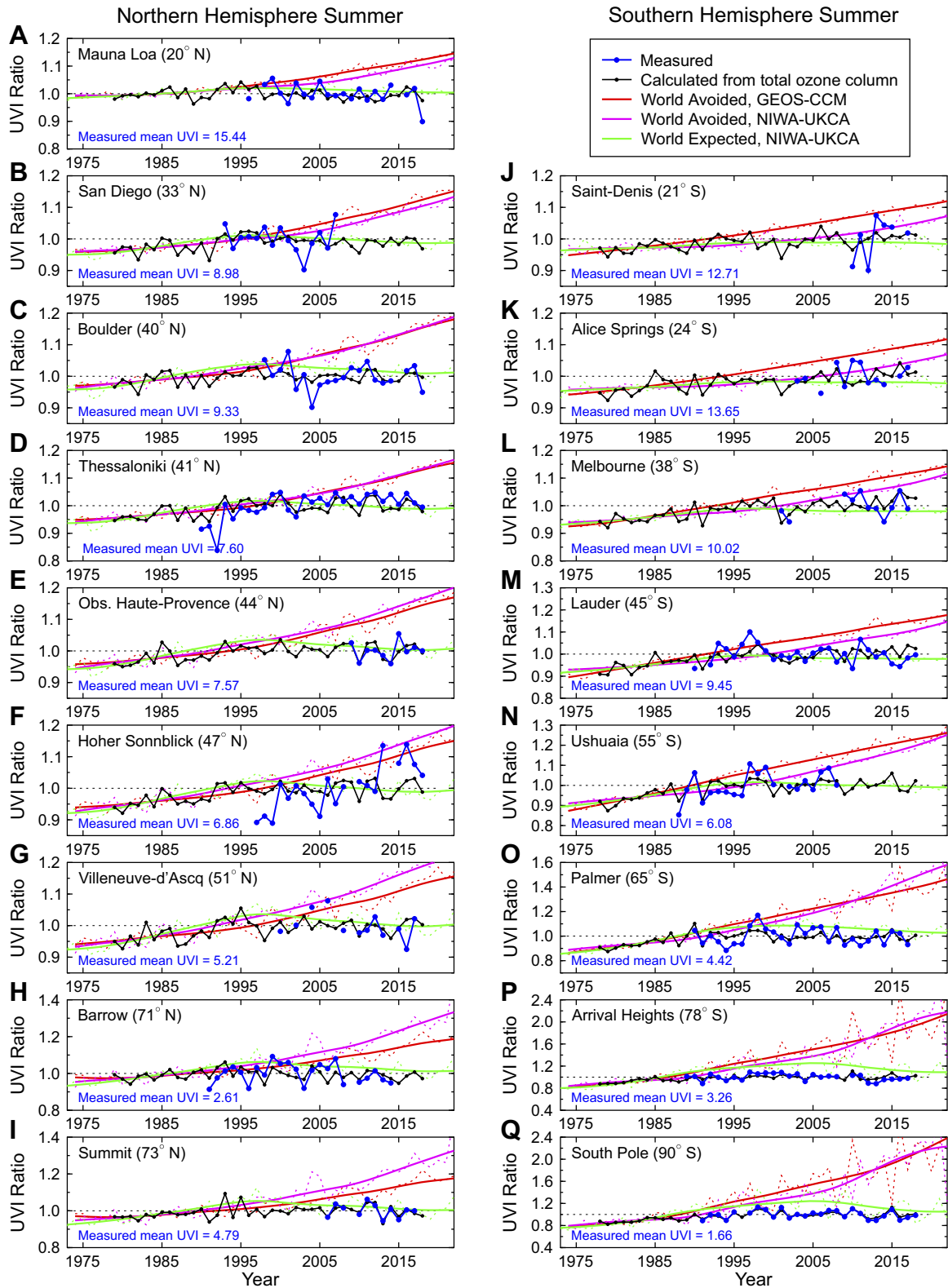
Northern Hemisphere Summer

Southern Hemisphere Summer

FIGURE 3. Comparison of normalized UV index (UVI) ratios for summer months at all sites between measurements, calculations for clear skies based on the ozone assimilation, and clear-sky models for the world avoided (evolution of the UVI if there were no Montreal Protocol provisions) and world expected (expected evolution of the UV index after the adoption of the Montreal Protocol) scenarios. *A–I*: Northern Hemisphere. *J–Q*: Southern Hemisphere. Note that the vertical axis scale varies between panels. GEOS-CCM, Goddard Earth Observing System-Chemistry-Climate Model; NIWA-UKCA, National Institute of Water & Atmospheric Research-UK Meteorological Office Climate Assessment. Reproduced from Ref. 111 under CC-BY license.
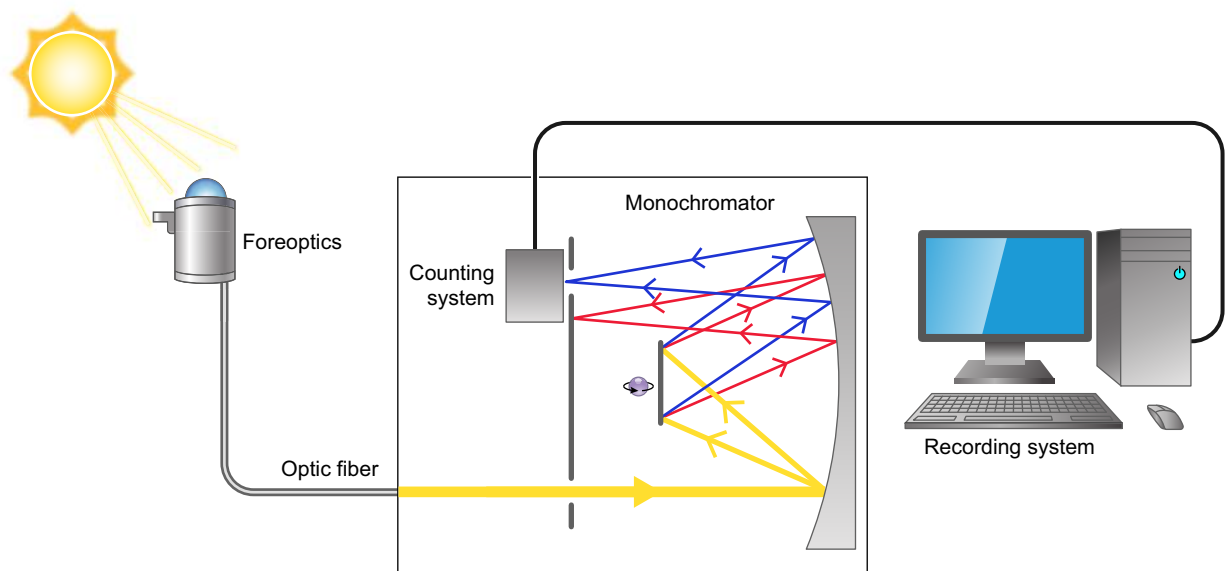
FIGURE 4. Basic principle of operations of the newest technology spectrophotometers used for measurements of the spectral global UV-B irradiance. Solar radiation enters the system through a diffuser that is usually covered by a UV-transparent quartz dome. Then, through an optical fiber, it is transferred to the monochromator, where it is analyzed at different wavelengths. In many instruments, the monochromatic beam at the exit of the first monochromator enters a second monochromator, where it is analyzed again. With the use of the second monochromator, better stray light rejection (i.e., more accurate wavelength separation) is achieved (134). At the exit of the monochromator there is the counting system, which is usually either a photon counter (with an adjusted photomultiplier tube) or a charge-coupled device (CCD). The signal is typically recorded to a PC or a data logger.

calibration and maintenance procedures and development of international reference standards led to great improvement in the quality of the measurements. Although in the 1990s one-fold uncertainties in the measurements of well-maintained and well-calibrated spectral instruments were of the order of 5% (139), currently uncertainties of the order of 1% are feasible (144, 145).

Instruments aboard satellite platforms cannot directly measure the surface solar UV-B irradiance. Nevertheless, analyses of their measurements can give information for the main atmospheric parameters that affect solar UV-B irradiance (i.e., total ozone, aerosols, clouds, and surface albedo). Then the surface solar UV-B irradiance can be simulated with radiative transfer modeling, where inputs can be either data sets from a single satellite instrument or a combination of data sets from different sensors. Satellite monitoring provides global coverage but, as discussed below, is in many cases less accurate or less representative for an area relative to ground-based monitoring.

The first efforts to measure the profile of ozone in the atmosphere with satellite-based sensors took place in the 1960s (146). Satellite-based monitoring of a complete set of parameters that affect (and can be used to model) surface solar UV-B irradiance (i.e., total ozone, aerosol optical properties, and cloud optical properties) started later, in 1978, when NASA's Nimbus-7 satellite was launched into orbit. Nimbus-7 carried the Total Ozone

Mapping Spectrometer (TOMS) and the Temperature Humidity Infrared Radiometer (THIR) sensors that provided all necessary information for the modeling of UV-B irradiance (147–150). TOMS/Nimbus-7 was substituted by TOMS-Earth Probe (TOMS-EP) aboard the Russian Meteor-3 satellite in 1994. In 1995 the Global Ozone Monitoring Experiment-1 (GOME-1) instrument onboard the second European Remote Sensing (ERS-2) satellite was also launched and provided total ozone retrievals. Newer satellite sensors that provide retrievals of atmospheric and Earth surface parameters that are commonly used to simulate surface UV-B irradiance are the Global Ozone Monitoring Experiment-2 (GOME-2) aboard MetOp satellites, the SCanning Imaging Absorption spectroMeter for Atmospheric CHartographY (SCIAMACHY) aboard the Envisat satellite, the Ozone Monitoring Instrument (OMI) aboard the Aura satellite, and the most recently launched TROPOspheric Monitoring Instrument (TROPOMI) onboard the Copernicus Sentinel-5 Precursor satellite.

Many satellite-based data sets, mainly relating UV-B doses to human health, are currently available (151–155). Although UV doses based on TOMS and GOME-1 measurement have been produced and used in UV-related studies (e.g., Ref. 156), these measurements are highly inexact, mainly because of high uncertainties in the optical properties of aerosols and clouds used for the measurements (157–160). More reliable satellite-based data sets have been available since the 2000s, when more

reliable satellite-based aerosol and cloud information became available (e.g., Refs. 155, 161). Nevertheless, the retrievals are still not sufficiently accurate over highly reflective terrains, mountainous sites, and highly polluted environments (162–168), mainly because of simplifications in the algorithms and the use of climatological data (for, e.g., surface albedo and aerosol absorption). Furthermore, each satellite pixel represents the average of a finite area, and the average atmospheric and surface conditions in the pixel may differ significantly relative to the conditions of each point of the pixel, especially over complex, inhomogeneous terrains (169). Thus, under the conditions described above, ground-based UV measurements and satellite-based estimates may differ by 20% for cloudless skies and >50% for cloudy skies (see for example Figure 4 in Ref. 165). For high-quality data sets the agreement with ground-based measurements is generally much better, within the uncertainty of the ground-based measurements, for low surface albedo, low aerosol, and cloudless-sky conditions (e.g., Refs. 163, 165). Some of the most widely used satellite-based climatological products are listed in **TABLE 1**.

In addition to the satellite-based climatological UV products, satellite-based forecast and nowcast services are also available and are used for the information of the public (e.g., Ref. 172 and references therein).

6. UV-B RADIATION AND HUMAN HEALTH

The depletion of stratospheric ozone took place in a period when skin cancer cases in light-skinned populations were already increasing rapidly (e.g., Refs. 173–176). These increases resulted mainly from changes in socio-cultural norms. Changes in style of clothing and consideration of tanned rather than pale skin as a sign of

Table 1. *Satellite-based climatological UV measurements*

Data Set (Ref.)	Products	Availability	Coverage	Spatial/Temporal Resolution
Tropospheric Emission Monitoring Internet Service (TEMIS) (153)	Daily doses of the erythemal irradiance	Clear-sky UV index and erythemal dose: 1970–present (high quality since 1979)	Clear-sky UV index and erythemal dose: world	$0.5° \times 0.5°$ or $0.25° \times 0.25°$
	Effective dose for the production of vitamin D in the human skin, effective dose for DNA damage, clear-sky UV index	All-sky products: 2004–present	All-sky doses: Europe	Daily
OMI UV data set (154)	Noontime UV index and daily erythemal doses	2004–present	Global	$1° \times 1°$ Daily
TROPOMI UV data set (155)	Noontime UV index and daily erythemal doses	2017–present	Global	$1° \times 1°$ Daily
AC SAF surface UV product (170)	daily biologically active doses, daily maximum dose rates, daily UV-B and UV-A radiation, solar noon UV index	2007–present	Global	$0.5° \times 0.5°$ Daily
Vitt et al. (152)	Noontime UV index	1983–2015	Europe	$0.05° \times 0.05°$ Daily
Vuilleumier et al. (151)	UV erythemal irradiance	2004–2018	Switzerland	1.5–2 km Hourly
SoDa Service (171)	UV-B and UV-A irradiance	2004–present	Europe	5 km 15 min

AC SAF, Atmospheric Chemistry Satellite Application Facility; OMI, Ozone Monitoring Instrument; SoDa, Solar Radiation Data; TROPOMI, TROPOspheric Monitoring Instrument.

health and affluence are considered the main contributors to this tendency ([177–179]).

UV radiation causes DNA damage and the development of somatic mutations, inflammation, oxidative stress, and defective activity of the immune cells ([180]). These events are milestones for the development of skin cancers. In this way, products such as 6-4-pyrimidone photoproducts (6-4PPs) and cyclobutane pyrimidine dimers (CPDs) are formed in a wavelength-dependent manner. Oxidative DNA damage leads to DNA mutations and contributes to the formation of melanoma. Nonmelanoma skin cancers (NMSCs), basal cell carcinoma (BCC) and squamous cell carcinoma (SCC), are far more frequently diagnosed types of skin cancer. The mechanism of NMSC formation from UV radiation is direct DNA damage and indirect DNA damage through errors in DNA repair and reactive oxygen species as well as immune suppression ([181–183]). In all types of skin cancer, UV radiation plays a crucial role in skin carcinogenesis. However, the frequency of indexes is inversely related to skin pigmentation, with higher incidence in individuals with fair skin ([184], [185]).

Nowadays, exposure to UV radiation is considered a major environmental risk factor for melanomas ([186]). Approximately 75% of melanomas have been attributed to UV overexposure. The incidence varies with the duration of UV exposure and skin sensitivity to UV radiation. For example, this proportion of melanomas attributed to UV radiation is lower in Canada (62%) but much higher (96%) in Oceania ([187]). Potrony et al. ([188]) showed that an increase of one-fold standard deviation for ambient UV radiation during summertime is associated with a statistically significant greater melanoma risk. It has been suggested that both intermittent high-dose and chronic exposures to sunlight contribute to various forms of melanoma ([189]).

Exposure to sunlight is a known or suspected risk factor for many eye diseases also. Cataract is usually an inevitable side effect of aging and remains the leading cause of impaired vision worldwide ([190]). Exposure of eyes to UV radiation increases the risk of developing cataract and is considered among the most important environmental risk factors in different geographically diverse populations (e.g., Refs. [189], [191], [192]). Hashemi et al. ([193]) analyzed 45 studies with a sample size of 161,947 and identified that the prevalence of cataracts related to exposure to UV radiation was ~8%. Rezvan et al. ([194]) identified 3,255 articles and finally reviewed 68 articles with >400,000 participants from 24 countries to determine the global prevalence for eye pterygium and the related demographic, environmental, and lifestyle factors. The results of this study provided a more exact and reliable value for the effect of sunlight exposure. Exposure to sunlight was proven to be associated with

pterygium via numerous factors including time spent outdoors, outdoor versus indoor occupations, and wearing of sunglasses.

Extremely high UV-B levels over populated areas of the world have been avoided because of the implementation of the Montreal Protocol ([111]). Nonetheless, it is crucial to recognize the possible dangers to human health that could be caused by severe ozone depletion. The analyses of the "world avoided" UV levels by the Montreal Protocol and its amendments were expanded to the beneficial effects on health risks, mainly erythema and skin cancers (**FIGURE 5**). Slaper et al. ([196]) simulated the evolution of total ozone and first demonstrated that successful implementation of the Montreal Protocol would lead to an ozone minimum around the year 2000 and a peak in skin cancers of almost 10% occurring 60 yr later. Newman and McKenzie ([109]) reported that, despite the limitations in their modeled results and the expected changes in atmospheric composition due to climate change, the Montreal Protocol would have been hugely beneficial to avoid the health risks associated with high UV exposures. van Dijk et al. ([108]) integrated, for the first time, results from chemistry-climate models (CCMs) and risk models to provide a full global scenario analysis of UV-related health risks. They showed that with the countermeasures taken to save the ozone layer, two million cases (a decrease of 14%) of skin cancer would be prevented in 2030, worldwide, with the largest effects in the United States Southwest and Australia.

The importance of ODS emission reduction, the corresponding increase of stratospheric ozone and decrease of ambient UV-B, and the consequent prevention of adverse health impacts were assessed by the US Environmental Protection Agency with the updated Atmospheric and Health Effects Framework (AHEF) model ([195]). It was concluded that the Montreal Protocol (and its future amendments) prevents ~443 million cases of skin cancer, 2.3 million skin cancer deaths, and 63 million cataract cases for people in the United States born in the years 1980–2100. Although many important issues remain to be explored, such as the expansion of calculations to other geographies and the relationship with other health effects, the importance of the Montreal Protocol and the UV radiation-related human health impacts are profound.

The vast majority of the world's population can be occasionally exposed to extreme UV levels ([197]). However, the spatial and temporal variation in atmospheric constituents such as ozone, aerosol, and, more significantly, clouds affects UV-B radiation reaching the ground (see sects. 7–9). Moreover, the actual personal dose received depends on behavior (time in the sun and amount of skin exposed). For example, Kazantzidis et al. ([198]) determined the
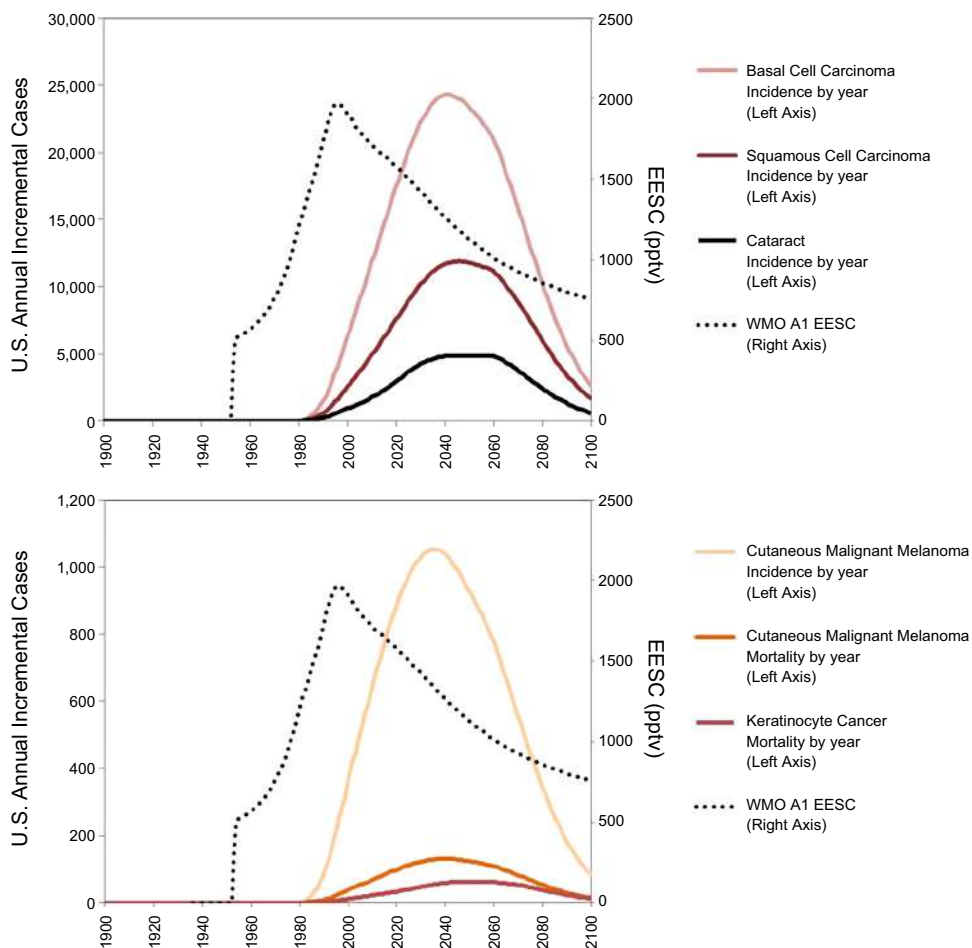
FIGURE 5. United States annual incremental health effects for full implementation of the Montreal Protocol as Amended and Adjusted [World Meteorological Organization (WMO) ozone-depleting substances (ODSs) emission scenario A1] relative to the "baseline" scenario with no ozone depletion (1980 ozone concentrations). *Top*: incidence by year for basal cell carcinoma, squamous cell carcinoma, and cataract. *Bottom*: incidence and mortality by year for malignant melanoma and mortality by year for keratinocyte cancer. EESC, equivalent effective stratospheric chlorine; pptv, parts per trillion by volume. Reproduced from Ref. 195 under CC-BY license.

ambient UV in the United Kingdom and concluded that the southern part of the country receives 1.5–2 times more UV than the north during spring, summer, and autumn. Moreover, even for the same latitude, regional variations of cloudiness result in doses at coastal sites being up to 25% higher than in inland areas. Webb et al. (199) combined those data with observation data (sun exposure, diet, and vitamin D status) and UV intervention studies performed with white Caucasian adults to quantify the sun exposure required to meet vitamin D targets year round and determine whether this can be safely achieved with short exposures [resulting in a dose < 1 standard erythemal dose (SED) (200)]. They concluded that white-skinned people in the United Kingdom (and similar latitudes) are able to meet vitamin D requirements by spending, from March to September, <10 min outdoors around noontime in season-appropriate clothing. The same methodology was followed with Fitzpatrick skin type V (brown) adults (201). Results showed that, under the same assumptions, a 25-min daily exposure could be adequate to meet vitamin D requirements at United Kingdom latitudes. O'Neill et al. (202) extended the investigation of the ambient UV-to-vitamin D relation across several European locations and illustrated the limits for cutaneous synthesis of the vitamin.

According to the results, there is not sufficient solar UV radiation to produce enough vitamin D for at least 4 mo during the winter in Iceland, Finland, Denmark, Ireland, and the United Kingdom. Moreover, the UV availability alone cannot explain a population's vitamin D status, so other factors must be considered in seeking solutions to vitamin D deficiency. Thus, although there is strong evidence that UV-B exposure is a risk factor for a range of adverse health effects, it is difficult to assess the proportion of those diseases that is ascribable to UV exposure, because of a range of complicating factors like genetics, type of skin, diet, and lifestyle.

Beneficial effects of exposure to UV radiation are not related only to the production of vitamin D in the human skin (27). Exposure to UV radiation contributes to the healing of diseases such as psoriasis, vitiligo, atopic dermatitis, and localized scleroderma as well as to suppression of the clinical symptoms of multiple sclerosis independently of vitamin D synthesis and the improvement of cardiovascular health. Through the release of endorphins, UV exposure contributes to the maintenance of good mental health. A debate relative to the potential beneficial effects of exposure to UV-B radiation for the prevention of infection and/or recovery from

SARS-CoV-2 has taken place since the emergence of the COVID-19 pandemic (203). Ambient UV-B radiation is believed to contribute toward protection from infection or serious illness through direct inactivation of the SARS-CoV-2 virus and through the formation of vitamin D or other substances such as nitric oxide produced by exposure of the skin to UV radiation that strengthen the human immune system. Although many studies report significant correlation between infection or mortality rates and UV-B radiation (e.g., Refs. 37, 204–206), the strong correlations between UV-B radiation and other environmental parameters increase the uncertainties in the determination of the extent to which it prevents infection or severe illness (203).

In general, the balance between risk and benefit of sun exposure needs to be more deeply investigated. Since there is convincing evidence that UV exposure is related to a risk factor for adverse health effects, the total UV exposure as well as the proportion that can be attributed to high or low exposure should be taken into account. For example, Petersen et al, (207) combined measures of simultaneous beneficial and adverse effects (personal UV exposure, DNA damage, and vitamin D data) in a real-life study of 1-wk sun or ski holidays. Their results indicate that UV-B exposure doses that caused and induced vitamin D synthesis also caused considerable DNA damage. Similar findings were reported for children in a similar study (208). On the contrary, Felton et al. (209) highlighted the importance of low-dose summer UV exposure: it resulted in vitamin D sufficiency in light-skinned people accompanied by low-level and nonaccumulating DNA damage. Moreover, the DNA damage was minimal and less vitamin D was produced in brown-skinned people under the same exposures.

7. FACTORS AFFECTING THE LEVELS OF UV-B RADIATION AT THE EARTH'S SURFACE

UV-B radiation that reaches the surface of the Earth exhibits periodical and nonperiodical changes. The former are mainly associated with periodicities in Earth-sun relative position, solar activity, and dynamic atmospheric phenomena. About 6.8% more solar radiation reaches the Earth's atmosphere at perihelion (January) than at aphelion (July). Furthermore, the angle between the sun and the zenith of a particular place on Earth [solar zenith angle (SZA)] changes periodically on different timescales (i.e., diurnally, annually), leading to corresponding changes in the solar radiation that reaches the surface. Solar activity also changes periodically, in cycles with different periodicities (e.g., 11-, 80-, and 210-yr cycles) (210, 211). On longer timescales, astronomical cycles with

periodicities of the order of 20,000–100,000 yr (Milankovitch cycles) slowly alter the amount of solar radiation that reaches the Earth's surface (212). Furthermore, solar radiation that reaches the atmosphere changes because of the 27-day apparent solar rotation. Dynamic atmospheric processes also induce changes in the levels of solar UV radiation that reach the Earth's surface. For example, the quasi-biennial oscillation (QBO) is related to periodic changes in total ozone (9, 213, 214) and subsequently to UV-B radiation at the Earth's surface (215). Life on Earth has adapted to changes in UV-B due to the above periodicities, which are predictable and thus can be easily modeled.

Nonperiodic changes in surface solar UV-B radiation are mainly related to changes in atmospheric composition and dynamics, and, in many cases, they cannot be easily predicted. Changes in total ozone, atmospheric aerosols, clouds, and surface albedo have been reported to play a dominant role in the variability of surface solar UV-B radiation (50, 123, 216–218). In **FIGURE 6**, projections of the past and future trends in the UV index due to changes in different atmospheric factors are presented. Despite the uncertainties in the magnitude of the changes due to each factor, it is clear that over different regions of the world the role of different atmospheric parameters was (in the past), and will be (in the future), dominant. It is also evident from **FIGURE 6** that there is a strong correlation between changes due to surface albedo and clouds (see sect. 9 for more details). Confidence in the presented results (**FIGURE 6,** *right*) is indicative for the level of understanding of how each factor affects UV-B radiation.

7.1. Total Ozone

A large fraction of the UV-B radiation at wavelengths longer than 290 nm is absorbed by stratospheric ozone. A metric that is commonly used to quantify the influence of total ozone (or any other atmospheric constituent) on UV-B radiation or UV-B effective doses is the radiation amplification factor (RAF), which is defined as the percentage of increase in UV-B (or any UV-B effective dose) that would result from a 1% decrease in the total ozone (219, 220). Hereafter, the RAF due to total ozone is referred as O_3 RAF. The O_3 RAF depends mainly on the SZA. It is also affected by the initial concentration of the considered atmospheric constituent (e.g., total ozone) and the concentration of other atmospheric constituents that are present in the atmosphere and affect UV-B (e.g., aerosols). Effective quantities that are affected more strongly by shorter UV wavelengths have higher RAFs because radiation at shorter wavelengths is affected more significantly by changes in total ozone. Bais et al. (123) estimated that at $SZA = 50°$ the O_3 RAF
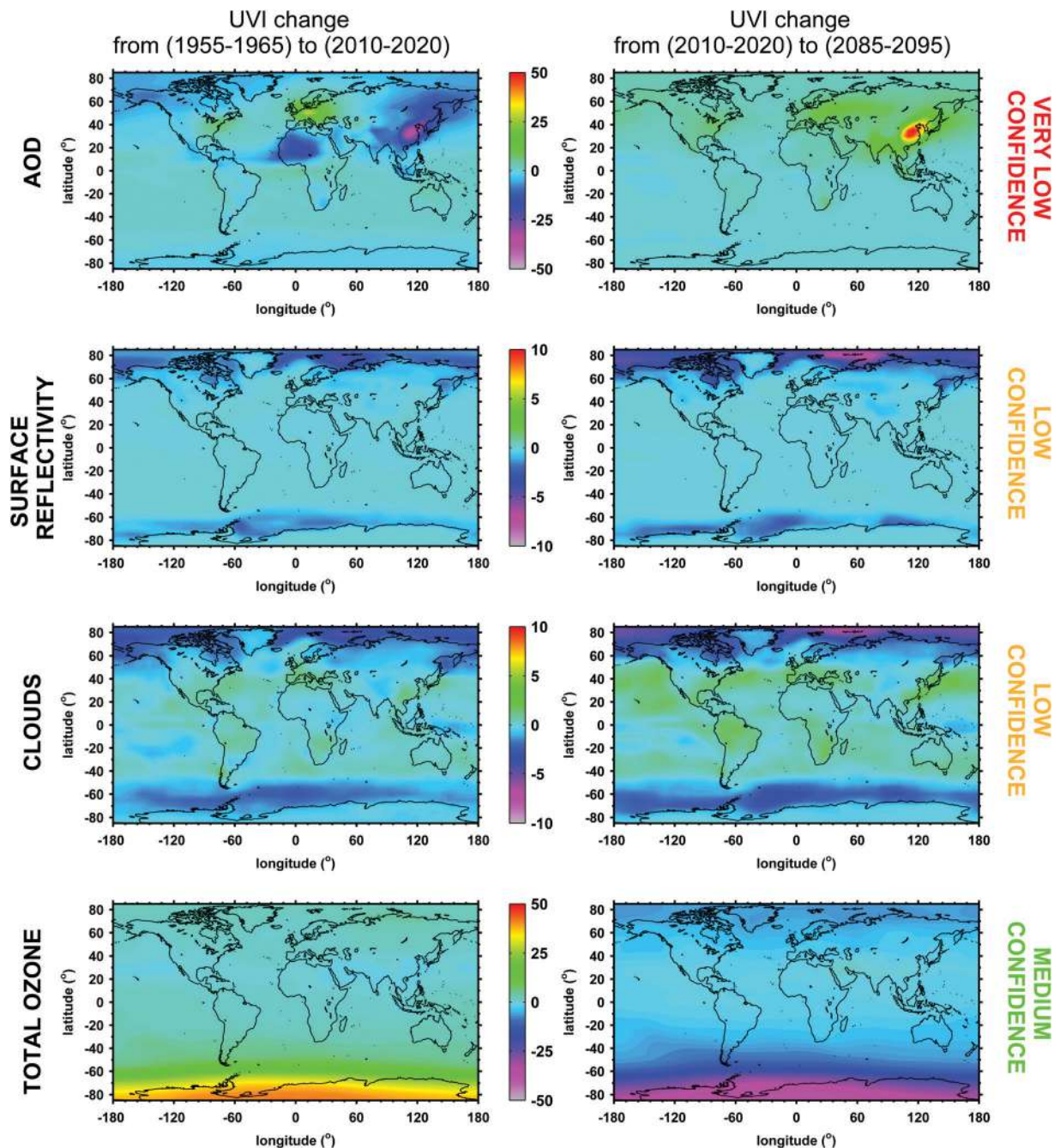
FIGURE 6. Simulated annually averaged percent changes in noontime UV index (UVI) (or erythemally weighted UV irradiance) relative to the "present" (i.e., 2010–2020), based on multimodel averages of projections of models participating in the 5th Phase of the Model Intercomparison Project (CMIP-5). *Left*: changes relative to the average 1955–1965 levels. *Right*: simulated changes expected from the present to the period 2085–2095. Effects of aerosols, surface reflectivity, cloud cover, and total ozone on UVI are shown in each row, with an assessment of the confidence in UVI projections. Note the 2 different color scales. AOD, aerosol optical depth. Reproduced from Ref. 50 with permission from *Photochemical and Photobiological Sciences*.

ranges between ∼20 and 1 for wavelengths between 295 and 315 nm, respectively. Blumthaler et al. (221) investigated the dependence of O_3 RAF on wavelength on a mountainous, practically aerosol-free, environment and estimated values from 2.4 to 1 for wavelengths from 305 to 315 nm at SZA = 30°. Similar results were derived by di Sarra et al. (222), who investigated O_3 RAF at

different wavelengths after taking into account and correcting for the effect of aerosols.

A detailed discussion of O_3 RAFs for different effective UV doses can be found in Refs. 61 and 223. For SZAs between 0° and 50° a RAF of 1.1 ± 0.1 can be used for erythemal radiation over middle latitudes. For higher SZAs and for very high total ozone the RAF generally

takes lower values (**FIGURE 7**). The results shown in **FIGURE 7** are in agreement with the results of other studies that also propose O_3 RAFs of 1.1–1.2 for moderate-ozone and low-SZA conditions under clear skies (224–226). According to the results of the latter studies, O_3 RAFs can range between 0.67 and 2 depending on the environment, the SZA, and the atmospheric conditions.

7.2. Aerosols

The effect of aerosols has been mainly studied with respect to aerosol optical depth (AOD). Kim et al. (226) estimated RAFs due to AOD changes (AOD RAFs) for erythemal radiation of 0.18–0.63 (average AOD RAF of 0.29) at Seoul, South Korea, depending on SZAs and total ozone. Palancar et al. (225) estimated lower AOD RAF values (again for erythemal radiation) of 0.06–0.27 (average 0.15) for Córdoba, Argentina. However, the effects of aerosols on UV-B also depend strongly on their other optical properties (mainly single scattering albedo and Ångstrom exponent), i.e., their chemical composition and physical characteristics (50, 218, 227), and thus vary locally and seasonally. Quantification of the effects of aerosols at UV-B wavelengths is very difficult because of the complex interactions between

aerosols, total ozone, and radiation, which in some cases are not completely understood (50, 228). Although aerosols are considered to mainly scatter and redistribute solar radiation, particular aerosol species absorb a significant amount of radiation at UV-B wavelengths (229, 230). Over polluted urban environments, aerosols have been found to absorb on average ~30% of the UV-B photons that they interact with, whereas the corresponding percentage for total solar radiation is usually below 10% (231–234). Mineral dust also absorbs UV-B radiation more effectively than radiation in the visible and infrared spectral regions (235). It is noteworthy that over sites that are strongly affected by aerosols, erythemal radiation can exceed/be below its climatological levels even under episodes of extremely high/low total ozone when aerosol load is very low/high (236, 237). Gaps in knowledge and uncertainties relative to the efficiency of aerosols in absorbing UV-B radiation, combined with the lack of systematic measurements of aerosol optical properties in UV-B, are responsible for large biases and uncertainties in the modeling of UV-B radiation over environments that are strongly affected by dust and/or urban aerosols (50). Thus, they are the main uncertainty source in clear-sky satellite products (e.g., Refs. 160, 238, 239). Absence of aerosols and other pollutants at high altitudes leads to a faster increase in UV-B radiation with altitude relative to what would be expected solely due to the exponential decrease of atmospheric density, i.e., the reduction in Rayleigh scattering (240, 241). As analytically discussed in sect. 10, when aerosols from, e.g., large volcanic eruptions enter the stratosphere they alter the equilibrium in the photochemistry at these altitudes, which can result in significant ozone decreases and subsequently in very large UV-B increases (for more information see for example Refs. 242, 243).

7.3. Clouds

Clouds also play a key role regarding both the short- and the long-term variability of UV-B radiation at the Earth's surface (50, 61, 105, 228, 244, 245). Clouds attenuate UV-B radiation less effectively relative to radiation at longer wavelengths, i.e., the cloud effect on UV radiation is 15–45% lower than the cloud effect on total solar radiation (246). It is noteworthy that UV-B radiation can increase by >20% relative to its expected clear-sky levels under broken cloud conditions due to reflections on clouds that do not cover the solar disk (247–249). Over high-surface albedo terrains the multiple reflections at the surface and at the bottom of the clouds can result in enhancement of the UV-B radiation by 60% relative to weakly reflective surfaces (6, 250, 251). Enhancement of 5–10% by clouds can also occur at mountainous sites when clouds are at a lower altitude
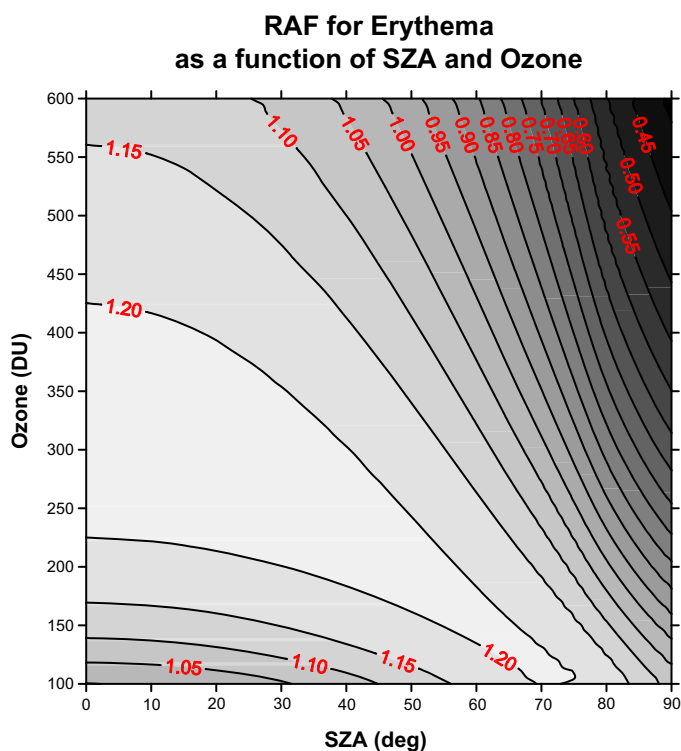

RAF for Erythema as a function of SZA and Ozone

FIGURE 7. The radiation amplification factor (RAF) for erythema, calculated as a function of solar zenith angle (SZA) and total ozone. DU, Dobson units. Reproduced from Ref. 61 with permission from *Photochemical and Photobiological Sciences*.

(252, 253). Although scattering by clouds is generally spectrally flat, complex interactions between clouds, aerosols, ozone, and UV-B radiation, in addition to the lack of systematic measurements of cloud optical properties, make the modeling of the effects of clouds a very challenging task (254–256).

7.4. Surface Reflectivity

Over most types of land surfaces and the ocean, surface reflectivity for UV-B is below 0.1. For snow- and ice-free surfaces a typical value of 0.05 is commonly used for UV-B radiation modeling. Over desert the surface albedo in UV is higher, 0.2–0.3, and over fresh snow it can exceed 0.9. The reflectivity of ice depends strongly on its characteristics and the underlying surface, and for UV it ranges from 0.2 to 0.8 (252, 257–260). Highly reflective terrains enhance surface solar UV-B radiation because of multiple scattering at the surface and in the atmosphere. Thus, the effect of surface albedo on the levels of surface UV-B radiation depends strongly on atmospheric composition (e.g., clouds or aerosols over highly reflective terrains can result in further enhancement). Although the effect of surface albedo on UV has been discussed in many studies (e.g., Refs. 6, 250, 255), modeling of UV-B radiation over highly reflective surfaces is still highly uncertain (165, 168, 261) and time-consuming simulations with three-dimensional models are needed to minimize uncertainties in the simulated surface solar UV-B radiation over complex terrains, even under cloudless skies and low-aerosol conditions (251, 262).

7.5. Sulfur Dioxide and Other Gases

Among atmospheric molecules, sulfur dioxide (SO_2) is the most effective absorber of UV-B radiation (e.g., Ref. 263). Nevertheless, absorption of the solar UV-B radiation by SO_2 is negligible compared with absorption by total ozone because the concentration of SO_2 is two orders of magnitude lower compared with total ozone for usual atmospheric conditions (e.g., Ref. 123). Volcanic eruptions and forest fires can result in elevated SO_2 levels, and thus to significant absorption of solar UV-B radiation (264–266). After volcanic eruptions, reduction of erythemal radiation by up to 50% has been reported due to increased levels of SO_2 in the atmosphere (267). SO_2 concentrations can also be high near strong anthropogenic emission sources (268, 269). Chlorine and bromine compounds and organic gases also absorb UV-B radiation, but their role is usually less significant relative to the role of other factors (71, 256). Nevertheless, erythemal radiation decreases of 10–15% have been reported in extremely polluted environments

because of combined absorption by different gases (270).

8. TRENDS IN SURFACE SOLAR UV-B RADIATION

Reliable UV-B (or UV-B effective dose) trends can be derived with high-quality ground-based measurements, which are available since the late 1980s for a few stations. Since the mid-1990s high-quality measurements are available for more stations, but again they do not provide global coverage (**FIGURE 8**). Most UV-B monitoring instruments are distributed at the Northern Hemisphere's middle and high latitudes, and very few instruments are deployed in the tropics and the Southern Hemisphere (50). Uncertainties in UV-B measurements and the large natural variability in UV-B radiation make the detection of trends a nontrivial task (271, 272).

Reconstructed UV-B data sets based on (ground or satellite based) atmospheric parameters can be used to study trends on wider spatial and/or temporal scales, but they are highly uncertain mainly because of the lack of systematic measurements of specific parameters (e.g., aerosol optical properties, surface albedo) that cannot be taken into account in the reconstruction, at least without making several assumptions (50, 61, 228). Furthermore, satellite sensors cannot accurately probe the lowest 1–2 km of the atmosphere, and thus they significantly underestimate the effects of air pollution and aerosols (228). It also must be noted that trends based on satellite products represent the average conditions within a satellite pixel and are not necessarily representative for each point of the pixel (169). Since satellite retrievals are very uncertain over highly reflective terrains [e.g., Lakkala et al. (165)], satellite-based UV-B trends are not available for Arctic and Antarctica. Because of the lack of continuous, reliable measurements of the total column of ozone, reconstruction of UV series is possible only at a very few stations before 1950. Information for aerosol optical properties is available at very few stations before 1980 (50, 228). Nevertheless, trends derived from reconstructed data sets can provide useful information on how changes in specific parameters have affected UV-B radiation on relatively wide spatial and/or temporal scales over middle latitudes and the tropics.

8.1. Trends Calculated with Reconstructed UV-B Series

Herman (273) analyzed satellite-based UV-B for 1979–2008 and detected positive trends in different UV-B
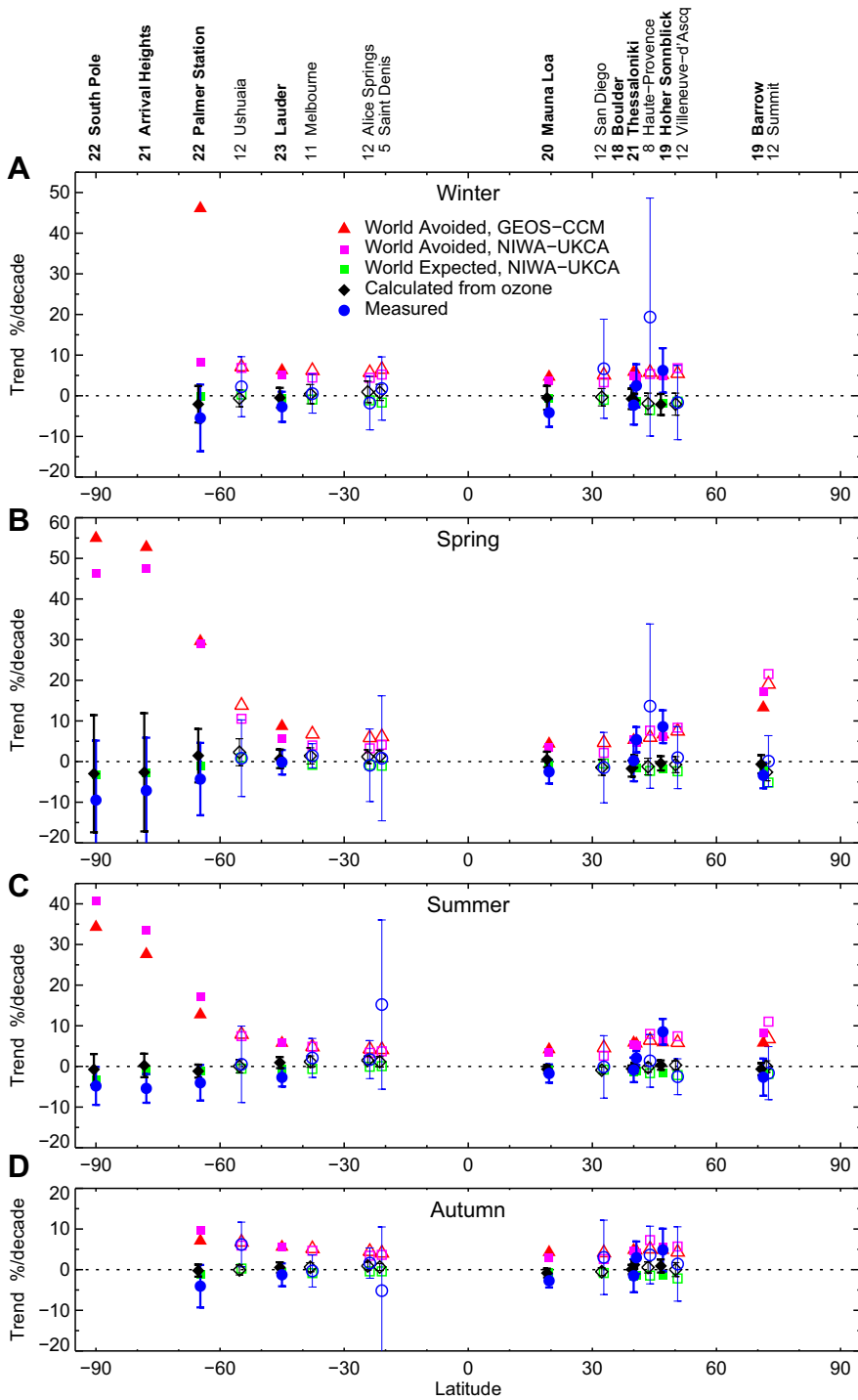
FIGURE 8. Calculated decadal trends in measured UV index since 1996 (or from the data start year if later than 1996) as a function of site latitude, compared with those calculated for clear skies from observed ozone and as calculated by two world avoided model runs and the world expected run for each season (*A–D*). Sites where the time series spans ≥20 yr are denoted by bold text and solid symbols. The number of years of data included in the trend analysis at each site is indicated beside the site name. If data from some seasons are missing, this number of used points can be less than the total number of years. Error bars shown are 2-σ uncertainties of the regression model. GEOS-CCM, Goddard Earth Observing System-Chemistry-Climate Model; NIWA-UKCA, National Institute of Water & Atmospheric Research-UK Meteorological Office Climate Assessment. Reproduced from Ref. 111 under CC-BY license.

doses over the middle latitudes of both hemispheres. The trends were stronger for the Southern Hemisphere in summer, of the order of 10–12% per decade for erythemal irradiance at latitudes 40° S to 55° S. Similar results were reported by Ialongo et al. (156), who reported positive trends of 0–5% per decade in erythemal irradiance at latitudes 55° S to 55° N for 1979–2010. The trends were again stronger over middle latitudes of the Southern Hemisphere in spring and summer. Herman et al. (274) calculated the trends in noon UV index for 191 specific cities distributed at latitudes between 60° S and 60° N, using OMI data for 2005–2018, and estimated positive average (not significant) increases of ~1% per decade at southern and northern middle latitudes and zero trends in the tropics.

Lindfors and Vuilleumier (275) reconstructed erythemal UV doses for Davos over 1926–2003, using one of the longest series of total ozone measurements globally as well as information for sunshine duration and snow depth. They found very large variability in erythemal

irradiance, especially before 1980, mainly due to the correspondingly large variability in sunshine duration. They also found a positive trend in erythemal doses in 1980–2003, which was attributed to a negative trend in total ozone. Posyniak et al. (276) reconstructed erythemal doses for Belsk, Poland for 1964–2014 and found positive trends of 5–6% per decade in 1974–1996 that were attributed to decreased attenuation by aerosols and stratospheric ozone. Čížková et al. (277) investigated the variability in erythemal radiation for Hradec Králové, Czech Republic for 1964–2013 based on reconstructed series. They estimated increases of the order of 15% per decade in erythemal UV radiation in the 1980s and the 1990s due to a decline of ~10% per decade in total ozone. den Outer et al. (278) simulated the erythemal irradiance for the period 1960–2006, using ground-based measurements from eight European stations. They found positive trends of 3–6%, which they attributed to changes in total column of ozone and cloudiness. Román et al. (279) used radiative transfer modeling and neural network techniques with inputs from nine Spanish stations and simulated daily erythemal doses for 1950–2011. They found an increase of ~6.5% in the period of study, which they attributed to changes in total ozone. More reconstructed series are available and have been analyzed for different sites around the world [e.g., Svalbard, Norway (280), China (281), Moscow, Russia (282)].

8.2. Trends Calculated with Ground-Based UV-B Measurements

Trends that have been calculated with high-quality ground-based measurements are more reliable than trends that have been calculated from reconstructed series. UV-B trends vary strongly depending on the region and the period to which they refer. A comprehensive summary of the erythemal irradiance trends in 1996–2018 for many sites around the world (where high-quality spectral UV measurements are available) is provided by McKenzie et al. (111). According to their findings, erythemal irradiance appears to be decreasing at higher latitudes of the Southern Hemisphere and has been stable in recent years at other locations. However, continued increases have been seen at some middle latitude sites in the Northern Hemisphere. The following is an effort to summarize the main findings of recent studies for different latitudinal zones.

8.2.1. Antarctica.

Continuous UV-B monitoring under the extreme climatic conditions of Antarctica is not an easy task. Nevertheless, a number of UV monitoring stations are deployed and maintained over Antarctica (e.g., Refs. 283–285) because

of the increased concern for the evolution of the ozone levels over the continent. In a recent study (286), the trends in erythemal irradiance at three Antarctic stations were investigated for 1996–2018. Negative trends were found for spring (−8% to −10%), which, however, were not statistically significant. Since the variability in erythemal irradiance is very large in spring, more measurements are necessary to verify that ozone recovery (113, 287) is depicted in the levels of erythemal irradiance. In particular stations, significant negative trends of 3–4% per decade were found for summer that were attributed to the positive trends in total ozone and/or the negative trends in surface albedo (111, 113, 287).

8.2.2. Southern Hemisphere middle latitudes.

Reliable UV-B measurements over the southern middle latitudes are available at very few stations (e.g., Refs. 167, 223, 288, 289). Trends in erythemal irradiance have been calculated for the period 1996–2018 for the sites of Lauder, New Zealand, Melbourne, Australia, and Ushuaia, Argentina (for 1996–2010 for the latter) and yielded insignificant small trends for all three sites (111).

8.2.3. Tropics.

People living or visiting tropical areas can be exposed to very high UV-B doses (290), and extremely high UV-B levels have been recorded at high-altitude tropical sites (291). Nevertheless, the number of UV-B monitoring stations over these latitudes is again very small (e.g., Refs. 288, 292). The only tropical site where high-quality spectral UV-B measurements are available for more than two decades is Mauna Loa, Hawaii, where UV has been continuously monitored since 1995 (292). Analysis of erythemal UV doses for Mauna Loa in 1996–2018 did not show any significant trend (111).

8.2.4. Northern middle latitudes.

Despite the increasing trends of upper stratospheric ozone over Northern Hemisphere middle latitudes since the mid-1990s, recent studies report increasing trends in UV-B irradiance, which in most cases are related to changes in clouds and/or aerosols (e.g., Refs. 166, 293). Over polluted urban sites, erythemal irradiance can be under/over its climatological levels even under extremely low/high total ozone, because of very high/low aerosol loads (236, 237). Over Rome, Italy decreasing trends in total ozone in 1996–2020, possibly related to decreasing lower stratospheric ozone, were found to induce positive trends in UV-B irradiance at 307.5 nm. The latter were statistically significant in April (2–5%), depending on the SZA (294). Recovery of upper stratospheric ozone

generally leads to positive total ozone trends over northern middle latitudes, which was found to induce statistically significant decreases in spring and summer erythemal doses during 1995–2015, of about −10% per decade at Chilton, United Kingdom (295, 296). Positive trends in UV radiation for different periods between 1995 and 2020 due to decreases in clouds and/or aerosols have been reported in many more studies (166, 293, 297–301).

8.2.5. The Arctic.

Whereas total ozone recovery has been reported for Antarctica (113, 114), this is not the case for the Arctic. The large year-to-year variability in total ozone over the Arctic (e.g., Refs. 302–304) currently does not allow the detection of statistically significant trends. Although studies reporting trends for 1995–2011 reported negative UV-B trends due to ozone recovery (305), analysis of extended data sets (including measurements for more years after 2011) reveals insignificant UV-B trends over the Arctic (166, 306). In the latest report of the Norwegian Institute for Air Research (NILU) (306), insignificant trends in total ozone and erythemal irradiance were estimated for different Norwegian stations covering latitudes between 60° N and 79° N for 1998–2020 (for total ozone) and 1995–2020 (for erythemal irradiance). Changing cloudiness and surface albedo conditions (related to climatic changes) have been also reported to affect the long-term UV-B changes in the Arctic. For example, Bernhard (307) calculated trends of −10% to −14% in October at Barrow, Alaska, for 1991–2011, that were mainly driven by changes in surface albedo.

9. UV-B IN THE FUTURE

Future changes in surface solar UV-B radiation will be mainly driven by changes in ozone, cloud cover, aerosols, and surface albedo (e.g., Ref. 228). Changes in the levels of the factors described in sect. 7 are not independent of each other (308), which complicates the description of the transfer of UV-B radiation in the atmosphere, and subsequently the projections of the future UV-B levels, especially in the context of global climate change (**FIGURE 9**). For example, reduced surface albedo due to sea ice melting would result in more evaporation, and thus more clouds. More clouds would, however, block solar radiation, resulting in lower surface temperatures. Increased surface temperatures would generally result in increases in aerosol load (e.g., Refs. 309, 310), which would again result in increased cloudiness. Changes in UV-B (e.g., decreased UV-B due to

stratospheric ozone recovery) that reaches the surface would also affect the levels of tropospheric ozone (e.g., less UV-B would result in less tropospheric ozone). The future levels of UV-B radiation and/or UV-B effective doses have been estimated in a few studies using radiative transfer model simulations with input parameters derived from global climate models. In this section we provide a summary of the results of these studies.

9.1. UV-B Irradiance

Simulations of the future levels of surface solar UV-B irradiance have been discussed in the study of Watanabe et al. (311), who used the radiative transfer code (mstrnX) of MIROC-ESM-CHEM (312) with inputs from the same Earth-System model. This study was the first that considered combined changes in total ozone, aerosol, clouds, and surface albedo. They performed simulations for 1960–2100 and for two different future socioeconomic scenarios representing different evolutions of the GHG concentrations: Representative Concentration Pathway (RCP) 4.5 (moderate scenario assuming peak emissions in 2040 and reduction thereafter) and RCP 8.5 (extreme scenario assuming that emissions continue to rise through the 21st century) (308). They showed that UV-B would increase (relative to 2000) over northern middle latitudes until the end of the century, by up to 10% over Europe and the United States and 20% over East Asia, because of reductions in aerosols and clouds that would overcompensate for the effect of ozone recovery. Large reductions, of 10–20%, were projected for high latitudes of both hemispheres because of the combined effects of increased total ozone increase and decreased surface reflectivity and cloudiness. In a study focused on UV-B changes over the Arctic Ocean (300), decreases of 10–30% in monthly UV-B relative to the 1950s levels were projected for northern high latitudes. According to the same study, absence of sea ice in the future would result in more than eight times higher monthly average levels of UV-B in the water over specific regions.

9.2. Erythemal Doses and Effective Doses for the Production of Vitamin D

The most commonly used parameter for assessing future evolution of the biological effects of UV radiation on human health is erythemal UV irradiance. The future evolution of clear (i.e., cloudless)-sky erythemal UV irradiance at local noon has been investigated in the studies of Hegglin and Shepherd (313) and Tourpali et al. (314). Both studies did not consider changes in aerosols, clouds, or surface albedo. Their results showed that surface erythemal irradiance would decrease globally until the end of the twenty-first century, more
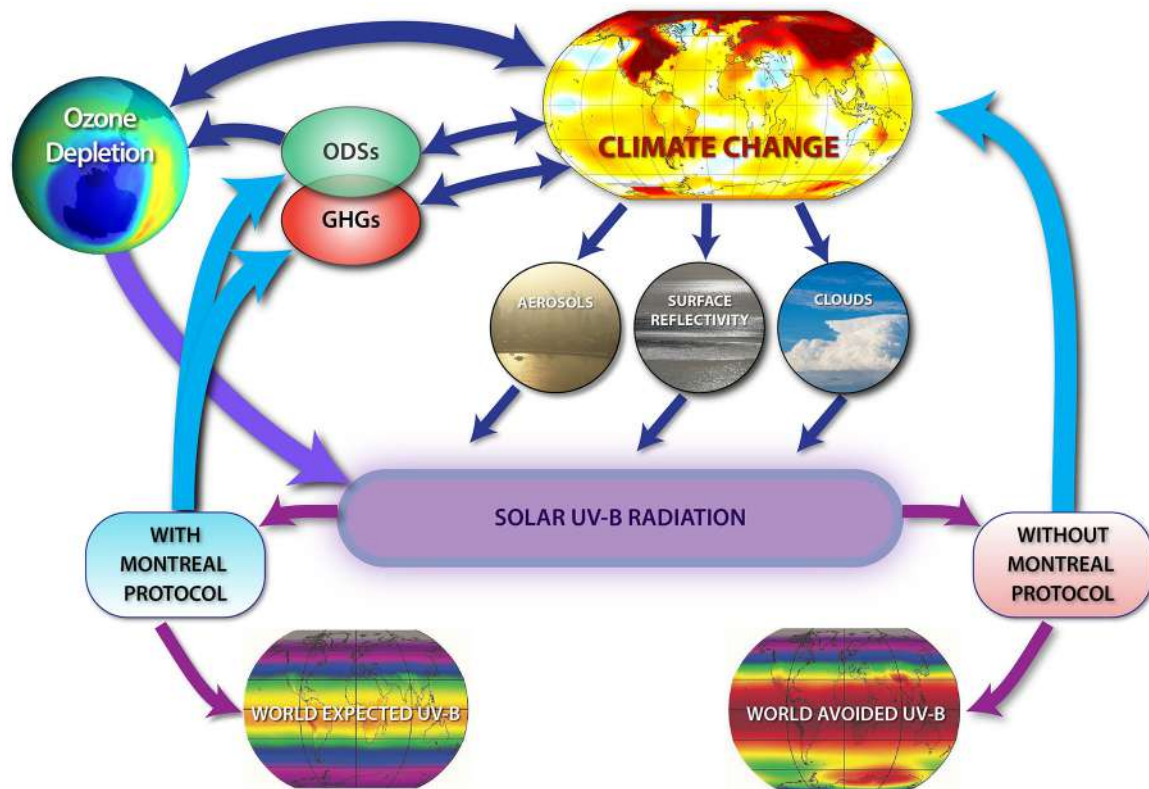
FIGURE 9. Conceptual representation of the interactive effects of changes in greenhouse gases (GHGs) and ozone-depleting substances (ODSs) on climate and solar UV-B radiation at the Earth's surface. Increases of ODSs in the atmosphere have led to stratospheric ozone depletion and the ozone "hole." Actions prompted by the Montreal Protocol have resulted in decreasing ODSs and have helped to avoid large increases of solar UV-B radiation that would otherwise have occurred by the middle of the 21st century. Continued emissions of GHGs (e.g., carbon dioxide, methane, and nitrous oxide) will change the climate and will also modify the recovery of stratospheric ozone, which is expected from decreasing concentrations of ODSs. Climate change will also affect clouds, surface reflectivity at high latitudes, where changes in sea ice and snow cover are expected, and aerosols near the Earth's surface. The combined effects of changes in ozone, aerosols, clouds, and reflectivity will determine future levels of UV-B radiation at the Earth's surface. Reproduced from Ref. 228 with permission from *Photochemical and Photobiological Sciences*.

strongly over higher latitudes, because of the recovery of total ozone.

Bais et al. (315) updated the results of Tourpali et al. (314), again using chemistry-climate model (CCM) simulations and parameterizations considering the effects of clouds. They concluded that erythemal UV irradiance would likely return to its 1980 levels by the first quarter of the twenty-first century in the northern middle and high latitudes and 20–30 yr later in the southern middle and high latitudes. After reaching the 1980 levels, it would continue to decrease toward 2100 in the Northern Hemisphere, whereas in the Southern Hemisphere it is highly uncertain whether the erythemal UV radiation would reach its 1960s levels by 2100. In the tropics, UV changes would be small and the erythemal UV radiation would remain roughly at 1980s levels or even higher by 2–3%. Nevertheless, the projections by Bais et al. (315) also did not consider changes in aerosols and surface albedo.

Another study (316) considering changes in clear-sky erythemal and vitamin D effective doses over Europe reported small reductions, of a few percent, in both

quantities from 2006 to 2100, which were attributed to ozone recovery and reduction in aerosol optical depth. Changes in erythemal and vitamin D effective doses over the Arctic were studied by Fountoulakis and Bais (317), again for RCP 4.5 and RCP 8.5. They reported large decreases, larger by ~10% for RCP 8.5, locally reaching ~30% for the noon UV index and ~50% for the noon effective UV dose for the production of vitamin D (hereafter referred as vitamin D dose) in April, which were attributed to the combined effects of changes in surface albedo, cloudiness, and total ozone.

Bais et al. (50) provided updated projections of the erythemal irradiance on a global scale taking into consideration the simulations of all available Global Climate Models (GCMs) that participated in the 5th Phase of the Model Intercomparison Project (CMIP-5) for the most significant factors affecting erythemal radiation such as cloud cover, ozone, surface reflectivity, and aerosols and for the moderate socioeconomic scenario RCP 4.5. The results showed that ozone would continue to be the dominant factor affecting the UV changes over Antarctica, whereas clouds and surface reflectivity would dominate

the changes over the Arctic. Although very uncertain, the effects of aerosols would probably dominate changes in erythemal irradiance over highly populated regions. Changes over the tropics were generally small and uncertain.

More recent estimates of future changes in erythemal irradiance were presented in a study in which changes in total ozone, surface reflectivity, and clouds according to the RCP 6.0 scenario were taken into account (228). FIGURE 10 shows the average differences (in %) in noontime UV index from the period 2010–2020 to the period 2085–2095. The projected changes are sensitive to latitude and season. Large decreases in the noontime UV index are projected at polar latitudes (>60° north and south). UV index decreases of >30% in October and >10% in January were estimated for Antarctica, which would be entirely due to the projected recovery of ozone. The picture is similar for the northern high latitudes, but with smaller decreases that in addition to total ozone are also partially attributed to changes in surface albedo. For the southern middle latitudes, the changes in the UV index are mostly negative, up to about −20%, and similar across seasons, whereas their spatial variability is large. Increases in stratospheric ozone and changes in cloudiness are major contributors of changes over these latitudes. There is a large spread in the UV index changes over the tropics, mainly

because of the large spread of the effects of aerosols, with increases that exceed 20% over regions that are currently highly affected by aerosols. Over the northern middle latitudes the UV index increases, locally by up to 40%, mainly because of decreases in aerosol optical depth. Changes in cloudiness can be very large over different regions of the world, though they are highly uncertain.

9.3. Other Biologically Effective Doses

The number of studies reporting future changes in quantities other than UV-B, erythemal irradiance, and the effective dose for the production of vitamin D are very limited. Kazantzidis et al. (318) investigated how five different UV dose rates would change in the future under cloud-free skies because of changes in total ozone on a global scale. They simulated erythemal doses (53), effective doses for DNA damage (48), effective doses for plant damage (319), effective doses for Skin Cancer Utrecht-Philadelphia-human (SCUP-h) (320), and vitamin D doses (67). Changes in aerosols were not taken into account in this study. The results for the southern polar latitudes showed that the DNA damage and vitamin D dose rates would decrease by ~62% and 53% in the 2070s relative to the mean of the period 1996–2005, whereas the erythema and SCUP-h dose rates would decrease by ~40%. The maximum reduction in all dose
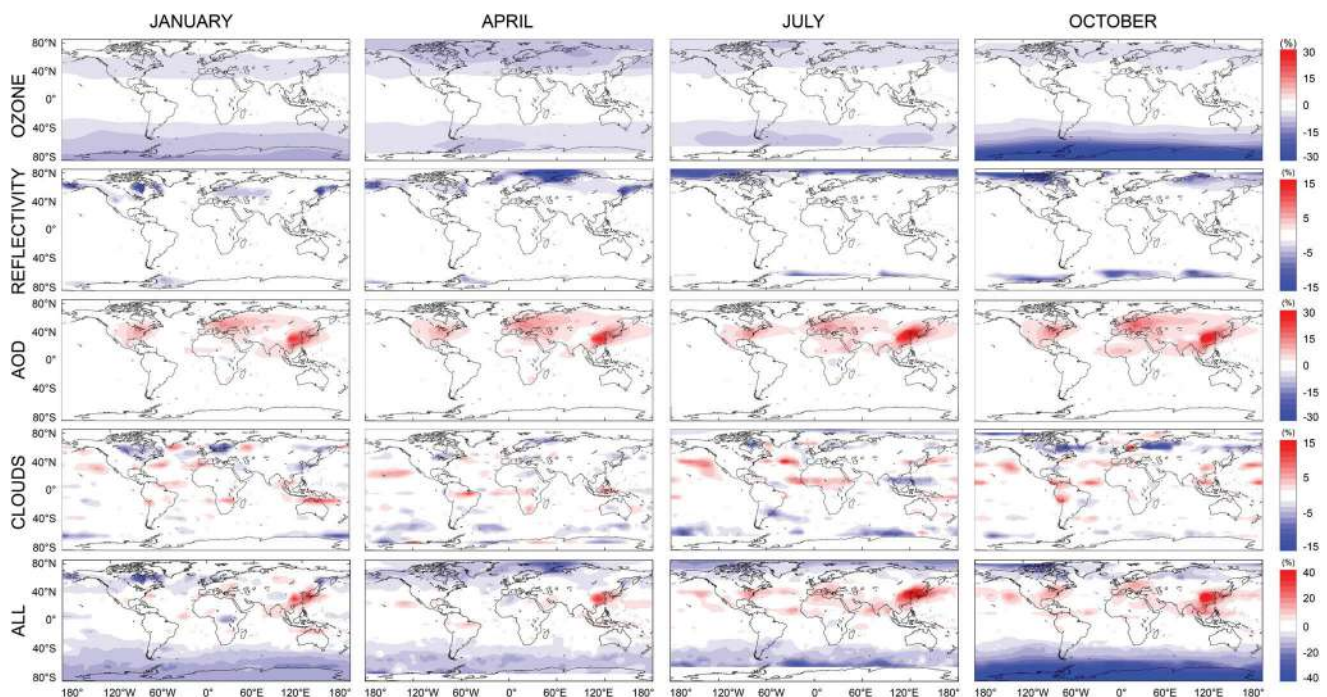

FIGURE 10. Monthly averaged percentage changes in noontime UV index (UVI) from 2010–2020 (present) to 2085–2095 (end of 21th century), as have been calculated from chemistry-climate model (CCM) simulations [Representative Concentration Pathway (RCP) 6.0 scenario] for 4 indicative months (January, April, July, and October), taking into account the effects from changes in total ozone, surface reflectivity, aerosol optical depth (AOD), and cloud cover. For each month, the individual changes in UVI due to changes in each of these parameters have been estimated while keeping the others constant. Note the different color scale for each individual parameter. Reproduced from Ref. 228 with permission from *Photochemical and Photobiological Sciences*.

rates at the Southern Hemisphere was almost double that of those at the Northern Hemisphere. At lower latitudes the estimated differences were generally smaller, decreases of <15% for middle latitudes and changes of the order of ±5% for the tropics.

In view of future increases in GHGs under RCP emissions scenario 6.0, Eleftheratos et al. (321) assessed the trends in DNA-damaging UV irradiance by using modeling, measurements and a thorough analysis, and discussion on complex atmospheric feedbacks and effects. The analysis compared trends in DNA-active UV irradiance at high latitudes with respective trends in the near-global mean. The key outcome was that DNA-active UV irradiance is expected to change differently at high latitudes than at near-global scale after around 2050. It will continue to decline at high latitudes mainly because of stratospheric ozone recovery from the reduction of ODSs (cloud cover changes are not significant), whereas it is expected to increase on a near-global scale, affected by greenhouse (GHG)-induced reductions in cloud cover and total ozone. It was also shown that decreasing surface albedo in the second half of the twenty-first century has a significant influence on the surface UV radiation at high latitudes.

FIGURE 11 shows the changes in total ozone, DNA-active UV irradiance, and cloud cover from model simulations and measurements averaged at four southern high-latitude stations (Ushuaia, Palmer, Arrival Heights, and South Pole). It was estimated that total ozone will increase by 4.2 ± 2.1% from 2050 to 2100 (P value = 0.049), DNA-active UV irradiance will decrease by 4.8 ± 2.9% (P value = 0.103), and cloud cover will decrease insignificantly by 1.1 ± 1.7% (P value = 0.548).

A similar picture with increasing ozone and decreasing DNA-harmful UV irradiance was presented for the northern high latitudes, but a completely different picture was found for the changes in the near-global mean. Here, the DNA-harmful UV radiation was shown to increase after 2050 because of decreasing cloud cover and decreasing total ozone associated with increasing GHGs. The results for the near-global mean were based on 13 station averages with contributions mainly from the middle latitudes, but a separate analysis using large-scale zonal means confirmed the findings of the station averages. The downward trend
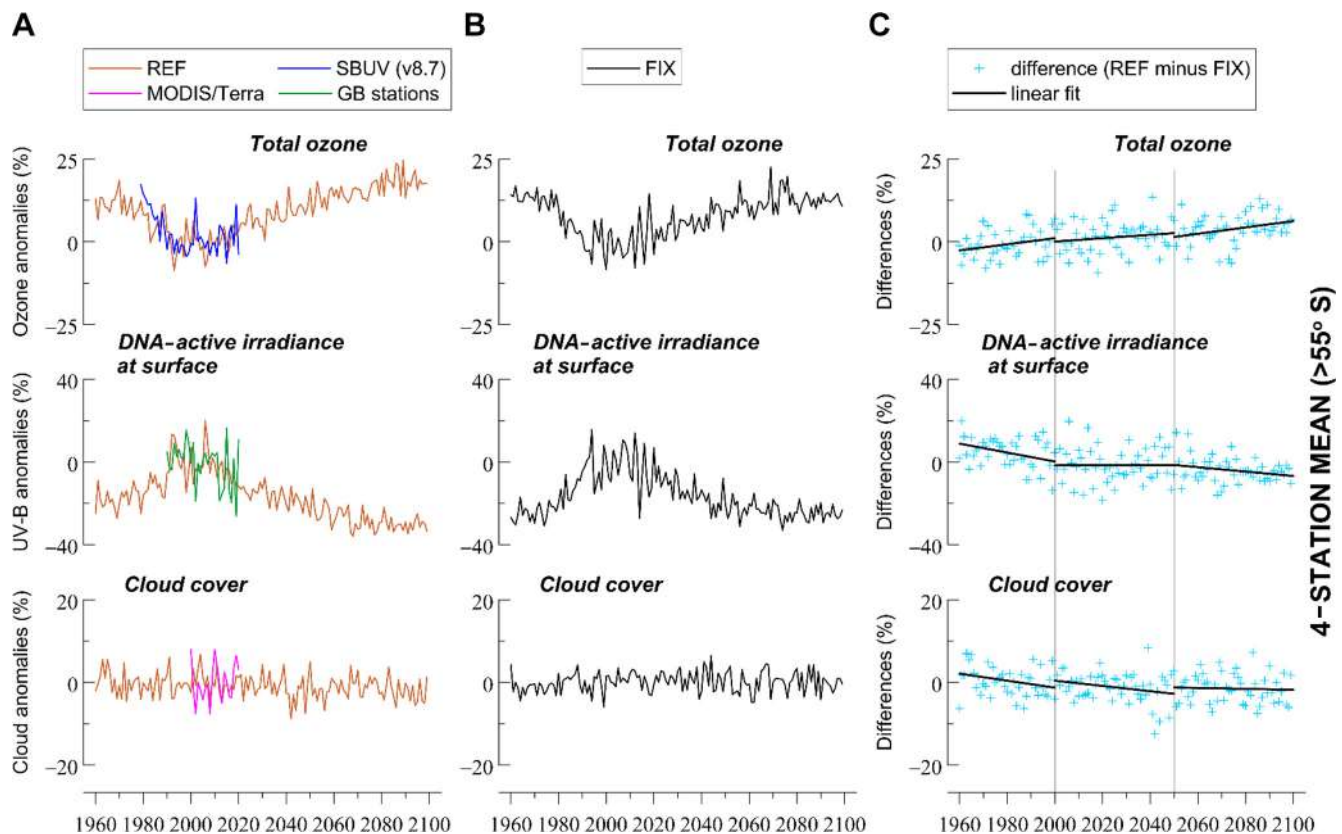

FIGURE 11. Changes in total ozone (*top*), DNA-active UV irradiance (*middle*), and cloud cover (*bottom*) averaged at 4 UV stations in the southern high latitudes (Ushuaia, Palmer, Arrival Heights, and South Pole) from chemistry-climate model (CCM) simulations for 1960–2100. *A*: simulation REF assumes increasing greenhouse gases (GHGs) [Representative Concentration Pathway (RCP) 6.0]. *B*: simulation FIX assumes constant GHGs at 1960 levels. *C* shows the difference between REF and FIX, as an indicator of the impact of increasing GHGs. *y*-Axes in *A* and *B* show averages (in %) calculated from deseasonalized monthly data. All data were deseasonalized with respect to the period 1990–2019. For the southern high latitude stations, the average refers to the average of monthly anomalies from September to March. GB, ground based; MODIS-Terra, MODerate-resolution Imaging Spectroradiometer (MODIS) Terra; SBUV, solar backscattered ultraviolet. Reproduced from Ref. 321 under CC-BY license.

in cloud cover was attributed to growing anthropogenic GHGs, which are responsible for fewer clouds in middle latitudes as has been shown by Norris et al. (322) and are capable for breaking up stratocumulus clouds into scattered clouds under greenhouse warming (323). The downward trend in total ozone was associated with decreasing ozone trends in the lower stratosphere due to increasing GHGs (324). **FIGURE 12** presents the results for the near-global mean based on results from 13 station averages.

Application of a multiple linear regression statistical model to quantify the contributions of total ozone and cloud cover to the DNA-active UV irradiance after 2050 showed that the primary parameter for determining the UV radiation change at high latitudes is total ozone, accounting for ~50% of the predicted trends in DNA-active UV irradiance. For stations averaged between 50° north and south, it was estimated that ~33% of the predicted DNA-active UV trend is caused by trends in ozone and ~41% by trends in clouds.

10. GAPS IN KNOWLEDGE AND CHALLENGES

After the agreement of the Montreal Protocol, there has been a lot of progress toward the quantification of the biological effects of solar UV-B radiation and toward understanding of the interactions between solar UV-B radiation and atmospheric constituents. Nevertheless, there are still many open questions, and, more significantly, despite the projected stratospheric ozone recovery, the evolution of surface solar UV-B irradiance in the future is far from certain.

10.1. Uncertainties in the Estimation of Biological Effects

Personal exposure depends on many parameters, and even the highest-quality ground-based UV measurements are not generally enough to quantify personal exposure. First, ground-based monitoring UV networks are constituted of instruments that are usually deployed in standard locations and are not representative of everyday personal exposure. Second, irradiance at the shortest UV-B wavelengths that reach the Earth's surface usually contributes most to human health-related effective UV-B doses. At such wavelengths, the low signal-to-noise ratio and difficulties in calibration and characterization procedures induce high uncertainties, [1-fold uncertainties of the order of 5–10% (139, 145)]. Lack of systematic calibration and maintenance may further
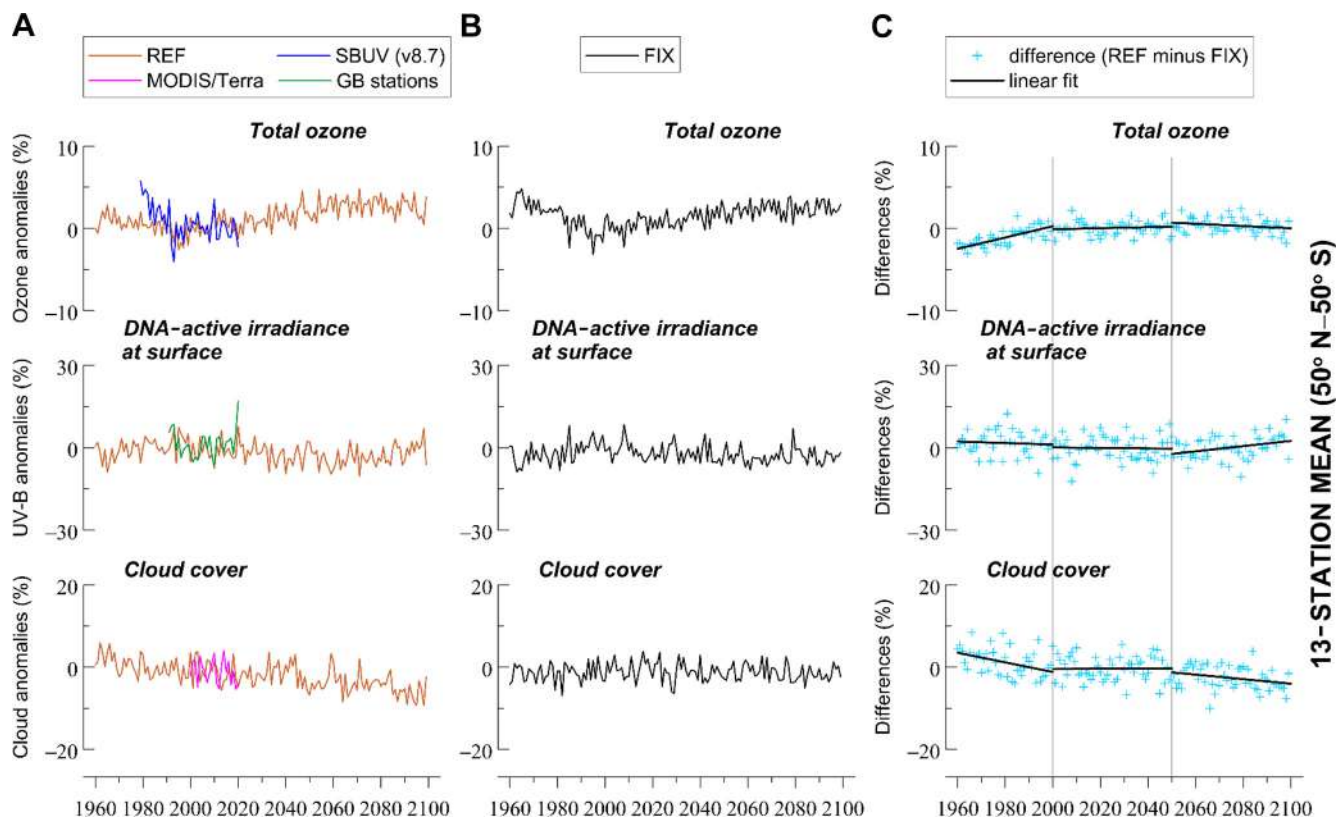

FIGURE 12. Same as **FIGURE 11** but for 13 UV stations averaged between 50° N and 50° S. *y*-Axes in *A* and *B* show annual averages (in %) calculated from deseasonalized monthly data. *C*: differences between A and B. The annual average was calculated from all monthly anomalies. GB, ground based; MODIS-Terra, MODerate-resolution Imaging Spectroradiometer (MODIS) Terra; SBUV, solar backscattered ultraviolet. Reproduced from Ref. 321 under CC-BY license.

increase the uncertainty ([135]). Furthermore, ground-based UV sensors measure the total irradiance that reaches a horizontal surface. Nevertheless, information about the directional distribution of solar radiation is necessary to model personal exposure more realistically. However, accurate and systematic measurements of the directional distribution of solar UV radiation are not widely available. Buildings, trees, or other obstacles (e.g., buildings forming man-made canyons in the cities) reduce the sky view and alter the radiation incident on a person and may reduce personal UV exposure noticeably ([325], [326]). Even at low SZAs a large fraction of the erythemal UV radiation received by a person is diffuse (i.e., photons that have been scattered in the atmosphere) and thus, even if the direct solar beam is not obscured, reductions due to obstacles can be significant.

For the same reason, protection from UV radiation cannot be achieved by only blocking the direct beam without also obstructing a large fraction of diffuse skylight. The effect of the orientation of obstructions on the exposure of a human with vertical posture to effective UV doses for vitamin D production was calculated for urban locations ([326]). In a typical mid-latitude urban area where 40% of the sky is hidden by obstructions, it was found that the exposure of a human model with winter clothing in spring depends on the orientation of the model to the sun and can vary by up to 25%. For the same conditions, it was found that obstructions from vegetation and buildings can reduce the exposure of a human with winter clothing walking around lunch time by 40%.

Exposure time is also critical for total personal exposure. Exposure to UV-B sunlight without protection throughout a summer's day at a typical mid-latitude site can result in exposure to >30 maximum erythemal doses (MEDs) ([327]). Nevertheless, personal exposure times are generally much shorter. Exposure times also vary significantly among individuals (sect. 6) as well as with location and time (e.g., Refs. [328], [329]).

Furthermore, there are still nonnegligible uncertainties in the human health-related biologically active spectra. For example, the contribution of irradiance with wavelengths beyond 400 nm to the induction of erythema in human skin has not been quantified yet. The action spectrum for the production of vitamin D in the human skin is also controversial ([63], [330]). The action spectra for various types of skin cancer in humans are also not accurately defined, and it is very difficult to obtain more accurate spectra (e.g., Ref. [331]).

The depletion of stratospheric ozone initiated the deeper investigation to understand the health risks and benefits of UV-B exposure. The consequences of overexposure to solar UV-B radiation, such as high rates of skin cancer, are expected to continue in the future because of the time lag between actual exposure and the appearance of adverse effects ([332]). Locally, lower levels of UV radiation in the future may result in receiving less of the current benefits. In contrast, longer-time exposure to smaller UV-B doses, without the risk of sunburn, contributes toward gaining more benefits of sun exposure ([203]). The biological significance of ambient UV should be carefully studied and addressed in biomedical studies for specific regions that are facing or expected to experience increasing levels of UV radiation.

10.2. Uncertainties in the Future Evolution of UV-B

Despite the successful implementation of the Montreal Protocol and the evidence for recovery of the stratospheric ozone layer, the future evolution of the levels of UV-B radiation at the Earth's surface is highly uncertain. An article dedicated to the uncertainties in the future evolution of surface solar UV-B levels has been recently published in a book for the 35th anniversary of the Montreal Protocol ([333]). Below, we provide a summary of the main uncertainty factors based on that article.

10.2.1. Future evolution of stratospheric ozone.

Although recent studies report increasing total ozone trends over Antarctica (e.g., Ref. [113]) and over some locations at northern middle latitudes since the mid-1990s (e.g., Ref. [166]), it is still not certain that ozone will return to its past levels before massive emissions of ODSs in the following decades.

10.2.1.1. DECREASING LOWER STRATOSPHERIC OZONE.
Recent studies report that although ozone at the upper stratosphere has been increasing since the mid-1990s as a result of reduced emissions of ODSs (e.g., Ref. [334]), lower stratospheric ozone is decreasing at middle and low latitudes ([335]–[339]). Lower stratospheric ozone decrease partially or fully counterbalances the increase in upper stratospheric ozone. Although the processes that drive the negative trends in lower stratospheric ozone are not completely understood yet, it is believed that they are dynamically driven ([340]). Over Rome, Italy, decreases in lower stratospheric ozone dominated over increases in upper atmospheric ozone in 1996–2020, resulting in an overall negative trend in total ozone and subsequently in statistically significant positive trends in 307.5-nm irradiance ([294]). The authors also found a significant negative correlation between the variability in total ozone and the tropopause height. This link has been already discussed in several studies (e.g., Refs. [341]–[343]). Warming of the troposphere due to increasing GHG concentrations in the future would induce elevation of the tropopause to higher altitudes (e.g., Refs.

344, 345), which would subsequently lead to reduced stratospheric ozone and increasing surface solar UV-B irradiance.

10.2.1.2. STRONG ARCTIC POLAR VORTICES. The wintertime boreal polar vortex is usually weaker and more perturbed than the polar vortex over Antarctica, and stratospheric temperatures are higher compared with temperatures in the Antarctic during austral winter (346). Every 3–5 yr dynamic conditions favor unusually strong, cold, and persistent Arctic polar vortices that result in extremely low levels of total ozone in early spring (302, 347). Such events also affect springtime ozone over middle latitudes of the Northern Hemisphere (304, 348). Low total ozone can then result in UV-B irradiance levels above climatological averages over the Arctic (349) and over the Northern Hemisphere's middle latitudes (304). The relative role of dynamic processes in determination of Arctic springtime ozone is expected to become more important (350). Changes in the frequency of such events would affect total ozone and UV-B irradiance over the Northern Hemisphere's middle and high latitudes. Low-ozone episodes that last for a few days and that are associated with synoptic weather systems can also take place over limited geographical areas at middle latitudes (351) and can affect the levels of UV-B irradiance.

10.2.1.3. ACCELERATED BREWER–DOBSON CIRCULATION. Increased levels of GHGs in the atmosphere lead to warming of the troposphere and cooling of the stratosphere. Stratospheric cooling results in accelerated ozone production. Annual mean Brewer–Dobson circulation (for more information see Ref. 352) has been accelerating since 1980, with a relative strengthening of ~1.7% per decade (353). In the future, ozone superrecovery is projected to lead to ozone levels that will exceed the pre-CFC era levels (117, 354, 355) and to less UV-B at the surface. However, there is a large spread in the projections of different models relative to the evolution of the Brewer–Dobson circulation in the future (356), which confirms that more in-depth understanding of the processes that drive these changes is necessary. Reduced CFC concentrations due to the implementation of the Montreal Protocol would counterbalance part of the Brewer–Dobson circulation enhancement due to the increase in other GHGs, especially at the Southern Hemisphere, since CFCs are among the gases that have a significant contribution to the acceleration of the Brewer–Dobson circulation (353).

10.2.1.4. NONCOMPLIANCE WITH THE MONTREAL PROTOCOL AND UNCONTROLLED ODS EMISSIONS. Trichlorofluoromethane (CFC-11) is one of the most significant ODSs that still contribute to the distraction of stratospheric ozone (CFC-11; Ref. 357). Concentrations of CFC-11 had been declining significantly since the implementation of the Montreal Protocol, but between 2012 and 2018 unexpected deceleration in the rate of decline was observed because of unreported production (358–362). If this unreported production were sustained it would delay the recovery of stratospheric ozone and would also imply unauthorized dichlorodifluoromethane (CFC-12) coproduction. Unreported CFC-11 emissions, however, have been limited drastically since 2019 (363). Nevertheless, emissions of uncontrolled short-lived anthropogenic ODSs such as methylene chloride (CH_2Cl_2) and chloroform ($CHCl_3$) have been increasing in the atmosphere in recent years, whereas further increase in the emissions of natural ODSs such as chloromethane (CH_3Cl) and bromomethane (CH_3Br) could emerge as a consequence of climate change (360), increasing the uncertainties relative to the recovery of total ozone and the evolution of surface solar UV-B radiation in the future.

10.2.1.5. VOLCANIC ERUPTIONS. Extremely low levels of total ozone can induce very high levels of surface solar UV-B irradiance over wide regions of the globe after volcanic eruptions (364, 365). This is because of the accelerated destruction of stratospheric ozone due to heterogeneous chemical reactions on surfaces of volcanically produced stratospheric aerosol particles (242, 366). For example, the Erebus volcano, located on Ross Island, Antarctica, emits gases that enter the stratosphere and contribute to the depletion of Antarctic ozone, decelerating its recovery. Tropical volcanic eruptions in preindustrial years could have been responsible for extremely low ozone levels in the tropics, the Arctic, and Antarctica and increases of 80–400% in biologically active UV irradiance over the same areas (367). About 74,000 yr ago there was a sharp decrease in human population that has been attributed to the eruption of the Toba supervolcano located in Lake Toba in Sumatra, Indonesia. It is estimated that the Toba eruption suppressed ozone production in the tropics and induced decreases of the order of 50% in columnar ozone that subsequently led to extremely high levels of surface solar UV-B radiation. The extreme UV-B radiation and the intense volcanic winter are the most likely explanations for the decrease in human population (243). Volcanic eruptions of similar magnitude in the future could be catastrophic for the ozone layer (368), causing large increases in UV-B.

10.2.1.6. SEVERE WILDFIRES. When wildfire smoke enters the stratosphere, it can also perturb stratospheric gas composition and enhance ozone destruction. Enormous amounts of biomass burning aerosols were

injected into the stratosphere during the 2019–2020 Australian wildfires. A record-breaking ozone hole over Antarctica was observed in September–November 2020 because of smoke that rose to altitudes exceeding 30 km ([369], [370]). Extremely low ozone levels resulted in 20-yr record-breaking levels of UV-B irradiance at the northern tip of the Antarctic Peninsula ([371]). Severe wildfires are projected to become more intense and more frequent in the future ([372]), with correspondingly growing impacts on global ozone and UV-B irradiance.

10.2.2. Changes in air quality and climate.

Combined changes in air quality (e.g., aerosol amount and properties, concentration of air pollutants) and climate (e.g., surface reflectivity, clouds, climate-driven changes in ozone and aerosols) have significantly affected the long-term variability in surface solar UV-B irradiance in the last three decades (sect. 8) and are also expected to play a very significant role in the future ([50], [228]). Aerosols and clouds are two of the main uncertainty factors in the simulations of global climate models, and their interactions with solar radiation, especially in the UV-B region, are not completely understood ([373]), which further increases the uncertainty in the projections of the future levels of surface solar UV-B irradiance. Although aerosols mainly scatter solar radiation, species such as soot, mineral dust, black carbon, and brown carbon absorb a significant fraction of UV-B radiation (e.g., Ref. [50]). Whereas in the case of soot and black carbon the absorption efficiency is spectrally flat, mineral dust and brown carbon absorb UV-B more effectively than radiation at longer wavelengths. Although brown carbon aerosols play a significant role over polluted urban environments, there are large gaps in knowledge relative to the spectral structure of their optical properties (e.g., Ref. [230]) and subsequently in the description of their effects in radiative transfer algorithms. Interactions between clouds and aerosols and their impact on UV-B radiation are also not completely understood yet ([50], [228]). In addition to the anthropogenic changes in air quality and climate, there are slowly varying natural modes of climatic variability that may affect UV-B in the future (e.g., Refs. [374], [375]) and have not been extensively investigated ([376]).

10.3. Challenges in UV-B Monitoring

Significant progress has been achieved in the last 40 years relative to UV-B monitoring instrumentation and techniques. Nevertheless, accurate, high-quality UV-B monitoring is performed in a limited number of monitoring sites. In the last decade most political bodies and governments considered that there was no possibility of very high UV-B levels in the future after the success of the Montreal Protocol, which, however, is not true. In addition to this misconception, economic and political instabilities in many countries led to cuts in the funding for ground-based UV-B monitoring. Many stations were closed, whereas others provide measurements of quality that is below the desired standards (e.g., Ref. [135]) because of inadequate calibration and maintenance of the sensors. Satellite-based UV-B monitoring has been improved, but it is still very uncertain, especially over areas of great interest such as polar and Alpine regions and areas that are strongly affected by tropospheric pollution and dust aerosols (e.g., Ref. [165]). Thus, maintenance and support of the existing UV-B monitoring networks and funding of UV-B related research are necessary not only for the study of time series and the accurate detection of trends but also for the continuous validation and improvement of satellite products.

11. CONCLUSIONS

This review is focused on the significance of solar UV-B radiation for humans, the main factors that control its levels on the Earth surface, and its present and future variability. The main conclusions are summarized in the as follows:

- The exposure to UV-B radiation is related to risks and benefits for human health. Globally, UV-B radiation is considered as the primary environmental risk for non-melanoma skin cancer. Other important adverse effects include melanoma skin cancer and eye cataract. Moreover, exposure to UV-B radiation is necessary for the production of vitamin D in the human skin. The balance between risk and benefit of sun exposure needs further research.
- Variability in UV-B radiation depends significantly on many factors, in addition to total ozone. Thus, over specific locations, trends in surface solar UV-B radiation in the past three decades were found to be mainly related to the variability in aerosols, clouds and surface reflectivity.
- In the future, man-made climate change is expected to play a major role in the evolution of the levels of UV-B radiation, despite the expected recovery of total ozone. Decreased cloudiness over northern mid-latitudes due to climatic changes would allow more UV-B to reach the Earth surface. Large decreases up to 30–50% (in spring and in autumn) in the monthly levels of biologically weighted UV-B doses are expected over northern high latitudes due to combined changes in surface albedo and cloudiness.

- Transient volcanic interferences can reduce total ozone amounts over large areas on Earth and result in increased global UV-B levels at the ground.
- Satellite- and ground-based monitoring of surface solar UV-B radiation should continue for accurate and on-time detection of transient elevated UV-B episodes and trends.
- Despite the positive total ozone trends recorded in the last 30 years over many regions in the world due to the implementation of the Montreal Protocol and the full recovery of stratospheric ozone expected by the mid-2060s, evolution of UV-B has additional uncertainties in view of the interference of clouds and aerosols, whose variability in space and time depends on man-made climate change.
- It is recommended that the usual precautionary measures to protect from excess exposure of humans to solar UV-B radiation should continue to apply in the decades to come.

CORRESPONDENCE

C. Zerefos (zerefos@geol.uoa.gr).

GRANTS

DISCLOSURES

No conflicts of interest, financial or otherwise, are declared by the authors.

AUTHOR CONTRIBUTIONS

C.Z. conceived and designed research; I.F., K.E., and A.K. prepared figures; I.F., K.E., and A.K. drafted manuscript; C.Z., I.F., K.E., and A.K. edited and revised manuscript; C.Z., I.F., K.E., and A.K. approved final version of manuscript.

REFERENCES

1. Tsonis AA, Zerefos CS. Aristotle's Meteōrologiká: Meteorology Then and Now (Online). Oxford, UK: Archaeopress Publishing Limited. https://books.google.gr/books?id=83eBzQEACAAJ.

2. Graedel TE, Crutzen PJ. **Atmospheric Change: An Earth System Perspective**. New York: WH Freeman, 1993.

3. Rubin MB. The history of ozone. The Schönbein period, 1839–1868. **Bull Hist Chem** 26: 40–56, 2001.

4. Fabry C, Buisson H. A study of the ultra-violet end of the Solar spectrum. **Astrophys J** 54: 297, 1921. doi:10.1086/142647.

5. Dobson GM, Harrison DN, Lindemann FA. Measurements of the amount of ozone in the earth's atmosphere and its relation to other geophysical conditions. **Proc R Soc Lond A Math Phys Sci** 110: 660–693, 1926. doi:10.1098/rspa.1926.0040.

6. Renaud A, Staehelin J, Fröhlich C, Philipona R, Heimo A. Influence of snow and clouds on erythemal UV radiation: analysis of Swiss measurements and comparison with models. **J Geophys Res Atmos** 105: 4961–4969, 2000. doi:10.1029/1999JD900160.

7. Angell JK, Korshover J. Quasi-biennial and long-term fluctuations in total ozone. **Mon Weather Rev** 101: 426–443, 1973. doi:10.1175/1520-0493(1973)101<0426:QALFIT>2.3.CO;2.

8. Angell JK, Korshover J. Comparison of stratospheric warmings following Agung and Chichon. **Mon Weather Rev** 111: 2129–2135, 1983. doi:10.1175/1520-0493(1983)111<2129:COSWFA>2.0.CO;2.

9. Angell JK, Korshover J. Quasi-biennial variations in temperature, total ozone, and tropopause height. **J Atmos Sci** 21: 479–492, 1964. doi:10.1175/1520-0469(1964)021<0479:QBVITT>2.0.CO;2.

10. Zerefos CS, Loon H, Repapis CC. Possible evidence of the Southern Oscillation in total ozone at Arosa. **Arch Meteorol Geophys Bioclimatol Ser A** 31: 231–235, 1982. doi:10.1007/BF02258034.

11. Zerefos CS, Crutzen PJ. Stratospheric thickness variations over the northern hemisphere and their possible relation to solar activity. **J Geophys Res** 80: 5041–5043, 1975. doi:10.1029/JC080i036p05041.

12. Chapman S. Discussion of memoirs. On a theory of upper-atmospheric ozone. **Q J R Meteorol Soc** 58: 11–13, 2007. doi:10.1002/qj.49705824304.

13. Brasseur GP, Solomon S (Editors). Dynamics and transport. In: *Aeronomy of the Middle Atmosphere: Chemistry and Physics of the Stratosphere and Mesosphere*. Dordrecht, The Netherlands: Springer, 2005, p. 51–149.

14. Bhartia PK, Klenk KF, Gordon D, Fleig AJ. Nimbus-7 total ozone algorithm. In: *5th Conference on Atmospheric Radiation*. Boston, MA: American Meteorological Society, 1983, p. 115–117.

15. Stolarski RS. Observation of global stratospheric ozone change. **Ber Bunsenges Phys Chem** 96: 257–263, 1992. doi:10.1002/bbpc.19920960305.

16. Solomon S, Garcia RR, Rowland FS, Wuebbles DJ. On the depletion of Antarctic ozone. **Nature** 321: 755–758, 1986. doi:10.1038/321755a0.

17. Godin-Beekmann S, Newman PA, Petropavlovskikh I. 30th anniversary of the Montreal Protocol: From the safeguard of the ozone layer to the protection of the Earth's climate. **C R Geosci** 350: 331–333, 2018. doi:10.1016/j.crte.2018.11.001.

18. Brasseur G, De Rudder A, Keating GM, Pitts MC. Response of middle atmosphere to short-term solar ultraviolet variations: 2. Theory. **J Geophys Res** 92: 903–914, 1987. doi:10.1029/JD092iD01p00903.

19. Brasseur G, Simon PC. Stratospheric chemical and thermal response to long-term variability in solar UV irradiance. **J Geophys Res** 86: 7343–7362, 1981. doi:10.1029/JC086iC08p07343.

20. Bass AM, Paur RJ. The ultraviolet cross-sections of ozone: I. The measurements. In: **Atmospheric Ozone**, edited by Zerefos CS, Ghazi A. Dordrecht, The Netherlands: Springer, 1985, p. 606–610.

21. Zerefos CS, Bais AF, Meleti C, Ziomas IC. A note on the recent increase of Solar UV-B radiation over northern middle latitudes. **Geophys Res Lett** 22: 1245–1247, 1995. doi:10.1029/95GL01187.

22. Kerr JB, McElroy CT. Evidence for large upward trends of ultraviolet-B radiation linked to ozone depletion. **Science** 262: 1032–1034, 1993. doi:10.1126/science.262.5136.1032.

23. Diffey BL. Solar ultraviolet radiation effects on biological systems. **Phys Med Biol** 36: 299–328, 1991. doi:10.1088/0031-9155/36/3/001.

24. Caldwell MM, Bornman JF, Ballaré CL, Flint SD, Kulandaivelu G. Terrestrial ecosystems, increased solar ultraviolet radiation, and interactions with other climate change factors. **Photochem Photobiol Sci** 6: 252–266, 2007. doi:10.1039/b700019g.

25. Häder DP, Kumar HD, Smith RC, Worrest RC. Effects of solar UV radiation on aquatic ecosystems and interactions with climate change. **Photochem Photobiol Sci** 6: 267–285, 2007. doi:10.1039/b700020k.

26. Gao K, Wu Y, Li G, Wu H, Villafañe VE, Helbling EW. Solar UV radiation drives CO_2 fixation in marine phytoplankton: a double-edged sword. **Plant Physiol** 144: 54–59, 2007. doi:10.1104/pp.107.098491.

27. Juzeniene A, Moan J. Beneficial effects of UV radiation other than via vitamin D production. **Dermatoendocrinol** 4: 109–117, 2012. doi:10.4161/derm.20013.

28. Holmes MG. Non-damaging and positive effects of UV radiation on higher plants. In: *Environmental UV Radiation: Impact on Ecosystems and Human Health and Predictive Models*, edited by Ghetti F, Checcucci G, Bornman JF. Dordrecht, The Netherlands: Springer, 2006, p. 159–177.

29. Moshammer H, Simic S, Haluza D. UV-radiation: from physics to impacts. **Int J Environ Res Public Health** 14: 200, 2017. doi:10.3390/ijerph14020200.

30. Jablonski NG, Chaplin G. The evolution of human skin coloration. **J Hum Evol** 39: 57–106, 2000. doi:10.1006/jhev.2000.0403.

31. Jablonski NG, Chaplin G. Human skin pigmentation as an adaptation to UV radiation. **Proc Natl Acad Sci USA** 107: 8962–8968, 2010. doi:10.1073/pnas.0914628107.

32. Juzeniene A, Brekke P, Dahlback A, Andersson-Engels S, Reichrath J, Moan K, Holick MF, Grant WB, Moan J. Solar radiation and human health. **Reports Prog Phys** 74: 066701, 2011. doi:10.1088/0034-4885/74/6/066701.

33. Hewison M. Vitamin D and immune function: an overview. **Proc Nutr Soc** 71: 50–61, 2012. doi:10.1017/S0029665111001650.

34. Berry DJ, Hesketh K, Power C, Hyppönen E. Vitamin D status has a linear association with seasonal infections and lung function in British adults. **Br J Nutr** 106: 1433–1440, 2011. doi:10.1017/S0007114511001991.

35. Almoosawi S, Palla L. Association between vitamin intake and respiratory complaints in adults from the UK National Diet and Nutrition Survey years 1–8. **BMJ Nutr Prev Health** 3: 403–408, 2020. doi:10.1136/bmjnph-2020-000150.

36. Borna M, Woloshynowych M, Schiano-Phan R, Volpi EV, Usman M. A correlational analysis of COVID-19 incidence and mortality and urban determinants of vitamin D status across the London boroughs. **Sci Rep** 12: 11741, 2022. doi:10.1038/s41598-022-15664-y.

37. Isaia G, Diémoz H, Maluta F, Fountoulakis I, Ceccon D, di Sarra A, Facta S, Fedele F, Lorenzetto G, Siani AM, Isaia G. Does solar ultraviolet radiation play a role in COVID-19 infection and deaths? An environmental ecological study in Italy. **Sci Total Environ** 757: 143757, 2021. doi:10.1016/j.scitotenv.2020.143757.

38. Sintzel MB, Rametta M, Reder AT. Vitamin D and multiple sclerosis: a comprehensive review. **Neurol Ther** 7: 59–85, 2018. doi:10.1007/s40120-017-0086-4.

39. Hewer S, Lucas R, van der Mei I, Taylor BV. Vitamin D and multiple sclerosis. **J Clin Neurosci** 20: 634–641, 2013. doi:10.1016/j.jocn.2012.10.005.

40. McGrath JJ, Eyles DW, Pedersen CB, Anderson C, Ko P, Burne TH, Norgaard-Pedersen B, Hougaard DM, Mortensen PB. Neonatal vitamin D status and risk of schizophrenia: a population-based case-control study. **Arch Gen Psychiatry** 67: 889–894, 2010. doi:10.1001/archgenpsychiatry.2010.110.

41. Allen KL, Byrne SM, Kusel MM, Hart PH, Whitehouse AJ. Maternal vitamin D levels during pregnancy and offspring eating disorder risk in adolescence. **Int J Eat Disord** 46: 669–676, 2013. doi:10.1002/eat.22147.

42. Yang L, Veierød MB, Löf M, Sandin S, Adami HO, Weiderpass E. Prospective study of UV exposure and cancer incidence among Swedish women. **Cancer Epidemiol Biomarkers Prev** 20: 1358–1367, 2011. doi:10.1158/1055-9965.EPI-11-0071.

43. Autier P, Boniol M, Pizot C, Mullie P. Vitamin D status and ill health: a systematic review. **Lancet Diabetes Endocrinol** 2: 76–89, 2014. doi:10.1016/S2213-8587(13)70165-7.

44. Shanafelt TD, Drake MT, Maurer MJ, Allmer C, Rabe KG, Slager SL, Weiner GJ, Call TG, Link BK, Zent CS, Kay NE, Hanson CA, Witzig TE, Cerhan JR. Vitamin D insufficiency and prognosis in chronic lymphocytic leukemia. **Blood** 117: 1492–1498, 2011. doi:10.1182/blood-2010-07-295683.

45. Gonzaga ER. Role of UV Light in photodamage, skin aging, and skin cancer. **Am J Clin Dermatol** 10: 19–24, 2009. doi:10.2165/0128071-200910001-00004.

46. Taylor HR, West SK, Rosenthal FS, Muñoz B, Newland HS, Abbey H, Emmett EA. Effect of ultraviolet radiation on cataract formation. **N Engl J Med** 319: 1429–1433, 1988. doi:10.1056/NEJM198812013192201.

47. Harm W. **Biological Effects of Ultraviolet Radiation**. Cambridge, UK: Cambridge University Press, 1980.

48. Setlow RB. The wavelengths in sunlight effective in producing skin cancer: a theoretical analysis. **Proc Natl Acad Sci USA** 71: 3363–3366, 1974. doi:10.1073/pnas.71.9.3363.

49. WHO. Environmental Health Criteria 160—Ultraviolet Radiation (Online). https://apps.who.int/iris/bitstream/handle/10665/39901/9241571608-eng.pdf?sequence=1.

50. Bais AF, McKenzie RL, Bernhard G, Aucamp PJ, Ilyas M, Madronich S, Tourpali K. Ozone depletion and climate change: impacts on UV radiation. **Photochem Photobiol Sci** 14: 19–52, 2015. doi:10.1039/C4PP90032D.

51. Bais AF, Lucas RM, Bornman JF, Williamson CE, Sulzberger B, Austin AT, et al. Environmental effects of ozone depletion, UV radiation and interactions with climate change: UNEP Environmental Effects Assessment Panel, update 2017. **Photochem Photobiol Sci** 17: 127–179, 2018. doi:10.1039/c7pp90043k.

52. Damian DL, Matthews YJ, Phan TA, Halliday GM. An action spectrum for ultraviolet radiation-induced immunosuppression in humans. **Br J Dermatol** 164: 657–659, 2011. doi:10.1111/j.1365-2133.2010.10161.x.

53. Mckinlay AF, Diffey BL. A reference action spectrum for ultraviolet induced erythema in human skin. **CIE J** 6: 17–22, 1987.

54. Cullen AP. Photokeratitis and other phototoxic effects on the cornea and conjunctiva. **Int J Toxicol** 21: 455–464, 2002. doi:10.1080/10915810290169882.

55. Taylor HR, West S, Muñoz B, Rosenthal FS, Bressler SB, Bressler NM. The long-term effects of visible light on the eye. **Arch Ophthalmol** 110: 99–104, 1992. doi:10.1001/archopht.1992.01080130101035.

56. Okuno T, Nakanishi-Ueda T, Ueda T, Yasuhara H, Koide R. Ultraviolet action spectrum for cell killing of primary porcine lens epithelial cells. **J Occup Health** 54: 181–186, 2012. doi:10.1539/joh.11-0215-OA.

57. Epe B. DNA damage spectra induced by photosensitization. **Photochem Photobiol Sci** 1: 98–106, 2002. doi:10.1039/c1pp05190c.

58. Jatana S, DeLouise LA. Understanding engineered nanomaterial skin interactions and the modulatory effects of ultraviolet radiation skin exposure. **Wiley Interdiscip Rev Nanomed Nanobiotechnol** 6: 61–79, 2014. doi:10.1002/wnan.1244.

59. Sallander E, Wester U, Bengtsson E, Wiegleb Edström D. Vitamin D levels after UVB radiation: effects by UVA additions in a randomized controlled trial. **Photodermatol Photoimmunol Photomed** 29: 323–329, 2013. doi:10.1111/phpp.12076.

60. Schmalwieser AW, Wallisch S, Diffey B. A library of action spectra for erythema and pigmentation. **Photochem Photobiol Sci** 11: 251–268, 2012. doi:10.1039/c1pp05271c.

61. McKenzie RL, Aucamp PJ, Bais AF, Björn LO, Ilyas M, Madronich S. Ozone depletion and climate change: impacts on UV radiation. **Photochem Photobiol Sci** 10: 182–198, 2011. doi:10.1039/c0pp90034f.

62. Caldwell MM, Camp LB, Warner CW, Flint SD. Action spectra and their key role in assessing biological consequences of solar UV-B radiation change. In: *Stratospheric Ozone Reduction, Solar Ultraviolet Radiation and Plant Life*, edited by Worrest RC, Caldwell MM. Berlin: Springer, 1986, p. 87–111.

63. Norval M, Björn LO, de Gruijl FR. Is the action spectrum for the UV-induced production of previtamin D3 in human skin correct? **Photochem Photobiol Sci** 9: 11–17, 2010. doi:10.1039/b9pp00012g.

64. Webb AR, Terenetskaya IP, Holick MF, van Dijk A, McKenzie RL, Lucas RM, Young AR, Philipsen PA, de Gruijl FR. Previtamin D action spectrum: challenging CIE towards a standard. **Light ResTechnol**: 2022. doi:10.1177/14771535221122937.

65. Bolsée D, Webb AR, Gillotay D, Dörschel B, Knuschke P, Krins A, Terenetskaya I. Laboratory facilities and recommendations for the characterization of biological ultraviolet dosimeters. **Appl Opt** 39: 2813–2822, 2000. doi:10.1364/AO.39.002813.

66. Olds WJ. *Elucidating the Links between UV Radiation and Vitamin D Synthesis: Using an In Vitro Model* (Online). Brisbane, Australia: Queensland University of Technology, 2010. https://eprints.qut.edu.au/32073/.

67. Bouillon R, Eisman J, Garabedian M, Holick M, Kleinschmidt J, Suda T, Terenetskaya I, Webb A. Action spectrum for the production of previtamin D3 in human skin. **CIE J** 174: 1–12, 2006.

68. Bernhard G, Mayer B, Seckmeyer G, Moise A. Measurements of spectral solar UV irradiance in tropical-Australia. **J Geophys Res Atmos** 102: 8719–8730, 1997. doi:10.1029/97JD00072.

69. Brühl C, Crutzen PJ. On the disproportionate role of tropospheric ozone as a filter against solar UV-B radiation. **Geophys Res Lett** 16: 703–706, 1989. doi:10.1029/GL016i007p00703.

70. Zerefos CS, Kourtidis KA, Melas D, Balis D, Zanis P, Katsaros L, Mantis HT, Repapis C, Isaksen I, Sundet J, Herman J, Bhartia PK, Calpini B. Photochemical activity and solar ultraviolet radiation (PAUR) modulation factors: an overview of the project. **J Geophys Res** 107: 1–15, 2002. doi:10.1029/2000JD000134.

71. Madronich S, Shao M, Wilson SR, Solomon KR, Longstreth JD, Tang XY. Changes in air quality and tropospheric composition due to depletion of stratospheric ozone and interactions with changing climate: implications for human and environmental health. **Photochem Photobiol Sci** 14: 149–169, 2015. doi:10.1039/C4PP90037E.

72. Erickson DJ 3rd, Sulzberger B, Zepp RG, Austin AT. Effects of stratospheric ozone depletion, solar UV radiation, and climate change on biogeochemical cycling: interactions and feedbacks. **Photochem Photobiol Sci** 14: 127–148, 2015. doi:10.1039/C4PP90036G.

73. Ritter JW. https://en.wikipedia.org/wiki/Johann_Wilhelm_Ritter. [date unknown].

74. Frercks J, Weber H, Wiesenfeldt G. Reception and discovery: the nature of Johann Wilhelm Ritter's invisible rays. **Stud Hist Philos Sci Part A** 40: 143–156, 2009. doi:10.1016/j.shpsa.2009.03.014.

75. Hockberger PE. A history of ultraviolet photobiology for humans, animals and microorganisms. **Photochem Photobiol** 76: 561–579, 2002. doi:10.1562/0031-8655(2002)076<0561:AHOUPF>2.0.CO;2.

76. Bojkov R. *International Ozone Commission: History and Activities*. Oberpfaffenhofen, Germany: IAMAS, 2012.

77. Cornu AM, Spottiswoode W. II. Sur la limite ultraviolette du spectre solaire. **Proc R Soc Lond** 29: 47–55, 1879. doi:10.1098/rspl.1879.0011.

78. Miethe A, Lehmann E. Sitzungsberichte der Königlich Preussischen Akademie der Wissenschaften zu Berlin (Online). Deutsche Akademie der Wissenschaften zu Berlin. https://www.biodiversitylibrary.org/item/92832.

79. Fabry C, Buisson H. L'absorption de l'ultra-violet par l'ozone et la limite du spectre solaire [Online]. **J Phys Theor Appl** 3: 196–206, 1913. doi:10.1051/jphystap:019130030019601.

80. Dorno C. **Physik der Sonnen und Himmelstrahlung**. Braunschweig, Germany: Nabu Press, 1919.

81. Schaeffer ER. Atmospheric attenuation of ultra-violet light. **Proc Am Acad Arts Sci** 57: 365–374, 1922. doi:10.2307/20025929.

82. Schultz LG. Weather and the ultra-violet radiations of the sun. **Nature** 90: 68–70, 1912. doi:10.1038/090068c0.

83. Finsen NR. **Phototherapy:(1) the Chemical Rays of Light and Small-Pox,(2) Light as a Stimulant,(3) the Treatment of Lupus Vulgaris by Concentrated Chemical Rays**. London: Arnold, 1901.

84. Peacock PR. The skin reaction to U-V radiation. **Br J Phys Med** 8: 173–176, 1934.

85. Clark JH. Ultraviolet radiation in relation to health. **Nutr Abstr Rev** 3: 13–21, 1933.

86. Luckiesh M, Holladay LL, Taylor AH. Reaction of untanned human skin to ultraviolet radiation. **J Opt Soc Am** 20: 423–432, 1930. doi:10.1364/JOSA.20.000423.

87. Gertrude R. Some aspects on the effect of solar radiation and other factors of the climatic environment on human beings: (Continued): C: the ultra-violet solar radiation. **S Afr Med J** 19: 308–310, 1921. doi:10.10520/AJA20785135_20882.

88. Pfeiffer NE. Anatomical Study of plants grown under glasses transmitting light of various ranges of wave lengths. **Bot Gaz** 85: 427–436, 1928. doi:10.1086/333854.

89. Popp HW, Brown F. A review of recent work on the effect of ultraviolet radiation upon seed plants. **Bull Torrey Bot Club** 60: 161–210, 1933. doi:10.2307/2480419.

90. Tonney FO, Somers PP, Marti WC. Actinic measurement of solar ultra-violet light and some correlations with the erythema dose (Online). **J Prev Med** 2: 493–511, 1928. https://eurekamag.com/research/029/866/029866898.php.

91. Clark JH. The Zinc sulphide method of measuring ultraviolet radiation and the results of three years' observations on Baltimore sunshine. **J Opt Soc Am** 21: 240–247, 1931. doi:10.1364/JOSA.21.000240.

92. Fleming WD. Solar ultraviolet radiometry. 2. Instruments and methods. **Philipp J Sci** 50: 279–300, 1933.

93. Strohecker HF. Measurements of solar ultraviolet in the Chicago Area. **Ecology** 19: 57–80, 1938. doi:10.2307/1930367.

94. Coblentz WW, Stair R. The evaluation of ultra-violet solar radiation of short wave-lengths. **Proc Natl Acad Sci USA** 22: 229–233, 1936. doi:10.1073/pnas.22.4.229.

95. Mayerson HS. Standardization of photochemical methods for the measurement of solar ultraviolet radiation. **Am J Epidemiol** 22: 106–136, 1935. doi:10.1093/oxfordjournals.aje.a118151.

96. Zerlaut GA. Solar radiation measurements: calibration and standardization efforts. In: *Advances in Solar Energy: An Annual Review of Research and Development, Volume 1*, edited by Böer KW, Duffie JA. New York: Springer, 1982, p. 19–60.

97. Chubachi S. A special ozone observation at Syowa Station, Antarctica from February 1982 to January 1983. In: **Atmospheric Ozone**, edited by Zerefos CS, Ghazi A. Dordrecht, The Netherlands: Springer, 1985, p. 285–289.

98. Farman JC, Murgatroyd RJ, Silnickas AM, Thrush BA. Ozone photochemistry in the Antarctic stratosphere in summer. **Q J R Meteorol Soc** 111: 1013–1025, 1985. doi:10.1002/qj.49711147006.

99. Stolarski R, Bojkov R, Bishop L, Zerefos C, Staehelin J, Zawodny J. Measured trends in stratospheric ozone. **Science** 256: 342–349, 1992. doi:10.1126/science.256.5055.342.

100. McConnell JC, Henderson GS, Barrie L, Bottenheim J, Niki H, Langford CH, Templeton EM. Photochemical bromine production implicated in Arctic boundary-layer ozone depletion. **Nature** 355: 150–152, 1992. doi:10.1038/355150a0.

101. Fan SM, Jacob DJ. Surface ozone depletion in Arctic spring sustained by bromine reactions on aerosols. **Nature** 359: 522–524, 1992. doi:10.1038/359522a0.

102. Solomon S. Stratospheric ozone depletion: a review of concepts and history. **Rev Geophys** 37: 275–316, 1999. doi:10.1029/1999RG900008.

103. Atkinson RJ, Matthews WA, Newman PA, Plumb RA. Evidence of the mid-latitude impact of Antarctic ozone depletion. **Nature** 340: 290–294, 1989. doi:10.1038/340290a0.

104. Zerefos C, Contopoulos G, Skalkeas G. **Twenty Years of Ozone Decline: Proceedings of the Symposium for the 20th Anniversary of the Montreal Protocol**. New York: Springer Science\& Business Media, 2009.

105. Lubin D, Jensen EH. Effects of clouds and stratospheric ozone depletion on ultraviolet radiation trends. **Nature** 377: 710–713, 1995. doi:10.1038/377710a0.

106. McKenzie R, Connor B, Bodeker G. Increased summertime UV radiation in New Zealand in response to ozone loss. **Science** 285: 1709–1711, 1999. doi:10.1126/science.285.5434.1709.

107. Madronich S. Implications of recent total atmospheric ozone measurements for biologically active ultraviolet radiation reaching the Earth's surface. **Geophys Res Lett** 19: 37–40, 1992. doi:10.1029/91GL02954.

108. van Dijk A, Slaper H, den Outer PN, Morgenstern O, Braesicke P, Pyle JA, Garny H, Stenke A, Dameris M, Kazantzidis A, Tourpali K, Bais AF. Skin cancer risks avoided by the Montreal Protocol–worldwide modeling integrating coupled climate-chemistry models with a risk model for UV. **Photochem Photobiol** 89: 234–246, 2013. doi:10.1111/j.1751-1097.2012.01223.x.

109. Newman PA, McKenzie R. UV impacts avoided by the Montreal Protocol. **Photochem Photobiol Sci** 10: 1152–1160, 2011. doi:10.1039/c0pp00387e.

110. Morgenstern O, Braesicke P, Hurwitz MM, O'Connor FM, Bushell AC, Johnson CE, Pyle JA. The world avoided by the Montreal Protocol. **Geophys Res Lett** 35: 16, 2008. doi:10.1029/2008GL034590.

111. McKenzie R, Bernhard G, Liley B, Disterhoft P, Rhodes S, Bais A, Morgenstern O, Newman P, Oman L, Brogniez C, Simic S. Success of Montreal Protocol demonstrated by comparing high-quality UV measurements with "World Avoided" calculations from two chemistry-climate models. **Sci Rep** 9: 12332, 2019. doi:10.1038/s41598-019-48625-z.

112. Hegglin MI, Fahey DW, McFarland M, Montzka SA, Nash ER. Twenty Questions and Answers About the Ozone Layer: 2014 Update—Scientific Assessment of Ozone Depletion (Online). 2014. https://wedocs.unep.org/20.500.11822/2.

113. Solomon S, Ivy DJ, Kinnison D, Mills MJ, Neely RR 3rd, Schmidt A. Emergence of healing in the Antarctic ozone layer. **Science** 353: 269–274, 2016. doi:10.1126/science.aae0061.

114. Weber M, Coldewey-Egbers M, Fioletov VE, Frith SM, Wild JD, Burrows JP, Long CS, Loyola D. Total ozone trends from 1979 to 2016 derived from five merged observational datasets – the emergence into ozone recovery. **Atmos Chem Phys** 18: 2097–2117, 2018. doi:10.5194/acp-18-2097-2018.

115. Montzka SA, Butler JH, Elkins JW, Thompson TM, Clarke AD, Lock LT. Present and future trends in the atmospheric burden of ozone-depleting halogens. **Nature** 398: 690–694, 1999. doi:10.1038/19499.

116. Chipperfield MP, Bekki S, Dhomse S, Harris NR, Hassler B, Hossaini R, Steinbrecht W, Thiéblemont R, Weber M. Detecting recovery of

the stratospheric ozone layer. **Nature** 549: 211–218, 2017. doi:10.1038/nature23681.

117. Li F, Stolarski RS, Newman PA. Stratospheric ozone in the post-CFC era. **Atmos Chem Phys** 9: 2207–2213, 2009. doi:10.5194/acp-9-2207-2009.

118. Kerr JB. The Brewer spectrophotometer. In: *UV Radiation in Global Climate Change: Measurements, Modeling and Effects on Ecosystems*, edited by Gao W, Slusser JR, Schmoldt DL. Berlin: Springer, 2010, p. 160.

119. Kerr JB, McElroy CT, Olafson RA. Measurements of ozone with the Brewer ozone spectrophotometer. In: **Quadrennial International Ozone Symposium, Boulder, CO**. 1981, p. 74–79.

120. Zerefos CS, Mantis HT, Bais AF, Ziomas IC, Zoumakis N. Solar ultraviolet absorption by sulphur dioxide in Thessaloniki, Greece. **Atmos-Ocean** 24: 292–300, 1986. doi:10.1080/07055900.1986.9649253.

121. Zerefos CS, Bais AF, Ziomas IC. Monochromatic UV-magnification factors and total ozone. In: **Atmospheric Ozone**, edited by Zerefos CS, Ghazi A. Dordrecht, The Netherlands: Springer, 1985, p. 686–690.

122. Kerr JB, McElroy CT, Wardle DI, Olafson RA, Evans WF. The automated Brewer spectrophotometer. In: **Atmospheric Ozone**, edited by Zerefos CS, Ghazi A. Dordrecht, The Netherlands: Springer, 1985, p. 396–401.

123. Bais AF, Zerefos CS, Meleti C, Ziomas IC, Tourpali K. Spectral measurements of solar UVB radiation and its relations to total ozone, SO_2, and clouds. **J Geophys Res Atmos** 98: 5199–5204, 1993. doi:10.1029/92JD02904.

124. Fioletov VE, Labow G, Evans R, Hare EW, Köhler U, McElroy CT, Miyagawa K, Redondas A, Savastiouk V, Shalamyansky AM, Staehelin J, Vanicek K, Weber M. Performance of the ground-based total ozone network assessed using satellite data. **J Geophys Res Atmos** 113, 2008. doi:10.1029/2008JD009809.

125. Rimmer JS, Redondas A, Karppinen T. EuBrewNet—a European Brewer network (COST Action ES1207), an overview. **Atmos Chem Phys** 18: 10347–10353, 2018. doi:10.5194/acp-18-10347-2018.

126. Zhao X, Fioletov V, Brohart M, Savastiouk V, Abboud I, Ogyu A, Davies J, Sit R, Lee SC, Cede A, Tiefengraber M, Müller M, Griffin D, McLinden C. The world Brewer reference triad—updated performance assessment and new double triad. **Atmos Meas Tech** 14: 2261–2283, 2021. doi:10.5194/amt-14-2261-2021.

127. Zuber R, Ribnitzky M, Tobar M, Lange K, Kutscher D, Schrempf M, Niedzwiedz A, Seckmeyer G. Global spectral irradiance array spectroradiometer validation according to WMO. **Meas Sci Technol** 29: 105801, 2018. doi:10.1088/1361-6501/aada34.

128. De Mazière M, Thompson AM, Kurylo MJ, Wild JD, Bernhard G, Blumenstock T, Braathen GO, Hannigan JW, Lambert JC, Leblanc T, McGee TJ, Nedoluha G, Petropavlovskikh I, Seckmeyer G, Simon PC, Steinbrecht W, Strahan SE. The Network for the Detection of Atmospheric Composition Change (NDACC): history, status and perspectives. **Atmos Chem Phys** 18: 4935–4964, 2018. doi:10.5194/acp-18-4935-2018.

129. Schmalwieser AW, Gröbner J, Blumthaler M, Klotz B, De Backer H, Bolsée D, et al. UV index monitoring in Europe. **Photochem Photobiol Sci** 16: 1349–1370, 2017. doi:10.1039/c7pp00178a.

130. Acosta LR, Evans WF. Design of the Mexico City UV monitoring network: UV-B measurements at ground level in the urban environment. **J Geophys Res Atmos** 105: 5017–5026, 2000. doi:10.1029/1999JD900250.

131. Blumthaler M. UV monitoring for public health. **Int J Environ Res Public Health** 15: 1723, 2018. doi:10.3390/ijerph15081723.

132. Bernhard G, Seckmeyer G. Uncertainty of measurements of spectral solar UV irradiance. **J Geophys Res Atmos** 104: 14321–14345, 1999. doi:10.1029/1999JD900180.

133. Lamy K, Portafaix T, Brogniez C, Lakkala K, Pitkänen MR, Arola A, Forestier JB, Amelie V, Toihir MA, Rakotoniaina S. UV-Indien network: ground-based measurements dedicated to the monitoring of UV radiation over the western Indian Ocean. **Earth Syst Sci Data** 13: 4275–4301, 2021. doi:10.5194/essd-13-4275-2021.

134. Nevas S, Gröbner J, Egli L, Blumthaler M. Stray light correction of array spectroradiometers for solar UV measurements. **Appl Opt** 53: 4313–4319, 2014. doi:10.1364/AO.53.004313.

135. Hülsen G, Gröbner J, Bais A, Blumthaler M, Diémoz H, Bolsée D, Diaz A, Fountoulakis I, Naranen E, Schreder J, Stefania F, Guerrero JM. Second solar ultraviolet radiometer comparison campaign UVC-II. **Metrologia** 57: 35001, 2020. doi:10.1088/1681-7575/ab74e5.

136. McKenzie RL, Kotkamp M, Seckmeyer G, Erb R, Roy CR, Gies HP, Toomey SJ. First southern hemisphere intercomparison of measured solar UV spectra. **Geophys Res Lett** 20: 2223–2226, 1993. doi:10.1029/93GL02359.

137. Seckmeyer G, Thiel S, Blumthaler M, Fabian P, Gerber S, Gugg-Helminger A, Häder DP, Huber M, Kettner C, Köhler U, Köpke P, Maier H, Schäfer J, Suppan P, Tamm E, Thomalla E. Intercomparison of spectral-UV-radiation measurement systems. **Appl Opt** 33: 7805–7812, 1994. doi:10.1364/AO.33.007805.

138. Diémoz H, Siani AM, Casale GR, di Sarra A, Serpillo B, Petkov B, Scaglione S, Bonino A, Facta S, Fedele F, Grifoni D, Verdi L, Zipoli G. First national intercomparison of solar ultraviolet radiometers in Italy. **Atmos Meas Tech** 4: 1689–1703, 2011. doi:10.5194/amt-4-1689-2011.

139. Bais AF, Gardiner BG, Slaper H, Blumthaler M, Bernhard G, McKenzie R, Webb AR, Seckmeyer G, Kjeldstad B, Koskela T, Kirsch PJ, Gröbner J, Kerr JB, Kazadzis S, Leszczynski K, Wardle D, Josefsson W, Brogniez C, Gillotay D, Reinen H, Weihs P, Svenoe T, Eriksen P, Kuik F, Redondas A. SUSPEN intercomparison of ultraviolet spectroradiometers. **J Geophys Res Atmos** 106: 12509–12525, 2001. doi:10.1029/2000JD900561.

140. Garane K, Bais AF, Kazadzis S, Kazantzidis A, Meleti C. Monitoring of UV spectral irradiance at Thessaloniki (1990–2005): data re-evaluation and quality control. **Ann Geophys** 24: 3215–3228, 2006. doi:10.5194/angeo-24-3215-2006.

141. Gröbner J, Blumthaler M, Kazadzis S, Bais A, Webb A, Schreder J, Seckmeyer G, Rembges D. Quality assurance of spectral solar UV measurements: results from 25 UV monitoring sites in Europe, 2002 to 2004. **Metrologia** 43: S66–S71, 2006. doi:10.1088/0026-1394/43/2/S14.

142. Gröbner J, Hülsen G, Wuttke S, Schrems O, De Simone S, Gallo V, Rafanelli C, Petkov B, Vitale V, Edvardsen K, Stebel K. Quality assurance of solar UV irradiance in the Arctic. **Photochem Photobiol Sci** 9: 384–391, 2010. doi:10.1039/b9pp00170k.

143. Lakkala K, Arola A, Heikkilä A, Kaurola J, Koskela T, Kyrö E, Lindfors A, Meinander O, Tanskanen A, Gröbner J, Hülsen G. Quality assurance of the Brewer spectral UV measurements in Finland. **Atmos Chem Phys** 8: 3369–3383, 2008. doi:10.5194/acp-8-3369-2008.

144. Hülsen G, Gröbner J, Nevas S, Sperfeld P, Egli L, Porrovecchio G, Smid M. Traceability of solar UV measurements using the Qasume reference spectroradiometer. **Appl Opt** 55: 7265–7275, 2016. doi:10.1364/AO.55.007265.

145. Fountoulakis I, Diémoz H, Siani AM, Hülsen G, Gröbner J. Monitoring of solar spectral ultraviolet irradiance in Aosta, Italy. **Earth Syst Sci Data** 12: 2787–2810, 2020. doi:10.5194/essd-12-2787-2020.

146. Toth G, Hillger T. A brief history of ozone-monitoring satellites and instruments (Online). **ORBIT** 91: 12–17, 2011. https://rammb.cira.colostate.edu/dev/hillger/pdf/A_brief_history_of_ozone-monitoring_satellites_and_instruments.pdf.

147. Torres O, Bhartia PK, Herman JR, Ahmad Z, Gleason J. Derivation of aerosol properties from satellite measurements of backscattered ultraviolet radiation: theoretical basis. **J Geophys Res Atmos** 103: 17099–17110, 1998. doi:10.1029/98JD00900.

148. Herman JR, Bhartia PK, Torres O, Hsu C, Seftor C, Celarier E. Global distribution of UV-absorbing aerosols from Nimbus 7/TOMS data. **J Geophys Res Atmos** 102: 16911–16922, 1997. doi:10.1029/96JD03680.

149. Herman JR, Hudson R, McPeters R, Stolarski R, Ahmad Z, Gu XY, Taylor S, Wellemeyer C. A new self-calibration method applied to TOMS and SBUV backscattered ultraviolet data to determine long-term global ozone change. **J Geophys Res Atmos** 96: 7531–7545, 1991. doi:10.1029/90JD02662.

150. Stowe LL, Wellemeyer CG, Yeh HY, Eck TF; The Nimbus-7 CLOUD DATA PROCecessing TEAM. Nimbus-7 global cloud climatology. part I: algorithms and validation. **J Clim** 1: 445–470, 1988. doi:10.1175/1520-0442(1988)001<0445:NGCCPI>2.0.CO;2.

151. Vuilleumier L, Harris T, Nenes A, Backes C, Vernez D. Developing a UV climatology for public health purposes using satellite data. **Environ Int** 146: 106177, 2021. doi:10.1016/j.envint.2020.106177.

152. Vitt R, Laschewski G, Bais AF, Diémoz H, Fountoulakis I, Siani AM, Matzarakis A. UV-index climatology for Europe based on satellite data. **Atmosphere** 11: 727, 2020. doi:10.3390/atmos11070727.

153. Zempila MM, van Geffen JH, Taylor M, Fountoulakis I, Koukouli ME, van Weele M, van der A RJ, Bais A, Meleti C, Balis D. TEMIS UV product validation using NILU-UV ground-based measurements in Thessaloniki, Greece. **Atmos Chem Phys** 17: 7157–7174, 2017. doi:10.5194/acp-17-7157-2017.

154. Tanskanen A, Krotkov NA, Herman JR, Arola A. Surface ultraviolet irradiance from OMI. **IEEE Trans Geosci Remote Sens** 44: 1267–1271, 2006. doi:10.1109/TGRS.2005.862203.

155. Lindfors AV, Kujanpää J, Kalakoski N, Heikkilä A, Lakkala K, Mielonen T, Sneep M, Krotkov NA, Arola A, Tamminen J. The TROPOMI surface UV algorithm. **Atmos Meas Tech** 11: 997–1008, 2018. doi:10.5194/amt-11-997-2018.

156. Ialongo I, Arola A, Kujanpää J, Tamminen J. Use of satellite erythemal UV products in analysing the global UV changes. **Atmos Chem Phys** 11: 9649–9658, 2011. doi:10.5194/acp-11-9649-2011.

157. Wang P, Li Z, Cihlar J, Wardle DI, Kerr J. Validation of an UV inversion algorithm using satellite and surface measurements. **J Geophys Res Atmos** 105: 5037–5048, 2000. doi:10.1029/1999JD900403.

158. Peeters P, Müller JF, Simon PC, Gillotay D, Celarier EA, Herman JR. Monitoring surface UV-B irradiance from space using GOME; comparisons with ground-based measurements. **Adv Space Res** 26: 1941–1947, 2000. doi:10.1016/S0273-1177(00)00177-0.

159. Menkhaus A, Weber M, Haite C, Burrows JP, Feister U. Surface UV modelling and validation using GOME data. In: *Proceedings of European Symposium on Atmospheric Measurements from Space*. Noordwijk, The Netherlands: European Symposium on Atmospheric Measurements from Space, 1999, p. 325–332.

160. Arola A, Kazadzis S, Krotkov N, Bais A, Gröbner J, Herman JR. Assessment of TOMS UV bias due to absorbing aerosols. **J Geophys Res Atmos** 110, 2005. doi:10.1029/2005JD005913.

161. Abalos M, Calvo N, Benito-Barca S, Garny H, Hardiman SC, Lin P, Andrews MB, Butchart N, Garcia R, Orbe C, Saint-Martin D, Watanabe S, Yoshida K. The Brewer–Dobson circulation in CMIP6. **Atmos Chem Phys** 21: 13571–13591, 2021. doi:10.5194/acp-21-13571-2021.

162. Zempila MM, Koukouli ME, Bais A, Fountoulakis I, Arola A, Kouremeti N, Balis D. OMI/Aura UV product validation using NILU-UV ground-based measurements in Thessaloniki, Greece. **Atmos Environ** 140: 283–297, 2016. doi:10.1016/j.atmosenv.2016.06.009.

163. Zempila MM, Fountoulakis I, Taylor M, Kazadzis S, Arola A, Koukouli ME, Bais A, Meleti C, Balis D. Validation of OMI erythemal doses with multi-sensor ground-based measurements in Thessaloniki, Greece. **Atmos Environ** 183: 106–121, 2018. doi:10.1016/j.atmosenv.2018.04.012.

164. Wagner JE, Angelini F, Arola A, Blumthaler M, Fitzka M, Gobbi G, Kift R, Kreuter A, Rieder HE, Simic S, Webb A, Weihs P. Comparison of surface UV irradiance in mountainous regions derived from satellite observations and model calculations with ground-based measurements. **Meteorol Z** 19: 481–490, 2010. doi:10.1127/0941-2948/2010/0347.

165. Lakkala K, Kujanpää J, Brogniez C, Henriot N, Arola A, Aun M, et al. Validation of the TROPOspheric Monitoring Instrument (TROPOMI) surface UV radiation product. **Atmos Meas Tech** 13: 6999–7024, 2020. doi:10.5194/amt-13-6999-2020.

166. Fountoulakis I, Diémoz H, Siani AM, Laschewski G, Filippa G, Arola A, Bais AF, De Backer H, Lakkala K, Webb AR, De Bock V, Karppinen T, Garane K, Kapsomenakis J, Koukouli ME, Zerefos CS. Solar UV irradiance in a changing climate: trends in Europe and the significance of spectral monitoring in Italy. **Environments** 7: 1, 2020. doi:10.3390/environments7010001.

167. Cadet JM, Bencherif H, Portafaix T, Lamy K, Ncongwane K, Coetzee GJ, Wright CY. Comparison of ground-based and satellite-derived solar UV index levels at six South African sites. **Int J Environ Res Public Health** 14: 1384, 2017. doi:10.3390/ijerph14111384.

168. Bernhard G, Arola A, Dahlback A, Fioletov V, Heikkilä A, Johnsen B, Koskela T, Lakkala K, Svendby T, Tamminen J. Comparison of OMI UV observations with ground-based measurements at high northern latitudes. **Atmos Chem Phys** 15: 7391–7412, 2015. doi:10.5194/acp-15-7391-2015.

169. Kazadzis S, Bais A, Balis D, Kouremeti N, Zempila M, Arola A, Giannakaki E, Amiridis V, Kazantzidis A. Spatial and temporal UV irradiance and aerosol variability within the area of an OMI satellite pixel. **Atmos Chem Phys** 9: 4593–4601, 2009. doi:10.5194/acp-9-4593-2009.

170. Kujanpää J, Kalakoski N. Operational surface UV radiation product from GOME-2 and AVHRR/3 data. **Atmos Meas Tech** 8: 4399–4414, 2015. doi:10.5194/amt-8-4399-2015.

171. Wald L. Elements on the computation of UV maps in the Eurosun database (Online). https://hal-mines-paristech.archives-ouvertes.fr/hal-00788420. [2022 Sep 12].

172. Kosmopoulos PG, Kazadzis S, Schmalwieser AW, Raptis PI, Papachristopoulou K, Fountoulakis I, et al. Real-time UV index retrieval in Europe using Earth observation-based techniques: system

description and quality assessment. **Atmos Meas Tech** 14: 5657–5699, 2021. doi:10.5194/amt-14-5657-2021.

173. Santmyire BR, Feldman SR, Fleischer AB Jr. Lifestyle high-risk behaviors and demographics may predict the level of participation in sun-protection behaviors and skin cancer primary prevention in the United States: results of the 1998 National Health Interview Survey. **Cancer** 92: 1315–1324, 2001. doi:10.1002/1097-0142(20010901)92:5<1315::AID-CNCR1453>3.0.CO;2-I.

174. Randle HW. Suntanning: differences in perceptions throughout history. **Mayo Clin Proc** 72: 461–466, 1997. doi:10.4065/72.5.461.

175. Rigel DS, Carucci JA. Malignant melanoma: prevention, early detection, and treatment in the 21st century. **CA Cancer J Clin** 50: 215–236, 2000. doi:10.3322/canjclin.50.4.215.

176. Glass AG, Hoover RN. The emerging epidemic of melanoma and squamous cell skin cancer. **JAMA** 262: 2097–2100, 1989. doi:10.1001/jama.1989.03430150065027.

177. Albert MR, Ostheimer KG. The evolution of current medical and popular attitudes toward ultraviolet light exposure: part 2. **J Am Acad Dermatol** 48: 909–918, 2003. doi:10.1067/mjd.2003.272.

178. Albert MR, Ostheimer KG. The evolution of current medical and popular attitudes toward ultraviolet light exposure: part 3. **J Am Acad Dermatol** 49: 1096–1106, 2003. doi:10.1016/S0190-9622(03)00021-5.

179. Albert MR, Ostheimer KG. The evolution of current medical and popular attitudes toward ultraviolet light exposure: part 1. **J Am Acad Dermatol** 47: 930–937, 2002. doi:10.1067/mjd.2002.127254.

180. Pfeifer GP, Besaratinia A. UV wavelength-dependent DNA damage and human non-melanoma and melanoma skin cancer. **Photochem Photobiol Sci** 11: 90–97, 2012. doi:10.1039/c1pp05144j.

181. Cives M, Mannavola F, Lospalluti L, Sergi MC, Cazzato G, Filoni E, Cavallo F, Giudice G, Stucci LS, Porta C, Tucci M. Non-melanoma skin cancers: biological and clinical features. **Int J Mol Sci** 21: 5394, 2020. doi:10.3390/ijms21155394.

182. Brash DE, Rudolph JA, Simon JA, Lin A, McKenna GJ, Baden HP, Halperin AJ, Pontén J. A role for sunlight in skin cancer: UV-induced p53 mutations in squamous cell carcinoma. **Proc Natl Acad Sci USA** 88: 10124–10128, 1991. doi:10.1073/pnas.88.22.10124.

183. McDaniel B, Badri T, Steele RB. Basal cell carcinoma (Online). Treasure Island, FL: StatPearls Publishing, 2018. http://europepmc.org/abstract/MED/29494046.

184. Halder RM, Bridgeman-Shah S. Skin cancer in African Americans. **Cancer** 75: 667–673, 1995. doi:10.1002/1097-0142(19950115)75:2+<667::AID-CNCR2820751409>3.0.CO;2-I.

185. Kricker A, Armstrong BK, McMichael AJ. Skin cancer and ultraviolet. **Nature** 368: 594, 1994. doi:10.1038/368594b0.

186. Gandini S, Sera F, Cattaruzza MS, Pasquini P, Picconi O, Boyle P, Melchi CF. Meta-analysis of risk factors for cutaneous melanoma: II. Sun exposure. **Eur J Cancer** 41: 45–60, 2005. doi:10.1016/j.ejca.2004.10.016.

187. Arnold M, de Vries E, Whiteman DC, Jemal A, Bray F, Parkin DM, Soerjomataram I. Global burden of cutaneous melanoma attributable to ultraviolet radiation in 2012. **Int J Cancer** 143: 1305–1314, 2018. doi:10.1002/ijc.31527.

188. Potrony M, Badenas C, Aguilera P, Puig-Butille JA, Carrera C, Malvehy J, Puig S. Update in genetic susceptibility in melanoma.

Ann Transl Med 3: 210, 2015. doi:10.3978/j.issn.2305-5839.2015.08.11.

189. Pasquale LR, Jiwani AZ, Zehavi-Dorin T, Majd A, Rhee DJ, Chen T, Turalba A, Shen L, Brauner S, Grosskreutz C, Gardiner M, Chen S, Borboli-Gerogiannis S, Greenstein SH, Chang K, Ritch R, Loomis S, Kang JH, Wiggs JL, Levkovitch-Verbin H. Solar exposure and residential geographic history in relation to exfoliation syndrome in the United States and Israel. **JAMA Ophthalmol** 132: 1439–1445, 2014. doi:10.1001/jamaophthalmol.2014.3326.

190. Bourne RR, Stevens GA, White RA, Smith JL, Flaxman SR, Price H, Jonas JB, Keeffe J, Leasher J, Naidoo K, Pesudovs K, Resnikoff S, Taylor HR; Vision Loss Expert Group. Causes of vision loss worldwide, 1990–2010: a systematic analysis. **Lancet Glob Health** 1: e339–e349, 2013. doi:10.1016/S2214-109X(13)70113-X.

191. Vashist P, Tandon R, Murthy GV, Barua CK, Deka D, Singh S, Gupta V, Gupta N, Wadhwani M, Singh R, Vishwanath K; ICMR-EYE SEE Study Group. Association of cataract and sun exposure in geographically diverse populations of India: the CASE study. First Report of the ICMR-EYE SEE Study Group. **PLoS One** 15: e0227868, 2020. doi:10.1371/journal.pone.0227868.

192. Mohan M, Sperduto RD, Angra SK, Milton RC, Mathur RL, Underwood BA, Jaffery N, Pandya CB, Chhabra VK, Vajpayee RB. India-US case-control study of age-related cataracts. India-US Case-Control Study Group. **Arch Ophthalmol** 107: 670–676, 1989. doi:10.1001/archopht.1989.01070010688028.

193. Hashemi H, Pakzad R, Yekta A, Aghamirsalim M, Pakbin M, Ramin S, Khabazkhoob M. Global and regional prevalence of age-related cataract: a comprehensive systematic review and meta-analysis. **Eye (Lond)** 34: 1357–1370, 2020. doi:10.1038/s41433-020-0806-3.

194. Rezvan F, Khabazkhoob M, Hooshmand E, Yekta A, Saatchi M, Hashemi H. Prevalence and risk factors of pterygium: a systematic review and meta-analysis. **Surv Ophthalmol** 63: 719–735, 2018. doi:10.1016/j.survophthal.2018.03.001.

195. US EPA. Updating the atmospheric and health effects framework model: stratospheric ozone protection and human health benefits (Online). https://www.epa.gov/sites/default/files/2020-04/documents/2020_ahef_report.pdf.

196. Slaper H, Velders GJ, Daniel JS, de Gruijl FR, van der Leun JC. Estimates of ozone depletion and skin cancer incidence to examine the Vienna Convention achievements. **Nature** 384: 256–258, 1996. doi:10.1038/384256a0.

197. Liley J, McKenzie R. Where on Earth has the highest UV (Online)? https://niwa.co.nz/sites/niwa.co.nz/files/import/attachments/Liley_2.pdf Last accesses: 23//03/2023 [23 Mar 2023].

198. Kazantzidis A, Smedley A, Kift R, Rimmer J, Berry JL, Rhodes LE, Webb AR. A modeling approach to determine how much UV radiation is available across the UK and Ireland for health risk and benefit studies. **Photochem Photobiol Sci** 14: 1073–1081, 2015. doi:10.1039/c5pp00008d.

199. Webb AR, Kazantzidis A, Kift RC, Farrar MD, Wilkinson J, Rhodes LE. Meeting vitamin D requirements in white caucasians at UK latitudes: providing a choice. **Nutrients** 10: 497, 2018. doi:10.3390/nu10040497.

200. Diffey BL, Jansén CT, Urbach F, Wulf HC. The standard erythema dose: a new photobiological concept. **Photodermatol Photoimmunol Photomed** 13: 64–66, 1997. doi:10.1111/j.1600-0781.1997.tb00110.x.

201. Webb AR, Kazantzidis A, Kift RC, Farrar MD, Wilkinson J, Rhodes LE. Colour counts: sunlight and skin type as drivers of vitamin D deficiency at UK latitudes. **Nutrients** 10: 457, 2018. doi:10.3390/nu10040457.

202. O'Neill CM, Kazantzidis A, Ryan MJ, Barber N, Sempos CT, Durazo-Arvizu RA, Jorde R, Grimnes G, Eiriksdottir G, Gudnason V, Cotch MF, Kiely M, Webb AR, Cashman KD. Seasonal changes in vitamin D-effective UVB availability in Europe and associations with population serum 25-hydroxyvitamin D. **Nutrients** 8: 533, 2016. doi:10.3390/nu8090533.

203. Barnes PW, Robson TM, Neale PJ, Williamson CE, Zepp RG, Madronich S, et al. Environmental effects of stratospheric ozone depletion, UV radiation, and interactions with climate change: UNEP Environmental Effects Assessment Panel, Update 2021. **Photochem Photobiol Sci** 21: 275–301, 2022. doi:10.1007/s43630-022-00176-5.

204. Moozhipurath RK, Kraft L, Skiera B. Evidence of protective role of ultraviolet-B (UVB) radiation in reducing COVID-19 deaths. **Sci Rep** 10: 17705, 2020. doi:10.1038/s41598-020-74825-z.

205. Merow C, Urban MC. Seasonality and uncertainty in global COVID-19 growth rates. **Proc Natl Acad Sci USA** 117: 27456–27464, 2020. doi:10.1073/pnas.2008590117.

206. Ma Y, Pei S, Shaman J, Dubrow R, Chen K. Role of meteorological factors in the transmission of SARS-CoV-2 in the United States. **Nat Commun** 12: 3602, 2021. doi:10.1038/s41467-021-23866-7.

207. Petersen B, Wulf HC, Triguero-Mas M, Philipsen PA, Thieden E, Olsen P, Heydenreich J, Dadvand P, Basagaña X, Liljendahl TS, Harrison GI, Segerbäck D, Schmalwieser AW, Young AR, Nieuwenhuijsen MJ. Sun and ski holidays improve vitamin D status, but are associated with high levels of DNA damage. **J Invest Dermatol** 134: 2806–2813, 2014. doi:10.1038/jid.2014.223.

208. Narbutt J, Philipsen PA, Lesiak A, Sandberg Liljendahl T, Segerbäck D, Heydenreich J, Chlebna-Sokol D, Olsen P, Harrison GI, Pearson A, Baczynska K, Rogowski-Tylman M, Wulf HC, Young AR. Children sustain high levels of skin DNA photodamage, with a modest increase of serum 25-hydroxyvitamin D3, after a summer holiday in Northern Europe. **Br J Dermatol** 179: 940–950, 2018. doi:10.1111/bjd.16668.

209. Felton SJ, Cooke MS, Kift R, Berry JL, Webb AR, Lam PM, de Gruijl FR, Vail A, Rhodes LE. Concurrent beneficial (vitamin D production) and hazardous (cutaneous DNA damage) impact of repeated low-level summer sunlight exposures. **Br J Dermatol** 175: 1320–1328, 2016. doi:10.1111/bjd.14863.

210. Eddy JA. The Maunder minimum. **Science** 192: 1189–1202, 1976. doi:10.1126/science.192.4245.1189.

211. Courtillot V, Lopes F, Le Mouël JL. On the prediction of solar cycles. **Sol Phys** 296: 21, 2021. doi:10.1007/s11207-020-01760-7.

212. Bennett KD. Milankovitch cycles and their effects on species in ecological and evolutionary time. **Paleobiology** 16: 11–21, 1990. doi:10.1017/S0094837300009684.

213. Lindzen RS, Holton JR. A theory of the quasi-biennial oscillation. **J Atmos Sci** 25: 1095–1107, 1968. doi:10.1175/1520-0469(1968)025<1095:ATOTQB>2.0.CO;2.

214. Bowman KP. Global patterns of the quasi-biennial oscillation in total ozone. **J Atmos Sci** 46: 3328–3343, 1989. doi:10.1175/1520-0469(1989)046<3328:GPOTQB>2.0.CO;2.

215. Zerefos C, Meleti C, Balis D, Tourpali K, Bais AF. Quasi-biennial and longer-term changes in clear sky UV-B solar irradiance. **Geophys Res Lett** 25: 4345–4348, 1998. doi:10.1029/1998GL900160.

216. Meleti C, Cappellani F. Measurements of aerosol optical depth at Ispra: analysis of the correlation with UV-B, UV-A, and total solar irradiance. **J Geophys Res Atmos** 105: 4971–4978, 2000. doi:10.1029/1999JD900459.

217. Liu SC, McKeen SA, Madronich S. Effect of anthropogenic aerosols on biologically active ultraviolet radiation. **Geophys Res Lett** 18: 2265–2268, 1991. doi:10.1029/91GL02773.

218. Balis DS, Amiridis V, Zerefos C, Kazantzidis A, Kazadzis S, Bais AF, Meleti C, Gerasopoulos E, Papayannis A, Matthias V, Dier H, Andreae MO. Study of the effect of different type of aerosols on UV-B radiation from measurements during EARLINET. **Atmos Chem Phys** 4: 307–321, 2004. doi:10.5194/acp-4-307-2004.

219. Madronich S. UV radiation in the natural and perturbed atmosphere. In: **Environmental Effects of UV**, edited by Tevini M. Boca Raton, FL: CRC Press, 1993.

220. McKenzie RL, Matthews WA, Johnston PV. The relationship between erythemal UV and ozone, derived from spectral irradiance measurements. **Geophys Res Lett** 18: 2269–2272, 1991. doi:10.1029/91GL02786.

221. Blumthaler M, Salzgeber M, Ambach W. Ozone and ultraviolet-B irradiances: experimental determination of the radiation amplification factor. **Photochem Photobiol** 61: 159–162, 1995. doi:10.1111/j.1751-1097.1995.tb03954.x.

222. di Sarra A, Cacciani M, Chamard P, Cornwall C, DeLuisi JJ, Di Iorio T, Disterhoft P, Fiocco G, Fuá D, Monteleone F. Effects of desert dust and ozone on the ultraviolet irradiance at the Mediterranean island of Lampedusa during PAUR II. **J Geophys Res** 107: 2–14, 2002. doi:10.1029/2000JD000139.

223. McKenzie R, Liley B, Kotkamp M, Geddes A, Querel R, Stierle S, Lantz K, Rhodes S, Madronich S. Relationship between ozone and biologically relevant UV at 4 NDACC sites. **Photochem Photobiol Sci** 21: 2095–2114, 2022. doi:10.1007/s43630-022-00281-5.

224. Micheletti MI, Piacentini RD, Madronich S. Sensitivity of biologically active UV radiation to stratospheric ozone changes: effects of action spectrum shape and wavelength range. **Photochem Photobiol** 78: 456–461, 2003. doi:10.1562/0031-8655(2003)0780456SOBAUR2.0.CO2.

225. Palancar GG, Olcese LE, Achad M, López ML, Toselli BM. A long term study of the relations between erythemal UV-B irradiance, total ozone column, and aerosol optical depth at central Argentina. **J Quant Spectrosc Radiat Transf** 198: 40–47, 2017. doi:10.1016/j.jqsrt.2017.05.002.

226. Kim J, Cho HK, Mok J, Yoo HD, Cho N. Effects of ozone and aerosol on surface UV radiation variability. **J Photochem Photobiol B** 119: 46–51, 2013. doi:10.1016/j.jphotobiol.2012.11.007.

227. Campanelli M, Diémoz H, Siani AM, di Sarra A, Iannarelli AM, Kudo R, Fasano G, Casasanta G, Tofful L, Cacciani M, Sanò P, Dietrich S. Aerosol optical characteristics in the urban area of Rome, Italy, and their impact on the UV index. **Atmos Meas Tech** 15: 1171–1183, 2022. doi:10.5194/amt-15-1171-2022.

228. Bais AF, Bernhard G, McKenzie RL, Aucamp PJ, Young PJ, Ilyas M, Jöckel P, Deushi M. Ozone–climate interactions and effects on solar ultraviolet radiation. **Photochem Photobiol Sci** 18: 602–640, 2019. doi:10.1039/c8pp90059k.

229. Chubarova N, Nezval' Y, Sviridenkov I, Smirnov A, Slutsker I. Smoke aerosol and its radiative effects during extreme fire event over Central Russia in summer 2010. **Atmos Meas Tech** 5: 557–568, 2012. doi:10.5194/amt-5-557-2012.

230. Hoffer A, Gelencsér A, Guyon P, Kiss G, Schmid O, Frank GP, Artaxo P, Andreae MO. Optical properties of humic-like substances

(HULIS) in biomass-burning aerosols. **Atmos Chem Phys** 6: 3563–3570, 2006. doi:10.5194/acp-6-3563-2006.

231. Fountoulakis I, Siomos N, Natsi A, Drosoglou T, Bais AF. Deriving aerosol absorption properties from solar ultraviolet radiation spectral measurements at Thessaloniki, Greece. **Remote Sens** 11: 2179, 2019. doi:10.3390/rs11182179.

232. Raptis IP, Kazadzis S, Eleftheratos K, Amiridis V, Fountoulakis I. Single scattering albedo's spectral dependence effect on UV irradiance. **Atmosphere** 9: 364, 2018. doi:10.3390/atmos9090364.

233. Mok J, Krotkov NA, Torres O, Jethva H, Li Z, Kim J, Koo JH, Go S, Irie H, Labow G, Eck TF, Holben BN, Herman J, Loughman RP, Spinei E, Lee SS, Khatri P, Campanelli M. Comparisons of spectral aerosol single scattering albedo in Seoul, South Korea. **Atmos Meas Tech** 11: 2295–2311, 2018. doi:10.5194/amt-11-2295-2018.

234. Kazadzis S, Raptis P, Kouremeti N, Amiridis V, Arola A, Gerasopoulos E, Schuster GL. Aerosol absorption retrieval at ultraviolet wavelengths in a complex environment. **Atmos Meas Tech** 9: 5997–6011, 2016. doi:10.5194/amt-9-5997-2016.

235. Bergstrom RW, Pilewskie P, Russell PB, Redemann J, Bond TC, Quinn PK, Sierau B. Spectral absorption properties of atmospheric aerosols. **Atmos Chem Phys** 7: 5937–5943, 2007. doi:10.5194/acp-7-5937-2007.

236. Raptis IP, Eleftheratos K, Kazadzis S, Kosmopoulos P, Papachristopoulou K, Solomos S. The combined effect of ozone and aerosols on erythemal irradiance in an extremely low ozone event during May 2020. **Atmosphere** 12: 145, 2021. doi:10.3390/atmos12020145.

237. Fragkos K, Bais AF, Fountoulakis I, Balis D, Tourpali K, Meleti C, Zanis P. Extreme total column ozone events and effects on UV solar radiation at Thessaloniki, Greece. **Theor Appl Climatol** 126: 505–517, 2016. doi:10.1007/s00704-015-1562-3.

238. Arola A, Kazadzis S, Lindfors A, Krotkov N, Kujanpää J, Tamminen J, Bais A, di Sarra A, Villaplana JM, Brogniez C, Siani AM, Janouch M, Weihs P, Webb A, Koskela T, Kouremeti N, Meloni D, Buchard V, Auriol F, Ialongo I, Staneck M, Simic S, Smedley A, Kinne S. A new approach to correct for absorbing aerosols in OMI UV. **Geophys Res Lett** 36: L22805, 2009. doi:10.1029/2009GL041137.

239. Kazadzis S, Bais A, Arola A, Krotkov N, Kouremeti N, Meleti C. Ozone Monitoring Instrument spectral UV irradiance products: comparison with ground based measurements at an urban environment. **Atmos Chem Phys** 9: 585–594, 2009. doi:10.5194/acp-9-585-2009.

240. Blumthaler M, Ambach W, Ellinger R. Increase in solar UV radiation with altitude. **J Photochem Photobiol B** 39: 130–134, 1997. doi:10.1016/S1011-1344(96)00018-8.

241. Seckmeyer G, Mayer B, Bernhard G, Erb R, Albold A, Jäger H, Stockwell WR. New maximum UV irradiance levels observed in Central Europe. **Atmos Environ** 31: 2971–2976, 1997. doi:10.1016/S1352-2310(97)00104-0.

242. Bais AF, Zerefos CS, Ziomas IC, Zoumakis N, Mantis HT, Hofmann DJ, Fiocco G. Decreases in the ozone and the SO2 columns following the appearance of the El Chichon aerosol cloud at midlatitude. In: **Atmospheric Ozone**, edited by Zerefos CS, Ghazi A. Dordrecht, The Netherlands: Springer, 1985, p. 353–356.

243. Osipov S, Stenchikov G, Tsigaridis K, LeGrande AN, Bauer SE, Fnais M, Lelieveld J. The Toba supervolcano eruption caused severe tropical stratospheric ozone depletion. **Commun Earth Environ** 2: 71, 2021. doi:10.1038/s43247-021-00141-7.

244. McKenzie RL, Björn LO, Bais A, Ilyasad M. Changes in biologically active ultraviolet radiation reaching the Earth's surface. **Photochem Photobiol Sci** 2: 5–15, 2003. doi:10.1039/b211155c.

245. Frederick JE, Snell HE. Tropospheric influence on solar ultraviolet radiation: the role of clouds. **J Climate** 3: 373–381, 1990. doi:10.1175/1520-0442(1990)003<0373:TIOSUR>2.0.CO;2.

246. Calbó J, Pagès D, González JA. Empirical studies of cloud effects on UV radiation: a review. **Rev Geophys** 43: RG2002, 2005. doi:10.1029/2004RG000155.

247. Sabburg J, Wong J. The effect of clouds on enhancing UVB irradiance at the Earth's surface: a one year study. **Geophys Res Lett** 27: 3337–3340, 2000. doi:10.1029/2000GL011683.

248. de Miguel A, Román R, Bilbao J, Mateos D. Evolution of erythemal and total shortwave solar radiation in Valladolid, Spain: effects of atmospheric factors. **J Atmos Solar-Terrestrial Phys** 73: 578–586, 2011. doi:10.1016/j.jastp.2010.11.021.

249. Crawford J, Shetter RE, Lefer B, Cantrell C, Junkermann W, Madronich S, Calvert J. Cloud impacts on UV spectral actinic flux observed during the International Photolysis Frequency Measurement and Model Intercomparison (IPMMI). **J Geophys Res** 108: 8545, 2003. doi:10.1029/2002JD002731.

250. Weihs P, Lenoble J, Blumthaler M, Martin T, Seckmeyer G, Philipona R, De la Casiniere A, Sergent C, Gröbner J, Cabot T, Masserot D, Pichler T, Pougatch E, Rengarajan G, Schmucki D, Simic S. Modeling the effect of an inhomogeneous surface albedo on incident UV radiation in mountainous terrain: determination of an effective surface albedo. **Geophys Res Lett** 28: 3111–3114, 2001. doi:10.1029/2001GL012986.

251. Kylling A, Mayer B. Ultraviolet radiation in partly snow covered terrain: observations and three-dimensional simulations. **Geophys Res Lett** 28: 3665–3668, 2001. doi:10.1029/2001GL013034.

252. Feister U, Grewe R. Spectral albedo measurements in the UV and visible region over different types of surfaces. **Photochem Photobiol** 62: 736–744, 1995. doi:10.1111/j.1751-1097.1995.tb08723.x.

253. Weihs P, Simic S, Laube W, Mikielewicz W, Rengarajan G, Mandl M. Albedo influences on surface UV irradiance at the Sonnblick High-Mountain Observatory (3106-m altitude). **J Appl Meteorol** 38: 1599–1610, 1999. doi:10.1175/1520-0450(1999)038<1599:AIOSUI>2.0.CO;2.

254. Solomon S, IPCC. *Climate Change 2007: The Physical Science Basis. Contribution of Working Group I to the Fourth Assessment Report of the Intergovernmental Panel on Climate Change*. Cambridge, UK: Cambridge University Press, 2007.

255. Bernhard G, Booth CR, Ehramjian JC, Stone R, Dutton EG. Ultraviolet and visible radiation at Barrow, Alaska: climatology and influencing factors on the basis of version 2 National Science Foundation network data. **J Geophys Res** 112: D09101, 2007. doi:10.1029/2006JD007865.

256. Kerr JB, Fioletov VE. Surface ultraviolet radiation. **Atmos Ocean** 46: 159–184, 2008. doi:10.3137/ao.460108.

257. Castro T, Mar B, Longoria R, Ruiz Suárez LG, Morales L. Surface albedo measurements in Mexico City metropolitan area. **Atmosfera** 14: 69–74, 2001.

258. Coulson KL, Reynolds DW. The spectral reflectance of natural surfaces. **J Appl Meteor** 10: 1285–1295, 1971. doi:10.1175/1520-0450(1971)010<1285:TSRONS>2.0.CO;2.

259. Eck TF, Bhartia PK, Hwang PH, Stowe LL. Reflectivity of Earth's surface and clouds in ultraviolet from satellite observations. **J Geophys Res** 92: 4287–4296, 1987. doi:10.1029/JD092iD04p04287.

260. Brandt RE, Warren SG, Worby AP, Grenfell TC. Surface albedo of the Antarctic sea ice zone. **J Clim** 18: 3606–3622, 2005. doi:10.1175/JCLI3489.1.

261. Pitkänen MR, Arola A, Lakkala K, Koskela T, Lindfors AV. Comparing OMI UV index to ground-based measurements at two Finnish sites with focus on cloud-free and overcast conditions. **Atmos Meas Tech Discuss** 2015: 487–516, 2015. doi:10.5194/amtd-8-487-2015.

262. Kreuter A, Buras R, Mayer B, Webb A, Kift R, Bais A, Kouremeti N, Blumthaler M. Solar irradiance in the heterogeneous albedo environment of the Arctic coast: measurements and a 3-D model study. **Atmos Chem Phys** 14: 5989–6002, 2014. doi:10.5194/acp-14-5989-2014.

263. Cede A, Herman J, Richter A, Krotkov N, Burrows J. Measurements of nitrogen dioxide total column amounts using a Brewer double spectrophotometer in direct Sun mode. **J Geophys Res** 111: D05304, 2006. doi:10.1029/2005JD006585.

264. Edmonds M, Herd RA, Galle B, Oppenheimer CM. Automated, high time-resolution measurements of SO_2 flux at Soufrière Hills Volcano, Montserrat. **Bull Volcanol** 65: 578–586, 2003. doi:10.1007/s00445-003-0286-x.

265. Weber JN, Kaufholdt D, Minner-Meinen R, Bloem E, Shahid A, Rennenberg H, Hänsch R. Impact of wildfires on SO_2 detoxification mechanisms in leaves of oak and beech trees. **Environ Pollut** 272: 116389, 2021. doi:10.1016/j.envpol.2020.116389.

266. Zerefos CS, Eleftheratos K, Kapsomenakis J, Solomos S, Inness A, Balis D, et al. Detecting volcanic sulfur dioxide plumes in the Northern Hemisphere using the Brewer spectrophotometers, other networks, and satellite observations. **Atmos Chem Phys** 17: 551–574, 2017. doi:10.5194/acp-17-551-2017.

267. Krueger AJ, Walter LS, Bhartia PK, Schnetzler CC, Krotkov NA, Sprod I, Bluth GJ. Volcanic sulfur dioxide measurements from the total ozone mapping spectrometer instruments. **J Geophys Res** 100: 14057–14076, 1995. doi:10.1029/95JD01222.

268. Johansson JK, Mellqvist J, Samuelsson J, Offerle B, Lefer B, Rappenglück B, Flynn J, Yarwood G. Emission measurements of alkenes, alkanes, SO_2, and NO_2 from stationary sources in Southeast Texas over a 5 year period using SOF and mobile DOAS. **J Geophys Res Atmos** 119: 1973–1991, 2014. doi:10.1002/2013JD020485.

269. Zhang Q, Tie X, Lin W, Cao J, Quan J, Ran L, Xu W. Variability of SO_2 in an intensive fog in North China Plain: evidence of high solubility of SO_2. **Particuology** 11: 41–47, 2013. doi:10.1016/j.partic.2012.09.005.

270. Koronakis PS, Sfantos GK, Paliatsos AG, Kaldellis JK, Garofalakis JE, Koronaki IP. Interrelations of UV-global/global/diffuse solar irradiance components and UV-global attenuation on air pollution episode days in Athens, Greece. **Atmos Environ** 36: 3173–3181, 2002. doi:10.1016/S1352-2310(02)00233-9.

271. Weatherhead EC, Reinsel GC, Tiao GC, Meng XL, Choi D, Cheang WK, Keller T, DeLuisi J, Wuebbles DJ, Kerr JB, Miller AJ, Oltmans SJ, Frederick JE. Factors affecting the detection of trends: statistical considerations and applications to environmental data. **J Geophys Res Atmos** 103: 17149–17161, 1998. doi:10.1029/98JD00995.

272. Glandorf M, Arola A, Bais A, Seckmeyer G. Possibilities to detect trends in spectral UV irradiance. **Theor Appl Climatol** 81: 33–44, 2005. doi:10.1007/s00704-004-0109-9.

273. Herman JR. Use of an improved radiation amplification factor to estimate the effect of total ozone changes on action spectrum weighted irradiances and an instrument response function. **J Geophys Res** 115: D23119, 2010. doi:10.1029/2010JD014317.

274. Herman J, Cede A, Huang L, Ziemke J, Torres O, Krotkov N, Kowalewski M, Blank K. Global distribution and 14-year changes in erythemal irradiance, UV atmospheric transmission, and total column ozone for 2005–2018 estimated from OMI and EPIC observations. **Atmos Chem Phys** 20: 8351–8380, 2020. doi:10.5194/acp-20-8351-2020.

275. Lindfors A, Vuilleumier L. Erythemal UV at Davos (Switzerland), 1926–2003, estimated using total ozone, sunshine duration, and snow depth. **J Geophys Res** 110: D02104, 2005. doi:10.1029/2004JD005231.

276. Posyniak M, Szkop A, Pietruczuk A, Podgórski J, Krzyścin J. The long-term (1964–2014) variability of aerosol optical thickness and its impact on solar irradiance based on the data taken at Belsk. **Acta Geophys** 64: 1858–1874, 2016. doi:10.1515/acgeo-2016-0026.

277. Čížková K, Láska K, Metelka L, Staněk M. Reconstruction and analysis of erythemal UV radiation time series from Hradec Králové (Czech Republic) over the past 50 years. **Atmos Chem Phys** 18: 1805–1818, 2018. doi:10.5194/acp-18-1805-2018.

278. den Outer PN, Slaper H, Kaurola J, Lindfors A, Kazantzidis A, Bais AF, Feister U, Junk J, Janouch M, Josefsson W. Reconstructing of erythemal ultraviolet radiation levels in Europe for the past 4 decades. **J Geophys Res** 115: D10102, 2010. doi:10.1029/2009JD012827.

279. Román R, Bilbao J, de Miguel A. Erythemal ultraviolet irradiation trends in the Iberian Peninsula from 1950 to 2011. **Atmos Chem Phys** 15: 375–391, 2015. doi:10.5194/acp-15-375-2015.

280. Krzyścin JW, Sobolewski PS. Trends in erythemal doses at the Polish Polar Station, Hornsund, Svalbard based on the homogenized measurements (1996–2016) and reconstructed data (1983–1995). **Atmos Chem Phys** 18: 1–11, 2018. doi:10.5194/acp-18-1-2018.

281. Liu H, Hu B, Zhang L, Zhao XJ, Shang KZ, Wang YS, Wang J. Ultraviolet radiation over China: spatial distribution and trends. **Renew Sustain Energy Rev** 76: 1371–1383, 2017. doi:10.1016/j.rser.2017.03.102.

282. Chubarova NE, Pastukhova AS, Galin VY, Smyshlyaev SP. Long-term variability of UV irradiance in the Moscow region according to measurement and modeling data. **Izv Atmos Ocean Phys** 54: 139–146, 2018. doi:10.1134/S0001433818020056.

283. Bernhard G, Booth CR, Ehramjian JC, Nichol SE. UV climatology at McMurdo Station, Antarctica, based on version 2 data of the National Science Foundation's Ultraviolet Radiation Monitoring Network. **J Geophys Res** 111: D11201, 2006. doi:10.1029/2005JD005857.

284. Bernhard GH, McKenzie RL, Lantz K, Stierle S. Updated analysis of data from Palmer Station, Antarctica (64° S), and San Diego, California (32° N), confirms large effect of the Antarctic ozone hole on UV radiation. **Photochem Photobiol Sci** 21: 373–384, 2022. doi:10.1007/s43630-022-00178-3.

285. Aun M, Lakkala K, Sanchez R, Asmi E, Nollas F, Meinander O, Sogacheva L, De Bock V, Arola A, de Leeuw G, Aaltonen V, Bolsée D, Cizkova K, Mangold A, Metelka L, Jakobson E, Svendby T, Gillotay D, Van Opstal B. Solar UV radiation measurements in

Marambio, Antarctica, during years 2017–2019. **Atmos Chem Phys** 20: 6037–6054, 2020. doi:10.5194/acp-20-6037-2020.

286. Bernhard G, Stierle S. Trends of UV radiation in Antarctica. **Atmosphere** 11: 795, 2020. doi:10.3390/atmos11080795.

287. Kuttippurath J, Kumar P, Nair PJ, Pandey PC. Emergence of ozone recovery evidenced by reduction in the occurrence of Antarctic ozone loss saturation. **npj Clim Atmos Sci** 1: 42, 2018. doi:10.1038/s41612-018-0052-6.

288. Cadet JM, Bencherif H, Du Preez DJ, Portafaix T, Sultan-Bichat N, Belus M, Brogniez C, Auriol F, Metzger JM, Ncongwane K, Coetzee GJ, Wright CY. Solar UV Radiation in Saint-Denis, La Réunion and Cape Town. South Africa: 10 years climatology and human exposure assessment at altitude. **Atmosphere** 10: 589, 2019. doi:10.3390/atmos10100589.

289. Lakkala K, Redondas A, Meinander O, Thölix L, Hamari B, Almansa AF, Carreno V, García RD, Torres C, Deferrari G, Ochoa H, Bernhard G, Sanchez R, de Leeuw G. UV measurements at Marambio and Ushuaia during 2000–2010. **Atmos Chem Phys** 18: 16019–16031, 2018. doi:10.5194/acp-18-16019-2018.

290. Cadet JM, Bencherif H, Cadet N, Lamy K, Portafaix T, Belus M, Brogniez C, Auriol F, Metzger JM, Wright CY. Solar UV radiation in the tropics: human exposure at Reunion Island (21° S, 55° E) during summer outdoor activities. **Int J Environ Res Public Health** 17: 8105, 2020. doi:10.3390/ijerph17218105.

291. Cabrol NA, Feister U, Häder DP, Piazena H, Grin EA, Klein A. Record solar UV irradiance in the tropical Andes. **Front Environ Sci** 2: 19, 2014. doi:10.3389/fenvs.2014.00019.

292. Bodhaine BA, McKenzie RL, Johnston PV, Hofmann DJ, Dutton EG, Schnell RC, Barnes JE, Ryan SC, Kotkamp M. New Ultraviolet spectroradiometer measurements at Mauna Loa Observatory. **Geophys Res Lett** 23: 2121–2124, 1996. doi:10.1029/96GL01954.

293. Fountoulakis I, Zerefos CS, Bais AF, Kapsomenakis J, Koukouli ME, Ohkawara N, Fioletov V, De Backer H, Lakkala K, Karppinen T, Webb AR. Twenty-five years of spectral UV-B measurements over Canada, Europe and Japan: trends and effects from changes in ozone, aerosols, clouds, and surface reflectivity. **Comptes Rendus Geosci** 350: 393–402, 2018. doi:10.1016/j.crte.2018.07.011.

294. Fountoulakis I, Diémoz H, Siani AM, di Sarra A, Meloni D, Sferlazzo DM. Variability and trends in surface solar spectral ultraviolet irradiance in Italy: on the influence of geopotential height and lower-stratospheric ozone. **Atmos Chem Phys** 21: 18689–18705, 2021. doi:10.5194/acp-21-18689-2021.

295. Hunter N, Rendell RJ, Higlett MP, O'Hagan JB, Haylock RG. Relationship between erythema effective UV radiant exposure, total ozone, cloud cover and aerosols in southern England, UK. **Atmos Chem Phys** 19: 683–699, 2019. doi:10.5194/acp-19-683-2019.

296. Hooke RJ, Higlett MP, Hunter N, O'Hagan JB. Long term variations in erythema effective solar UV at Chilton, UK, from 1991 to 2015. **Photochem Photobiol Sci** 16: 1596–1603, 2017. doi:10.1039/c7pp00053g.

297. Smedley AR, Rimmer JS, Moore D, Toumi R, Webb AR. Total ozone and surface UV trends in the United Kingdom: 1979–2008. **Int J Climatol** 32: 338–346, 2012. doi:10.1002/joc.2275.

298. Fitzka M, Simic S, Hadzimustafic J. Trends in spectral UV radiation from long-term measurements at Hoher Sonnblick, Austria. **Theor Appl Climatol** 110: 585–593, 2012. doi:10.1007/s00704-012-0684-0.

299. De Bock V, De Backer H, Van Malderen R, Mangold A, Delcloo A. Relations between erythemal UV dose, global solar radiation, total ozone column and aerosol optical depth at Uccle. **Atmos Chem Phys** 14: 12251–12270, 2014. doi:10.5194/acp-14-12251-2014.

300. Fountoulakis I, Bais AF, Tourpali K, Fragkos K, Misios S. Projected changes in solar UV radiation in the Arctic and sub-Arctic Oceans: effects from changes in reflectivity, ice transmittance, clouds, and ozone. **J Geophys Res Atmos** 119: 8073–8090, 2014. doi:10.1002/2014JD021918.

301. Zerefos CS, Tourpali K, Eleftheratos K, Kazadzis S, Meleti C, Feister U, Koskela T, Heikkilä A. Evidence of a possible turning point in solar UV-B over Canada. **Atmos Chem Phys** 12: 2469–2477, 2012. doi:10.5194/acp-12-2469-2012.

302. Dameris M, Loyola DG, Nützel M, Coldewey-Egbers M, Lerot C, Romahn F, van Roozendael M. Record low ozone values over the Arctic in boreal spring 2020. **Atmos Chem Phys** 21: 617–633, 2021. doi:10.5194/acp-21-617-2021.

303. Inness A, Chabrillat S, Flemming J, Huijnen V, Langenrock B, Nicolas J, Polichtchouk I, Razinger M. Exceptionally low arctic stratospheric ozone in Spring 2020 as seen in the CAMS reanalysis. **J Geophys Res Atmos** 125: e2020JD033563, 2020. doi:10.1029/2020JD033563.

304. Petkov B, Vitale V, Di Carlo P, Mazzola M, Lupi A, Diémoz H, Fountoulakis I, Drofa O, Mastrangelo D, Casale GR, Siani AM. The 2020 Arctic ozone depletion and signs of its effect on the ozone column at lower latitudes. **Bull Atmos Sci Technol** 2: 8, 2021. doi:10.1007/s42865-021-00040-x.

305. Eleftheratos K, Kazadzis S, Zerefos CS, Tourpali K, Meleti C, Balis D, Zyrichidou I, Lakkala K, Feister U, Koskela T, Heikkilä A, Karhu JM. Ozone and spectroradiometric UV changes in the past 20 years over high latitudes. **Atmos Ocean** 53: 117–125, 2015. doi:10.1080/07055900.2014.919897.

306. Svendby TM, Hansen GH, Bäcklund A, Nilsen AC, Schulze D, Johnsen B. Monitoring of the Atmospheric Ozone Layer and Natural Ultraviolet Radiation. Annual Report 2020. (NILU report 18/2021; Norwegian Environment Agency M-2091|2021). Kjeller, Norway: NILU, 2021.

307. Bernhard G. Trends of solar ultraviolet irradiance at Barrow, Alaska, and the effect of measurement uncertainties on trend detection. **Atmos Chem Phys** 11: 13029–13045, 2011. doi:10.5194/acp-11-13029-2011.

308. IPCC. **Climate Change 2013: The Physical Science Basis. Contribution of Working Group I to the Fifth Assessment Report of the Intergovernmental Panel on Climate Change**, edited by Stocker TF, Qin D, Plattner GK, Tignor M, Allen SK, Boschung J, Nauels A, Xia Y. Cambridge, UK: Cambridge University Press, 2013.

309. Zhang C, Gao R, Wu J, Yang Z. Combating climate change, desertification and sandstorms: a collaborative approach. In: *Annual Report on China's Response to Climate Change (2017): Implementing The Paris Agreement*, edited by Wang W, Liu Y. Singapore: Springer, 2017, p. 145–153.

310. Liu S, Liu CC, Froyd KD, Schill GP, Murphy DM, Bui TP, Dean-Day JM, Weinzierl B, Dollner M, Diskin GS, Chen G, Gao RS. Sea spray aerosol concentration modulated by sea surface temperature. **Proc Natl Acad Sci USA** 118: e2020583118, 2021. doi:10.1073/pnas.2020583118.

311. Watanabe S, Sudo K, Nagashima T, Takemura T, Kawase H, Nozawa T. Future projections of surface UV-B in a changing climate. **J Geophys Res** 116: D16118, 2011. doi:10.1029/2011JD015749.

312. Sekiguchi M, Nakajima T. A k-distribution-based radiation code and its computational optimization for an atmospheric general circulation model. **J Quant Spectrosc Radiat Transf** 109: 2779–2793, 2008. doi:10.1016/j.jqsrt.2008.07.013.

313. Hegglin MI, Shepherd TG. Large climate-induced changes in ultraviolet index and stratosphere-to-troposphere ozone flux. **Nat Geosci** 2: 687–691, 2009. doi:10.1038/ngeo604.

314. Tourpali K, Bais AF, Kazantzidis A, Zerefos CS, Akiyoshi H, Austin J, Brühl C, Butchart N, Chipperfield MP, Dameris M, Deushi M, Eyring V, Giorgetta MA, Kinnison DE, Mancini E, Marsh DR, Nagashima T, Pitari G, Plummer DA, Rozanov E, Shibata K, Tian W. Clear sky UV simulations for the 21st century based on ozone and temperature projections from Chemistry-Climate Models. **Atmos Chem Phys** 9: 1165–1172, 2009. doi:10.5194/acp-9-1165-2009.

315. Bais AF, Tourpali K, Kazantzidis A, Akiyoshi H, Bekki S, Braesicke P, Chipperfield MP, Dameris M, Eyring V, Garny H, Iachetti D, Jöckel P, Kubin A, Langematz U, Mancini E, Michou M, Morgenstern O, Nakamura T, Newman PA, Pitari G, Plummer DA, Rozanov E, Shepherd TG, Shibata K, Tian W, Yamashita Y. Projections of UV radiation changes in the 21st century: impact of ozone recovery and cloud effects. **Atmos Chem Phys** 11: 7533–7545, 2011. doi:10.5194/acp-11-7533-2011.

316. Corrêa MD, Godin-Beekmann S, Haeffelin M, Bekki S, Saiag P, Badosa J, Jégou F, Pazmiño A, Mahé E. Projected changes in clear-sky erythemal and vitamin D effective UV doses for Europe over the period 2006 to 2100. **Photochem Photobiol Sci** 12: 1053–1064, 2013. doi:10.1039/c3pp50024a.

317. Fountoulakis I, Bais AF. Projected changes in erythemal and vitamin D effective irradiance over northern-hemisphere high latitudes. **Photochem Photobiol Sci** 14: 1251–1264, 2015. doi:10.1039/c5pp00093a.

318. Kazantzidis A, Tourpali K, Bais AF. Variability of cloud-free ultraviolet dose rates on global scale due to modeled scenarios of future ozone recovery. **Photochem Photobiol** 86: 117–122, 2010. doi:10.1111/j.1751-1097.2009.00645.x.

319. Caldwell MM. Solar ultraviolet radiation as an ecological factor for alpine plants. **Ecol Monogr** 38: 243–268, 1968. doi:10.2307/1942430.

320. de Gruij FR. Action spectrum for photocarcinogenesis. In: *Skin Cancer: Basic Science, Clinical Research and Treatment*, edited by Garbe C, Schmitz S, Orfanos CE. Berlin: Springer, 1995, p. 21–30.

321. Eleftheratos K, Kapsomenakis J, Fountoulakis I, Zerefos CS, Jöckel P, Dameris M, Bais AF, Bernhard G, Kouklaki D, Tourpali K, Stierle S, Liley JB, Brogniez C, Auriol F, Diémoz H, Simic S, Petropavlovskikh I. Ozone and DNA active UV radiation changes for the near global mean and at high latitudes due to enhanced greenhouse gas concentrations. **Atmos Chem Phys** 2022: 12827–12855, 2022. doi:10.5194/acp-22-12827-2022.

322. Norris JR, Allen RJ, Evan AT, Zelinka MD, O'Dell CW, Klein SA. Evidence for climate change in the satellite cloud record. **Nature** 536: 72–75, 2016. doi:10.1038/nature18273.

323. Schneider T, Kaul CM, Pressel KG. Possible climate transitions from breakup of stratocumulus decks under greenhouse warming. **Nat Geosci** 12: 163–167, 2019. doi:10.1038/s41561-019-0310-1.

324. Eleftheratos K, Kapsomenakis J, Zerefos CS, Bais AF, Fountoulakis I, Dameris M, Jöckel P, Haslerud AS, Godin-Beekmann S, Steinbrecht W, Petropavlovskikh I, Brogniez C, Leblanc T, Liley JB, Querel R, Swart DP. Possible effects of greenhouse gases to ozone

325. profiles and DNA active UV-B irradiance at ground level. **Atmosphere** 11: 228, 2020. doi:10.3390/atmos11030228.

325. Wright CY, du Preez DJ, Martincigh BS, Allen MW, Millar DA, Wernecke B, Blesic S. A comparison of solar ultraviolet radiation exposure in urban canyons in Venice, Italy and Johannesburg, South Africa. **Photochem Photobiol** 96: 1148–1153, 2020. doi:10.1111/php.13291.

326. Schrempf M, Thuns N, Lange K, Seckmeyer G. Impact of orientation on the vitamin D weighted exposure of a human in an urban environment. **Int J Environ Res Public Health** 14: 980, 2017. doi:10.3390/ijerph14080920.

327. McKenzie RL, Lucas RM. Reassessing impacts of extended daily exposure to low level solar UV radiation. **Sci Rep** 8: 13805, 2018. doi:10.1038/s41598-018-32056-3.

328. Modenese A, Gobba F, Paolucci V, John SM, Sartorelli P, Wittlich M. A one-month monitoring of exposure to solar UV radiation of a group of construction workers in Tuscany. **Energies** 13: 6035, 2020. doi:10.3390/en13226035.

329. Siani AM, Casale GR, Sisto R, Colosimo A, Lang CA, Kimlin MG. Occupational Exposures to solar ultraviolet radiation of vineyard workers in Tuscany (Italy). **Photochem Photobiol** 87: 925–934, 2011. doi:10.1111/j.1751-1097.2011.00934.x.

330. Webb AR, Slaper H, Koepke P, Schmalwieser AW. Know your standard: clarifying the CIE erythema action spectrum. **Photochem Photobiol** 87: 483–486, 2011. doi:10.1111/j.1751-1097.2010.00871.x.

331. Moan J, Grigalavicius M, Baturaite Z, Dahlback A, Juzeniene A. The relationship between UV exposure and incidence of skin cancer. **Photodermatol Photoimmunol Photomed** 31: 26–35, 2015. doi:10.1111/phpp.12139.

332. Lucas RM, Yazar S, Young AR, Norval M, de Gruijl FR, Takizawa Y, Rhodes LE, Sinclair CA, Neale RE. Human health in relation to exposure to solar ultraviolet radiation under changing stratospheric ozone and climate. **Photochem Photobiol Sci** 18: 641–680, 2019. doi:10.1039/c8pp90060d.

333. UNEP. **Protecting the Ozone Layer—35th Anniversary Edition**. Nairobi: UNEP Ozone Secretariat, 2022.

334. Sofieva VF, Kyrölä E, Laine M, Tamminen J, Degenstein D, Bourassa A, Roth C, Zawada D, Weber M, Rozanov A, Rahpoe N, Stiller G, Laeng A, von Clarmann T, Walker KA, Sheese P, Hubert D, van Roozendael M, Zehner C, Damadeo R, Zawodny J, Kramarova N, Bhartia PK. Merged SAGE II, Ozone_cci and OMPS ozone profile dataset and evaluation of ozone trends in the stratosphere. **Atmos Chem Phys** 17: 12533–12552, 2017. doi:10.5194/acp-17-12533-2017.

335. Ball WT, Alsing J, Mortlock DJ, Staehelin J, Haigh JD, Peter T, Tummon F, Stübi R, Stenke A, Anderson J, Bourassa A, Davis SM, Degenstein D, Frith S, Froidevaux L, Roth C, Sofieva V, Wang R, Wild J, Yu P, Ziemke JR, Rozanov EV. Evidence for a continuous decline in lower stratospheric ozone offsetting ozone layer recovery. **Atmos Chem Phys** 18: 1379–1394, 2018. doi:10.5194/acp-18-1379-2018.

336. Wargan K, Orbe C, Pawson S, Ziemke JR, Oman LD, Olsen MA, Coy L, Emma Knowland KE. Recent decline in extratropical lower stratospheric ozone attributed to circulation changes. **Geophys Res Lett** 45: 5166–5176, 2018. doi:10.1029/2018GL077406.

337. Godin-Beekmann S, Azouz N, Sofieva V, Hubert D, Petropavlovskikh I, Effertz P, Ancellet G, Degenstein D, Zawada D, Froidevaux L, Frith S, Wild J, Davis S, Steinbrecht W, Leblanc T, Querel R, Tourpali K, Damadeo R, Maillard-Barras E, Stübi R,

Vigouroux C, Arosio C, Nedoluha G, Boyd I, van Malderen R. Updated trends of the stratospheric ozone vertical distribution in the 60°S-60°N latitude range based on the LOTUS regression model. **Atmos Chem Phys Discuss** 2022: 1–28, 2022. doi:10.5194/acp-2022-137.

338. Zerefos C, Kapsomenakis J, Eleftheratos K, Tourpali K, Petropavlovskikh I, Hubert D, Godin-Beekmann S, Steinbrecht W, Frith S, Sofieva V, Hassler B. Representativeness of single lidar stations for zonally averaged ozone profiles, their trends and attribution to proxies. **Atmos Chem Phys** 18: 6427–6440, 2018. doi:10.5194/acp-18-6427-2018.

339. Bognar K, Tegtmeier S, Bourassa A, Roth C, Warnock T, Zawada D, Degenstein D. Stratospheric ozone trends for 1984–2021 in the SAGE II–OSIRIS–SAGE III/ISS composite dataset. **Atmos Chem Phys** 22: 9553–9569, 2022. doi:10.5194/acp-22-9553-2022.

340. Szelaôg ME, Sofieva VF, Degenstein D, Roth C, Davis S, Froidevaux L. Seasonal stratospheric ozone trends over 2000–2018 derived from several merged data sets. **Atmos Chem Phys** 20: 7035–7047, 2020. doi:10.5194/acp-20-7035-2020.

341. Hoinka KP, Claude H, Köhler U. On the correlation between tropopause pressure and ozone above central Europe. **Geophys Res Lett** 23: 1753–1756, 1996. doi:10.1029/96GL01722.

342. Dobson GM, Brewer AW, Cwilong BM. Meteorology of the lower stratosphere. **Proc R Soc Med** 185: 144–175, 1946. doi:10.1098/rspa.1946.0010.

343. Steinbrecht W, Claude H, Köhler U, Hoinka KP. Correlations between tropopause height and total ozone: Implications for long-term changes. **J Geophys Res Atmos** 103: 19183–19192, 1998. doi:10.1029/98JD01929.

344. Lin P, Paynter D, Ming Y, Ramaswamy V. Changes of the tropical tropopause layer under global warming. **J Clim** 30: 1245–1258, 2017. doi:10.1175/JCLI-D-16-0457.1.

345. Meng L, Liu J, Tarasick DW, Randel WJ, Steiner AK, Wilhelmsen H, Wang L, Haimberger L. Continuous rise of the tropopause in the Northern Hemisphere over 1980–2020. **Sci Adv** 7: eabi8065, 2021. doi:10.1126/sciadv.abi8065.

346. Waugh DW, Sobel AH, Polvani LM. What is the polar vortex and how does it influence weather? **Bull Am Meteorol Soc** 98: 37–44, 2017. doi:10.1175/BAMS-D-15-00212.1.

347. Manney GL, Santee ML, Rex M, Livesey NJ, Pitts MC, Veefkind P, Nash ER, Wohltmann I, Lehmann R, Froidevaux L, Poole LR, Schoeberl MR, Haffner DP, Davies J, Dorokhov V, Gernandt H, Johnson B, Kivi R, Kyrö E, Larsen N, Levelt PF, Makshtas A, McElroy CT, Nakajima H, Parrondo MC, Tarasick DW, von der Gathen P, Walker KA, Zinoviev NS. Unprecedented Arctic ozone loss in 2011. **Nature** 478: 469–475, 2011. doi:10.1038/nature10556.

348. Petkov BH, Vitale V, Tomasi C, Siani AM, Seckmeyer G, Webb AR, Smedley ARD, Casale GR, Werner R, Lanconelli C, Mazzola M, Lupi A, Busetto M, Diémoz H, Goutail F, Köhler U, Mendeva BD, Josefsson W, Moore D, Bartolomé ML, Moreta González JR, Mišaga O, Dahlback A, Tóth Z, Varghese S, De Backer H, Stübi R, Vaníček K. Response of the ozone column over Europe to the 2011 Arctic ozone depletion event according to ground-based observations and assessment of the consequent variations in surface UV irradiance. **Atmos Environ** 85: 169–178, 2014. doi:10.1016/j.atmosenv.2013.12.005.

349. Bernhard GH, Fioletov VE, Grooß JU, Ialongo I, Johnsen B, Lakkala K, Manney GL, Müller R, Svendby T. Record-breaking increases in Arctic solar ultraviolet radiation caused by exceptionally large ozone depletion in 2020. **Geophys Res Lett** 47: e2020GL090844, 2020. doi:10.1029/2020GL090844.

350. Bednarz EM, Maycock AC, Abraham NL, Braesicke P, Dessens O, Pyle JA. Future Arctic ozone recovery: the importance of chemistry and dynamics. **Atmos Chem Phys** 16: 12159–12176, 2016. doi:10.5194/acp-16-12159-2016.

351. Siani A, Casale GR, Galliani A. Investigation on a low ozone episode at the end of November 2000 and its effect on ultraviolet radiation. **Opt Eng** 41: 3082–3089, 2002. doi:10.1117/1.1516821.

352. Butchart N. The Brewer-Dobson circulation. **Rev Geophys** 52: 157–184, 2014. doi:10.1002/2013RG000448.

353. Polvani LM, Wang L, Abalos M, Butchart N, Chipperfield MP, Dameris M, Deushi M, Dhomse SS, Jöckel P, Kinnison D, Michou M, Morgenstern O, Oman LD, Plummer DA, Stone KA. Large impacts, past and future, of ozone-depleting substances on Brewer-Dobson circulation trends: a multimodel assessment. **J Geophys Res Atmos** 124: 6669–6680, 2019. doi:10.1029/2018JD029516.

354. McLandress C, Shepherd TG. Simulated anthropogenic changes in the Brewer–Dobson circulation, including its extension to high latitudes. **J Clim** 22: 1516–1540, 2009. doi:10.1175/2008JCLI2679.1.

355. Butchart N, Scaife AA, Bourqui M, de Grandpré J, Hare SH, Kettleborough J, Langematz U, Manzini E, Sassi F, Shibata K, Shindell D, Sigmond M. Simulations of anthropogenic change in the strength of the Brewer–Dobson circulation. **Clim Dyn** 27: 727–741, 2006. doi:10.1007/s00382-006-0162-4.

356. Fu Q, Solomon S, Pahlavan HA, Lin P. Observed changes in Brewer–Dobson circulation for 1980–2018. **Environ Res Lett** 14: 114026, 2019. doi:10.1088/1748-9326/ab4de7.

357. Carpenter L, Reimann S, Burkholder J, Clerbaux C, Hall B, Hossaini R, Laube J. Scientific assessment of ozone depletion: 2014 (Online). Geneva: World Meteorological Organization, 2014. https://library.wmo.int.

358. Montzka SA, Dutton GS, Yu P, Ray E, Portmann RW, Daniel JS, Kuijpers L, Hall BD, Mondeel D, Siso C, Nance JD, Rigby M, Manning AJ, Hu L, Moore F, Miller BR, Elkins JW. An unexpected and persistent increase in global emissions of ozone-depleting CFC-11. **Nature** 557: 413–417, 2018. doi:10.1038/s41586-018-0106-2.

359. Lickley M, Solomon S, Fletcher S, Velders GJ, Daniel J, Rigby M, Montzka SA, Kuijpers LJ, Stone K. Quantifying contributions of chlorofluorocarbon banks to emissions and impacts on the ozone layer and climate. **Nat Commun** 11: 1380, 2020. doi:10.1038/s41467-020-15162-7.

360. Fang X, Pyle JA, Chipperfield MP, Daniel JS, Park S, Prinn RG. Challenges for the recovery of the ozone layer. **Nat Geosci** 12: 592–596, 2019. doi:10.1038/s41561-019-0422-7.

361. Dhomse SS, Feng W, Montzka SA, Hossaini R, Keeble J, Pyle JA, Daniel JS, Chipperfield MP. Delay in recovery of the Antarctic ozone hole from unexpected CFC-11 emissions. **Nat Commun** 10: 5781, 2019. doi:10.1038/s41467-019-13717-x.

362. Keeble J, Abraham NL, Archibald AT, Chipperfield MP, Dhomse S, Griffiths PT, Pyle JA. Modelling the potential impacts of the recent, unexpected increase in CFC-11 emissions on total column ozone recovery. **Atmos Chem Phys** 20: 7153–7166, 2020. doi:10.5194/acp-20-7153-2020.

363. Montzka SA, Dutton GS, Portmann RW, Chipperfield MP, Davis S, Feng W, Manning AJ, Ray E, Rigby M, Hall BD, Siso C, Nance JD, Krummel PB, Mühle J, Young D, O'Doherty S, Salameh PK, Harth CM, Prinn RG, Weiss RF, Elkins JW, Walter-Terrinoni H, Theodoridi C. A decline in global CFC-11 emissions during 2018−2019. **Nature** 590: 428−432, 2021. doi:10.1038/s41586-021-03260-5.

364. Reuder J, Dameris M, Koepke P. Future UV radiation in Central Europe modelled from ozone scenarios. **J Photochem Photobiol B** 61: 94–105, 2001. doi:10.1016/S1011-1344(01)00143-9.

365. Vogelmann AM, Ackerman TP, Turco RP. Enhancements in biologically effective ultraviolet radiation following volcanic eruptions. **Nature** 359: 47–49, 1992. doi:10.1038/359047a0.

366. Grant WB, Browell EV, Fishman J, Brackett VG, Veiga RE, Nganga D, Minga A, Cros B, Butler CF, Fenn MA, Long CS, Stowe LL. Aerosol-associated changes in tropical stratospheric ozone following the eruption of Mount Pinatubo. **J Geophys Res** 99: 8197–8211, 1994. doi:10.1029/93JD03314.

367. Brenna H, Kutterolf S, Krüger K. Global ozone depletion and increase of UV radiation caused by pre-industrial tropical volcanic eruptions. **Sci Rep** 9: 9435, 2019. doi:10.1038/s41598-019-45630-0.

368. Wade DC, Vidal CM, Abraham NL, Dhomse S, Griffiths PT, Keeble J, Mann G, Marshall L, Schmidt A, Archibald AT. Reconciling the climate and ozone response to the 1257 CE Mount Samalas eruption. **Proc Natl Acad Sci U S A** 117: 26651–26659, 2020. doi:10.1073/pnas.1919807117.

369. Ohneiser K, Ansmann A, Kaifler B, Chudnovsky A, Barja B, Knopf DA, Kaifler N, Baars H, Seifert P, Villanueva D, Jimenez C, Radenz M, Engelmann R, Veselovskii I, Zamorano F. Australian wildfire smoke in the stratosphere: the decay phase in 2020/2021 and impact on ozone depletion. **Atmos Chem Phys** 22: 7417–7442, 2022. doi:10.5194/acp-22-7417-2022.

370. Bernath P, Boone C, Crouse J. Wildfire smoke destroys stratospheric ozone. **Science** 375: 1292–1295, 2022. doi:10.1126/science.abm5611.

371. Cordero RR, Feron S, Damiani A, Redondas A, Carrasco J, Sepúlveda E, Jorquera J, Fernandoy F, Llanillo P, Rowe PM, Seckmeyer G. Persistent extreme ultraviolet irradiance in Antarctica despite the ozone recovery onset. **Sci Rep** 12: 1266, 2022. doi:10.1038/s41598-022-05449-8.

372. UNEP. **Spreading like Wildfire—The Rising Threat of Extraordinary Landscape Fires. A UNEP Rapid Response Assessment**. Nairobi: UNEP, 2022.

373. Fountoulakis I, Natsis A, Siomos N, Drosoglou T, Bais AF. Deriving aerosol absorption properties from solar ultraviolet radiation spectral measurements at Thessaloniki, Greece. **Remote Sens** 11: 2179, 2019. doi:10.3390/rs11182179.

374. Iglesias-Suarez F, Wild O, Kinnison DE, Garcia RR, Marsh DR, Lamarque JF, Ryan EM, Davis SM, Eichinger R, Saiz-Lopez A, Young PJ. Tropical stratospheric circulation and ozone coupled to Pacific multi-decadal variability. **Geophys Res Lett** 48: e2020GL092162, 2021. doi:10.1029/2020GL092162.

375. Gerber EP, Baldwin MP, Akiyoshi H, Austin J, Bekki S, Braesicke P, Butchart N, Chipperfield M, Dameris M, Dhomse S, Frith SM, Garcia RR, Garny H, Gettelman A, Hardiman SC, Karpechko A, Marchand M, Morgenstern O, Nielsen JE, Pawson S, Peter T, Plummer DA, Pyle JA, Rozanov E, Scinocca JF, Shepherd TG, Smale D. Stratosphere-troposphere coupling and annular mode variability in chemistry-climate models. **J Geophys Res** 115: D00M06, 2010. doi:10.1029/2009JD013770.

376. Mann ME, Park J, Bradley RS. Global interdecadal and century-scale climate oscillations during the past five centuries. **Nature** 378: 266–270, 1995. doi:10.1038/378266a0.

377. World Meteorological Organization (WMO). **Scientific Assessment of Ozone Depletion: 2022, GAW Report No. 278**. Geneva, Switzerland: World Meteorological Organization, p. 509, 2022.